The Dissertation Committee for Christopher Eric Bailey certifies that this is the approved version of the following dissertation:

TYROSINE NITRATION AND ALTERED GLYCERALDEHYDE-3-PHOSPHATE DEHYDROGENASE PROTEIN LEVELS FOLLOWING ISCHEMIA/REPERFUSION: THE INFLUENCE OF AGING IN GLYCOLYTIC SKELETAL MUSCLE

Committee:

_____

John Papaconstantinou, Ph.D. Supervisor

_____

Jeffrey Rabek, Ph.D.

_____

Giulio Taglialatela, Ph.D.

_____

Golda A. Leonard, Ph.D.

_____

Roger Farrar, Ph.D.

_____

Cary W. Cooper, Ph.D.

Dean, Graduate School

TYROSINE NITRATION AND ALTERED GLYCERALDEHYDE-3-PHOSPHATE DEHYDROGENASE PROTEIN LEVELS FOLLOWING ISCHEMIA/REPERFUSION: THE INFLUENCE OF AGING IN GLYCOLYTIC SKELETAL MUSCLE

by

Christopher Eric Bailey, B.A.

Dissertation

Presented to the Faculty of the Graduate School of

The University of Texas Medical Branch

in Partial Fulfillment

of the Requirements

for the Degree of

Doctor of Philosophy

The University of Texas Medical Branch

June 2009

Dedication

To my wife, Dr. Kimberly Shilling Bailey, for her love, support, and understanding in letting me follow this dream even thought it meant living apart for the first three years of our marriage. You were a thousand miles away, but you were always in my heart.

To my maternal grandparents, N.L. and Lynn Spears, for their incalculable support throughout my lifetime. We are poorer that you are no longer with us, but find rich comfort knowing you are together again.

Acknowledgments

I would like to thank Dr. John Papaconstantinou, for being not only my mentor but also my supporter for the past 5 years. I have appreciated your enthusiasm and dedication. To have a long, productive career and to be excited about your work is true success. It's readily apparent that he has learned some secrets about aging well that he has not published for the rest of us.

I also want to thank the past and present members of Dr.Papaconstantinou's laboratory who have contributed greatly to my education and research endeavors –Dr. James Deford, Dr. C. C. "Winston" Hsieh, Dr. William Boylston, Dr. Kashyap Choksi, Dr. Jonathon Nuss, Dr. Veronica Tovar Sepulveda, Vincent Dimayuga, James Amaning, and Amama Chalawalla,

Another person who has played a significant role in my academic journey is Dr. Golda Leonard. As director of the Cell Biology Graduate Program, as confidant, sounding board, encourager, and finally as committee member, you made invaluable contributions to my academic progress and the maintenance of my small store of sanity. Perhaps only those students who have had the blessing of working with you truly understand the loss this university will undergo at your departure.

I greatly appreciate the involvement of my other committee members, Dr. Jeffrey Rabek, Dr. Giulio Taglialatela, and Dr. Roger Farrar. You offered advice and knowledge throughout your tenures on my committee, but I can recall specific instances when each of you contributed at a crucial juncture. One regret that I have about my time in graduate school is that I did not interact more with each of you, to benefit more fully from your knowledge and experience.

Tyrosine Nitration and Altered Protein Pool Levels of Glyceraldehyde-3-Phosphate Dehydrogenase Following Ischemia/Reperfusion: The Influence of Aging in Glycolytic Skeletal Muscle

Publication No._____

Christopher Eric Bailey, Ph.D.

The University of Texas Medical Branch, 2009

Supervisor: John Papaconstantinou

Aging and skeletal muscle ischemia/reperfusion (I/R) injury both lead to skeletal muscle dysfunction, evidenced by decreased contractile force generation, particularly in glycolytic muscle. The deficits in I/R are more severe and persistent in aged animals. Previous studies in our lab led us to hypothesize that the expression of the glycolytic enzyme glyceraldehyde-3-phosphate dehydrogenase may be altered following I/R. We further hypothesized that aging would enhance the oxidative stress and oxidative damage experienced by the muscle. GAPDH protein levels were measured by Western blotting. We observed that the enzyme is significantly decreased at 3 and 5 days of reperfusion in the young muscle, while the enzyme was significantly decreased in the aged muscle at 1, 3, 5, and 7 days. Using PCR, we compared GAPDH mRNA levels at 5 days reperfusion and found that the I/R tissue from both young and old have significant increases in GAPDH transcript at this time point compared to control, suggesting that the protein deficit is not due to decreased transcription. Finally, we examined tyrosine nitration. A

spot selected following 2D gel electrophoresis and nitrotyrosine western blotting of young and old muscle lysate was identified as GAPDH by mass spectrometry. We compared tyrosine nitration over the time course of reperfusion. While total tyrosine nitration does not increase in the I/R tissue in the young, nitration of GAPDH is significantly increased at 1 and 3 days reperfusion. In contrast to the young, total tyrosine nitration in the aged muscle was significantly increased at 1, 3, and 5 days of reperfusion, with significant increases in nitration of GAPDH at the same time points. We conclude that GAPDH protein levels are decreased following I/R, which could interfere with metabolism and ATP generation. Further, this decrease is not likely transcriptionally mediated. Based on the increases in tyrosine nitration, we propose that oxidative modification enhances the degradation of GAPDH following I/R, and that the persistence of decreased GAPDH in the aged muscle is due to the prolonged increases in oxidative modification seen in that age group. This suggests that the aged muscle experiences greater oxidative stress, protein modification, and GAPDH degradation, possibly contributing to the decreased muscle function reported in the literature.

TABLE OF CONTENTS

Table of Figures

Introduction: Chapter 1 - Aging and Ischemia/Reperfusion Injury in Glycolytic Skeletal Muscle

Aging and skeletal muscle ischemia/reperfusion injury both result in skeletal muscle dysfunction [8,40,58,64,119,120]. In these conditions, oxidative protein modifications are often cited not only as evidence for increased oxidative stress, but as a possible mechanistic feature that promotes skeletal muscle dysfunction. As aging and skeletal muscle ischemia/reperfusion injury have overlapping pathologic features, it is reasonable to expect that age-related muscle dysfunction and ischemia/reperfusion (I/R) injury would have a synergistic effect upon muscle function. Recent research has indeed substantiated this idea [40]; however, the degree to which oxidative modification may play a role in this cumulative effect and the mechanisms by which oxidative protein modification may lead to muscle dysfunction are not well understood.

Sarcopenia, which is decreased strength due to loss of skeletal muscle function or mass, is a characteristic manifestation of the progressive loss of tissue function in aging [119,120]. One component of this dysfunction is the oxidation of proteins and free amino acids. The overall amount of oxidative post-translational modifications increases during aging, likely due to an increased rate of modification or decreased degradation of modified proteins [71,113]. Changes in protein structure and function due to oxidative modification have been postulated to be a significant cause of muscle dysfunction

[19,49,106]. Sarcopenia is a significant cause of loss of independence and frailty in older adults [58]. It has been reported that decreased thigh muscle mass, decreased leg strength, and increased fat infiltration are inversely correlated with mobility in normally functioning older adults [122]. In another prospective study of individuals aged 70-79, muscle strength was inversely related to mortality over a mean follow-up interval of 4.9 years [86]. While some of the correlation may be explained by metabolic or biochemical factors, it is likely that part of the association is directly due to decreased mobility, increased susceptibility to falls and other trauma, and decreased independence and self-care that accompany muscle and strength decreases [42]. This is particularly true in individuals whose level of muscle strength barely exceeds the amount necessary for a given task (i.e., low reserve capacity) [95,96] In these individuals, small changes in strength can have a disproportionate impact upon the ability to perform a given function, as the ability to perform a function usually requires a minimum level of strength below which individuals are unable to perform a given task [13,30]. While this can have devastating consequences when strength is lost, it also means that small increases in strength or reductions in the loss of strength can provide major improvements to the quality of life and potentially to morbidity and mortality of older individuals [61].

In addition to aging, another factor that has direct influence on the susceptibility of muscle cells to oxidative stress during I/R is the metabolic phenotype of the cell. This is supported by several lines of evidence. During aging, there is a preferential decrease in fiber number and fiber size for glycolytic skeletal muscles[119,120]. Oxidative stress appears to have a greater impact upon mitochondrial electron transport chain function in

glycolytic skeletal muscles compared to mitochondria isolated from more oxidative muscles [19]. Furthermore, the degree of glycolytic phenotype in skeletal muscle correlates with susceptibility to cachexia as a result of chronic disease in humans and in models of cachexia both in mouse muscle *in vivo* or mouse cell lines [130]. It is suggested that this is the result of increased anti-oxidant defenses and inducible nitric oxide synthase. The increased susceptibility of primarily glycolytic muscle to oxidative stress in both ischemic or hypoxic injury and in aging is the rational for studying glycolytic skeletal muscle in the present work.

Ischemia/reperfusion is also characterized by increased oxidative stress. ROS production increases during hypoxia, although it is unclear whether mitochondria are the only source. In one study using a FRET-based technique, a redox-sensitive thiol probe was oxidized in the cytosol of hypoxic wild-type 143B osteosarcoma cells, while p^o 143B cells (which are deficient in mitochondrial respiration, due to siRNA knockdown of Riske iron sulfur protein in complex III) did not oxidize the same probe in hypoxia, suggesting that a functional mitochondrial electron transport chain contributes to ROS production in hypoxia [38]. However, measurements of mitochondrial superoxide production via a fluorescent probe which selectively interacts with superoxide suggest that mitochondrial ROS production actually decreases during hypoxia or anoxia in cardiac myocytes. During reoxygenation following anoxia, however, increased mitochondrial superoxide was detected, suggesting that mitochondria are a source of ROS during reperfusion [124]. Finally, the inflammatory response resulting from the action of cytokines and the infiltration of inflammatory cells also contributes to ROS

following reperfusion [8]. The increase in ROS from these various sources is thought to lead to an accumulation of oxidized proteins. Ischemia and hypoxia are common problems in clinical practice. It is estimated that by 2030, there will be 1 to 2 million major vascular surgery cases per year in the United States [1], and I/R is a major component of vascular surgery cases [123]. In addition to vascular surgery, utilization of flaps during reconstructive surgery, tourniquets during orthopedic surgery, compartment syndrome following surgery or trauma, sepsis, critical limb ischemia, and thromboembolic events can all lead to I/R injury [17,40,125]. Many of these clinical situations are more common in older patients, who may already be experiencing age-related muscle dysfunction. While it is suggested in the literature that an ischemic interval of 4 hours is needed before skeletal muscle death is readily apparent [8], changes in muscle function and physiology occur with ischemic intervals as short as two hours [40].

While nitric oxide may be a protective factor in certain tissue stress signaling processes at specific concentrations [6,130], excess nitric oxide can be detrimental. When combined with the presence of reactive oxygen species (ROS) such as superoxide, nitric oxide can lead to the formation of damaging products [7], whether peroxynitrite [112] or one of peroxynitrite's potential end products, tyrosine nitration[128].

Nitric oxide is generated enzymatically in cells by nitric oxide synthase (NOS), which converts L-arginine to citrulline via two successive oxidation reactions (Figure 1.1) [21].
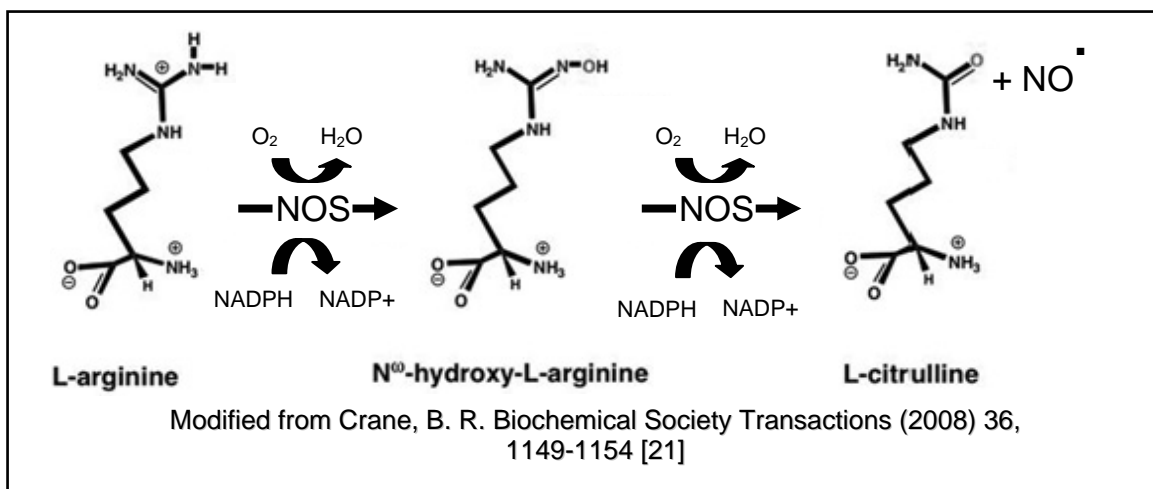
Figure 1.1: Production of Nitric Oxide From L-Arginine by Nitric Oxide Synthase: Conversion of l-arginine to citrulline occurs via two oxidation reactions

There are at least three forms of NOS in mammals [43,87] Endothelial NOS (eNOS) and neuronal NOS (nNOS) are constitutively expressed in a variety of tissue types. Inducible NOS (iNOS) is responsive to inflammatory stimuli. While all three isoforms share similar enzymatic mechanisms, the NOS isoforms are controlled by several different means. In addition to tissue-dependent expression levels, other factors which regulate NOS activity include subcellular localization, access to substrates, formation of complexes with regulatory proteins or other NOS proteins, and posttranslational modification [87]. Calcium is required for the activity of the constitutively expressed nNOS and eNOS isoforms, as this mediates their binding to calmodulin. Calmodulin binding is necessary for full activity for all isoforms, although iNOS binds calmodulin at much lower calcium levels [87]. These multiple regulatory mechanisms function in concert to control NO production. For instance, phosphorylation of certain cysteine

5

residues of eNOS in bovine aortic endothelial cells has been shown to alter the calcium

levels needed for activation [82]. This layering of multiple regulatory mechanisms

provides the ability for precise control of NO production.

Experiments measuring nitric oxide production in ischemia and reperfusion are

difficult to interpret, due to the variation in animal models, ischemic times, and methods

for measuring NO. An increase in nitric oxide production from vascular endothelium

early in ischemia has been reported in several studies of rabbit muscle ischemia, with NO

concentrations decreasing as ischemic time lengthens [10,39]. This early increase in

endothelium-derived NO might be interpreted as an expected physiological response to

vasoconstriction, while the following decline in NO production would occur due to

decreased oxygen availability (oxygen is a substrate of NOS; Figure 1). Following

ischemia, nitric oxide production increases within the first fifteen minutes of reperfusion

due to eNOS activation. This initial increase is followed by a second peak in NO

production resulting from iNOS activated by the immune response [64]. The precise

timing and duration of the second flux of NO production is difficult to determine. Direct

electrochemical measurement using porphyrinic microsensors allows real-time

measurement of NO production and is well-suited for measuring endothelial NO

production; however, it is limited to a detection area within 50 μM of the probe. It also

cannot account for NO which reacts with ROS before contacting the probe [10]. This

could be a major limitation during situations of high oxidative stress, as the reaction of

NO with superoxide is diffusion-limited (k approximately $1\mathrm{x}10^{10}\ \mathrm{M}^{-1}\ \mathrm{s}^{-1}$) [90]. Electron

paramagnetic resonance (EPR) spectroscopy has also been used to measure NO

concentration following reperfusion of ischemic rat skeletal muscle [70], with the result

that NO production was not detected until 24 hours after reperfusion. The reported NO

production after 24 hours was not blocked by administration of the NOS inhibitors N-

nitro-L-arginine methyl ester or S-methylisothiourea; however, it was decreased by

glucocorticoid administration, suggesting that iNOS might contribute to the observed NO

production at 24 hours. A potential difficulty in interpreting the results of EPR

spectroscopy in this study, however, is the possibility the signal detected after 24 hours of

reperfusion may represent the accumulation of the nitroso-heme adducts measured by

EPR in this experiment to a detectable level, rather than a flux of NO synthesis [64].

Difficulties in experimental details aside, the consensus of the experiments suggests that

an iNOS-mediated increase in NO production occurs after the initial eNOS-mediated

flux.

Nitric oxide can interact with ROS, leading to several different types of post-

translational modifications (for reviews, see [80,113,118]. While some nitrosative

modifications such as cysteine nitrosylation have been shown convincingly to be

involved in signaling mechanisms[41,44,114], tyrosine nitration is usually considered to

be an indication of high oxidative and nitrative stress that has resulted in protein damage.

Further studies are necessary, however, to elucidate the potential significance of tyrosine

nitration as a signaling mechanism *in vivo* [80].

Nitrotyrosine adducts are formed *in vivo* by two primary reaction pathways, as

shown in Figure 1.2. These include (a) the reaction of nitric oxide with superoxide

leading to peroxynitrite production and (b) the reaction of nitrite and hydrogen peroxide

7

with various heme peroxidases. Both of these reactions lead to formation of a tyrosyl

radical, followed by addition of nitrogen dioxide to yield 3-nitrotyrosine [90]. In I/R

injury, levels of nitrotyrosine due to both mechanisms are likely to be elevated, as a result

of the infiltration of immune cells, activation of iNOS, and increased ROS production

[64].
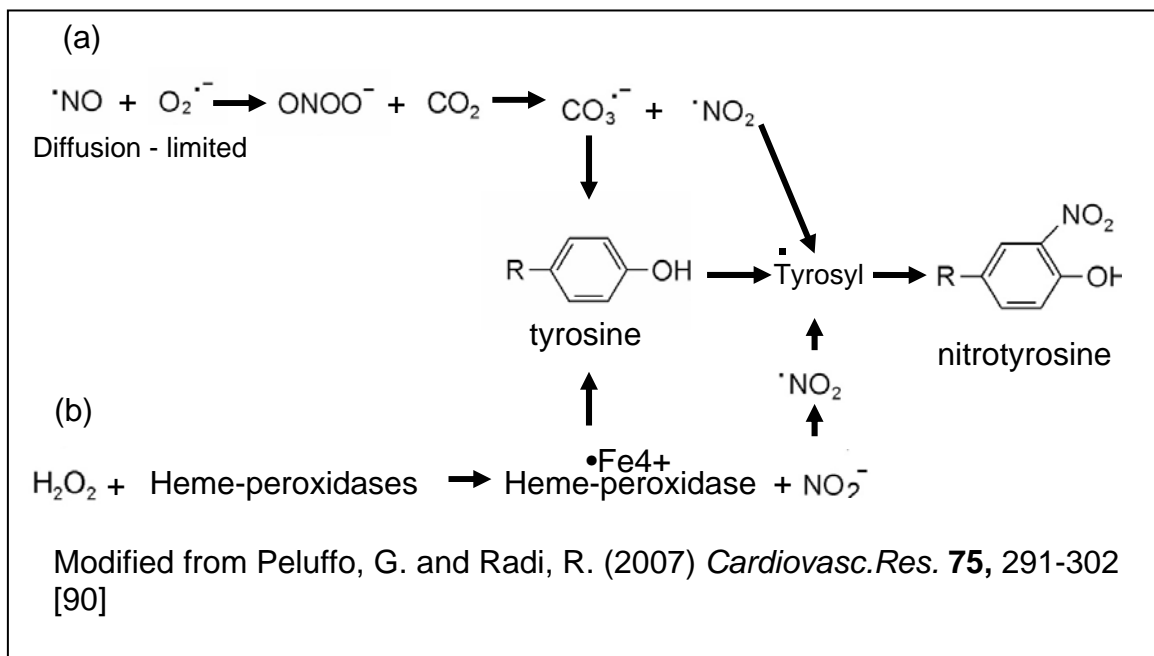
Figure 1.2: Mechanisms of in vivo Nitrotyrosine Formation:
(a) Reaction of Nitric oxide with superoxide to yield peroxynitrite, followed by reaction
of peroxynitrite with carbon dioxide, which decomposes into carbonate anion and
nitrogen dioxide; (b) reaction of hydrogen peroxide and heme-peroxidase enzymes to
yield an activated heme center. Both (a) and (b) result in a tyrosyl radical, which reacts
with nitrogen dioxide to yield nitrotyrosine.

It has been suggested that nitrotyrosine could in fact be involved in signaling

reactions, with specificity being provided by subcellular trafficking of NOS as a potential

mechanism for targeting NO-induced nitration of specific proteins [87,127]. Regardless

of the ultimate conclusions concerning tyrosine nitration as a signaling molecule *in vivo*,

it is apparent that tyrosine nitration alters the biochemical characteristics of proteins. One

example of this is the ability of nitration to prevent the tyrosine phosphorylation of

synthetic peptide substrates by lymphocyte-specific tyrosine kinase p56^{lck}.

Phosphorylation of the synthetic peptide is completely inhibited when the nitration

occurred at the phosphorylation site; however, nitration of a tyrosine four residues away

from the phosphorylation site was still sufficient to decrease tyrosine phosphorylation

significantly [67], suggesting that nitration may alter protein structure and alter enzyme

activation even if the nitration occurs outside of the catalytic site. The potential *in vivo*

relevance is that the sequence of the synthetic peptides used is a phosphorylation site in

p34^{cdc2} kinase, which is activated by tyrosine phosphorylation of this site as part of

progression through the G2/M checkpoint [28]. In a broader sense, this demonstrates that

tyrosine nitration could have widespread implications for signaling cascades involving

tyrosine phosphorylation, including those for insulin, growth factors, and MAPK stress

responses. Indeed, it has recently been suggested that nitration of the MAPK ERK plays

a role in the vulnerability to injury and the decreased mucosal healing seen in a rat model

of portal hypertension [66]. Another indication that tyrosine nitration can alter protein

function is the binding of nitrated SH2-specific peptides to the regulatory SH2 domain of

src kinases, thus preventing intramolecular interactions which block src kinase activation

[79]. Finally, there are multiple examples of tyrosine nitration correlating with decreased

enzyme activity. One such example is the manganese superoxide dismutase (Mn-SOD).

Nitration of Y34 has been reported to inactivate the enzyme following treatment with peroxynitrite. The crystal structures of nitrated and non-nitrated Mn-SOD show that although there are not large scale alterations in enzyme structure, the nitration of Y34 introduces steric hindrance at the active site which may hinder substrate accessibility [94].

Debate continues concerning the effects of tyrosine nitration *in vivo*. Sharov et. al [107] reported an age-related increase in nitration of glycogen phosphorylase b in rat skeletal muscle that correlated with inactivation of the enzyme. Other studies [24] based upon *in vitro* nitration of the purified protein suggested a particular tyrosine of glycogen phosphorylase as the site responsible for inactivation. Further experiments by Sharov et. al. [106] suggest however that the nitrated tyrosine identified by *in vitro* treatment with peroxynitrite is not responsible for inactivation of glycogen phosphorylase, but that this enzyme inactivation is due to modification of cysteine. This is in contrast to the hypothesis presented in their previous publication. These three publications illustrate some of the difficulties encountered in the study of non-enzymatic post-translational modifications.

In vitro studies can provide insight into the basic mechanisms of modification or the ways in which modification may alter cellular functions. One particularly relevant area of investigation concerns the effect of oxidative protein modification on the rate of protein degradation. Chaperone-mediated autophagy (CMA) is one mechanism used by cells for the removal of oxidized proteins [62]. Proteins containing a specific exposed pentapeptide sequence [77] are recognized by cytosolic heat shock cognate 70 (hsc70),

which is a constitutively expressed heat shock family member known to participate in trans-membrane transport in mitochondria and ER [18,27]. The hsc70/unfolded protein complex is then bound by the lysosomal membrane protein lamp2a. The lamp2a/protein complex is translocated across the lysosomal membrane with the help of lysosomal-heat shock cognate 70 [62]. In a series of experiments, it was reported that treatment of mouse fibroblasts with hydrogen peroxide causes increased localization of lamp2a to the lysosomal membrane. To further examine the possibility that CMA was increased by oxidative stress, investigators treated rats with paraquat, which is known to cause increased ROS generation. Lamp2a was again found to be increased at the lysosomal membrane. In both instances, lysosomal heat shock cognate 70, which works in conjunction with lamp2a, was also upregulated, potentially explaining the increased levels of oxidized proteins also reported in both fibroblast and liver lysosomes [65]. Experiments with isolated lysosomes are particularly telling, however. GAPDH is known to be a substrate of the CMA pathway [2,22]. GAPDH which had been oxidized with iron and ascorbate or non-oxidized GAPDH were incubated with isolated lysosomes for 30 minutes. Lysosomes were then washed, and associated GAPDH was removed by proteinase K digestion. The lysosomes were then examined by gel electrophoresis. It was found that the oxidized GAPDH was imported to a greater degree than non-oxidized GAPDH, and that increasing the oxidation time of GAPDH increased the amount of GAPDH imported into the lysosomes [65]. Further experiments showed that the oxidized GAPDH was more susceptible to proteolytic degradation by lysosomal enzymes or proteinase K, making it unlikely that the increase in oxidized lysosomal GAPDH is due

11

to lower rates of degradation. Further, the increased importation of oxidized GAPDH

occurred in the absence of direct oxidation of the lysosomes themselves, suggesting that

it is not mediated by increased expression of lamp2a or lysosomal heat shock cognate 70.

These experiments support the concept of CMA as an important means of disposing of

oxidatively modified protein.

The stimulation of protein degradation by oxidative stress is not unique to

lysosomal autophagy, however. Another mechanism for clearing oxidatively modified

proteins from the cell is the proteasomal system [37]. The proteasomal system includes

several different proteasome complexes: the 26S proteasome, the 20S proteasome, and

the immunoproteasome [5]. These complexes are formed in a modular manner by

assembly of several subcomplexes, each named according to their sedimentation

coefficients [117]. The 20S core subunit is the catalytic component of the proteasome,

possessed of proteolytic activities similar to trypsin, chymotrypsin, and peptidylglutamyl-

peptide hydrolase [5]. The 20S proteasome recognizes hydrophobic regions of unfolded

proteins [37] and is more resistant to oxidative inactivation than the 26S proteasome

[97,98]. These two key factors, along with experimental evidence, suggest that the 20S

proteasome is the major proteasomeal system responsible for removing oxidized proteins

[5].   The 26S proteasome consists of both the 20S core and the 19S regulatory domain.

The 26S proteasome recognizes ubiquitinated proteins and operates in an ATP-dependent

manner.   The specificity for ubiquitinated proteins is provided by the 19S regulatory

domain, which is thought to utilize ATP for unfolding recognized proteins and

translocating them into the 20S core [117].

A series of experiments carried out by Buchczyk et. al. [12] provide insight into proteasomal degradation of GAPDH after exposure to peroxynitrite. Purified GAPDH was treated with doses of peroxynitrite from 135 nanomolar to over 1 mM. The protein was dialyzed to remove excess peroxynitrite, and glycolytic enzyme activity was measured. Approximately 20 μM peroxynitrite was needed to reduce the activity of 8.8 μM GAPDH by 50% (or a peroxynitrite:GAPDH molar ratio of 2.5:1). At this peroxynitrite concentration, tyrosine nitration was not detected by western blot. Peroxynitrite-treated GAPDH was then incubated with 20S proteasomes isolated from rat liver. The degradation rate of GAPDH was increased by peroxynitrite treatment. Surprisingly, maximal rates of degradation were achieved using GAPDH that had been treated with peroxynitrite concentrations two orders of magnitude lower than that required for half-maximal inhibition of GAPDH enzyme activity. Consequently, the rate of GAPDH degradation was decreased in GAPDH treated with a peroxynitrite:GAPDH ratio higher than approximately 0.03:1 (although the degradation rate was still greater than for untreated GAPDH). Nitration became detectible when peroxynitrite:GAPDH molar ratios were approximately 8:1. Thus, it appears that *in vitro*, the reaction of peroxynitrite with GAPDH increases rates of proteasomal degradation of GAPDH at very low levels of enzyme inactivation. Increasing levels of peroxynitrite lead to further loss of GAPDH enzymatic activity, decreasing rates of proteasomal degradation (although still greater than untreated GAPDH), and eventually cause tyrosine nitration. At extremely high levels of peroxynitrite treatment (> 2 mM), the treated GAPDH is degraded by the proteasome at the same rate as untreated GAPDH. Experiments

13

measuring the rate of degradation of oxidatively modified proteins by isolated proteasomal or lysozomal systems provide an underlying understanding of possible *in vivo* effects of protein modification. While studies such as this provide valuable mechanistic insight, the relationship to *in vivo* situations can be difficult to establish.

It should not necessarily be concluded that tyrosine nitration does not alter protein function, even in cases where enzyme inactivation can be shown to occur *in vitro* at peroxynitrite concentrations below that required for facile detection of tyrosine nitration. Many enzymes have multiple functions that are not measured by standard enzymatic assays. Further, while kinetics of enzyme activity are important, the effective activity of enzymes or other proteins requires appropriate localization and coordination with other cellular systems. Coordination and localization of activity are often accomplished via protein-protein interactions. These interactions are not measured in commonly used enzymatic assays. Also, exposure of proteins to oxidants or peroxynitrite *in vitro* often ignores the influence of substrate, cofactors, or interacting proteins which may shield or alter the nitration/oxidation characteristics of the protein, as well as the necessary concentration of oxidants/nitrating agents necessary to achieve a specific modification. Finally, while enzyme inactivation may occur *in vitro* at levels of peroxynitrite that are below the threshold for tyrosine nitration, this does not imply that tyrosine nitration *in vivo* has no effect on enzyme activity following the resolution of oxidative or nitrative stress. Many enzymes catalyzing oxidation-reduction reactions contain cysteine in their active sites and are inactivated by cysteine modification. These modifications (see Figure 1.3) are reversible, provided the oxidative stress is not so severe as to drive the

14

modification to higher oxidation states [111]. It has even been suggested that the

formation of disulfide bonds, cysteine sulfenic acids, nitrosothiols, or glutathiolation are

reversible, protective features of many enzymes, preventing irreversible oxidation of

cysteine residues which are critical for enzyme activity [45,126].

Adapted from Spickett et. al, BBA, 1764(12):1823-41 [111]
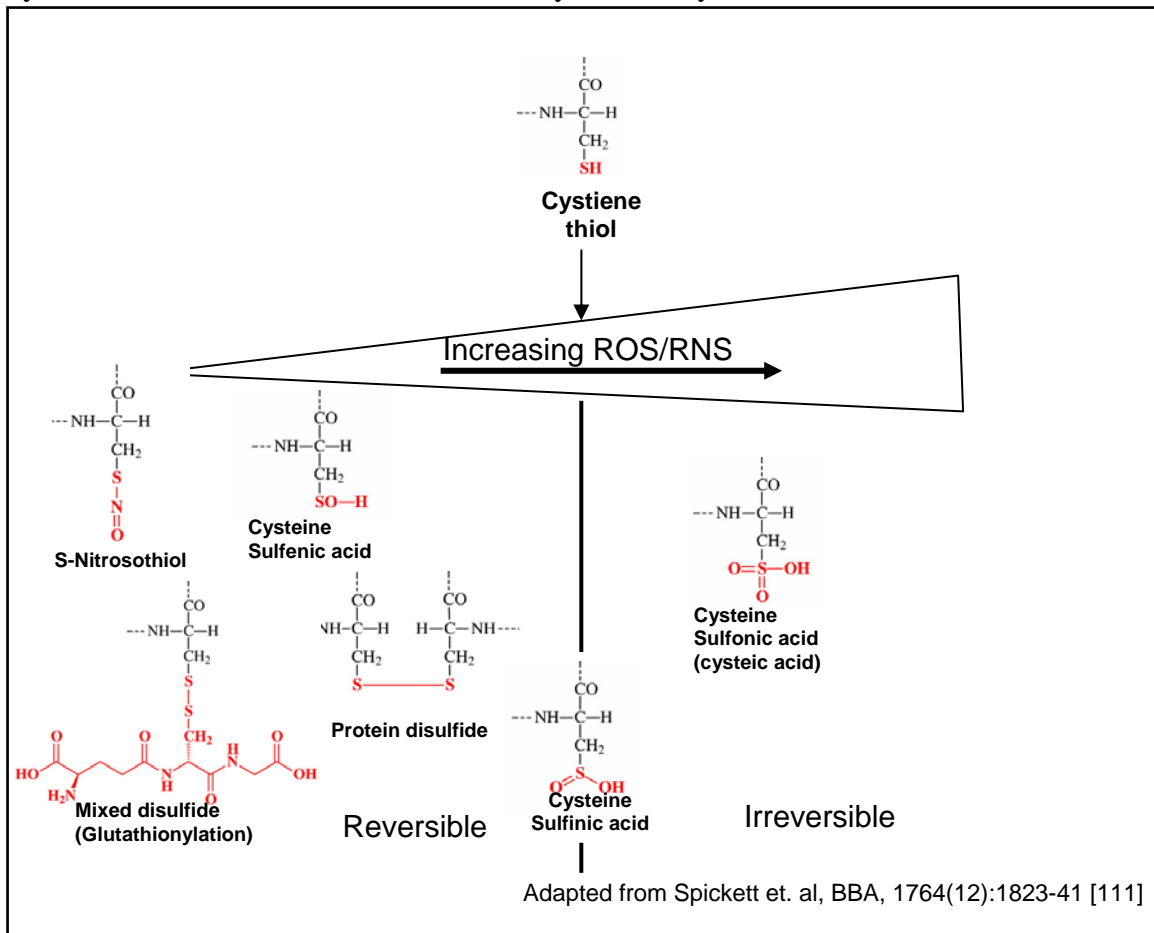
Figure 1.3: Cysteine Modifications:
Reversible and irreversible cysteine modifications resulting from oxidative/nitrative
stress

However, modifications which are not readily reversible upon the re-

establishment of normal glutathione levels could prevent the reactivation of enzymes or

15

alter protein-protein interactions, thereby preventing proper localization or regulation. This has been suggested by experimental results showing altered activity of GAPDH in erythrocytes treated with ferric protoporphyrin IX [88]. Tyrosine phosphorylation of the anion transporter protein Band 3 prevents the binding of GAPDH to the erythrocyte membrane and subsequent GAPDH inactivation; however, ferric protoporphyrin IX inhibits GAPDH-Band 3 association even in the presence of staurosporine (and presumably, phosphorylation of Band 3). It is possible that tyrosine nitration of Band 3 could mimic tyrosine phosphorylation and disrupt GAPDH binding, leading to an increase in erythrocyte GAPDH activity. Alternately, it is possible that oxidative modification (including tyrosine nitration) of GAPDH could affect the Band 3-GAPDH binding domain. These possibilities are supported by the finding that antioxidant treatment prevents stimulation of GAPDH activity in erythrocytes treated with ferric protoporphyrin IX [88]. However, since nitration of Band 3 or modification of Band 3 binding sites of GAPDH would not involve the catalytic site of GAPDH, it is conceivable that neither would alter the results of an *in vitro* enzyme assay, in spite of having measurable consequences upon erythrocyte metabolic function by allowing unsequestered GAPDH to remain active in the cytoplasm.

Given the importance of I/R of skeletal muscle in the clinical setting and the basic laboratory data concerning age-related changes in skeletal muscle, we undertook a series of experiments to examine the contribution of tyrosine nitration and oxidative stress to I/R injury of glycolytic skeletal muscle, including an examination into the impact of aging on tyrosine nitration and oxidative stress in I/R injury. Further, GAPDH has been

16

reported to be a target for oxidative modification in skeletal muscle in a number of

different physiological and pathological states [60,92,93]. Recent studies have

highlighted the realization that GAPDH is a multi-functional protein, with roles as

diverse as initiating apoptosis [41], enhancing neurite growth [78], contributing to the

regulation of glucose uptake[131], linking transcription to cell redox status [133], and

reactivating DNA repair enzyme APE-1 [4]. As GAPDH has been found to be a target

for tyrosine nitration in a number of different situations outside of I/R injury

[59,60,102,116] and has been shown to possess multiple cellular functions in addition to

its canonical role in glycolysis, we concluded that GAPDH would be an important

molecule for investigation.

Chapter 2: Glyceraldehyde-3-Phosphate Dehydrogenase in Young and Old Glycolytic Skeletal Muscle Following Ischemia/Reperfusion Injury

SUMMARY

We undertook a series of proteomics experiments to test our hypothesis that protein expression is altered in glycolytic skeletal muscle of young and aged mice after ischemia/reperfusion (I/R) injury. To address this hypothesis, protein expression was examined in glycolytic skeletal muscle of young and aged mice after I/R injury. We identified proteins whose expression was altered following I/R injury via preliminary experiments (data not shown) using two dimensional gel electrophoresis and MALDI-TOF mass spectrometry. One of these proteins is the glycolytic enzyme glyceraldehyde-3-phosphate dehydrogenase (GAPDH). A decrease in GAPDH pool levels was verified via one dimensional gel electrophoresis and Western blotting in both young and old mouse plantaris/flexor hallicus longus muscle lysate. Furthermore, a time course analysis revealed differences in the timing of GAPDH pool level changes between young and aged muscles. These studies confirm our hypothesis that protein expression is altered following I/R injury and that age influences the protein expression pattern for some proteins following I/R.

INTRODUCTION

Ischemic injury to rat skeletal muscle of only 2 hours duration and subsequent reperfusion is known to result in decreased specific force production of the *triceps surae* muscle group [40]. It has further been reported that the decrease in specific force production is greater and the recovery delayed for old rats. The ischemic muscle is also

atrophied compared to the uninjured contralateral muscle of the same animal [40], perhaps suggesting decreased protein content. Ischemia/reperfusion (I/R) injury is also known to increase oxidative stress, both in skeletal muscle and in other tissues [17,46], potentially leading to increased protein degradation due to oxidative protein modification [57]. However, insulin-like growth factor-1 (IGF-1) expression is reported to be increased following several forms of muscle injury, including I/R injury [40,81,115,132]. IGF-1 is known to be involved in protein synthesis at transcriptional [55] and translational levels [99]. These findings suggest that the levels of many proteins are likely altered following I/R injury, either due to increased synthesis or due to degradation induced by oxidative modification. We hypothesized that oxidative protein modification or altered protein synthesis would result in changes in protein expression, which could explain the observed phenotype of decreased specific force production and atrophy. Further, as the literature suggests a chronic state of oxidative stress develops during aging [48,49,71], we hypothesized that protein expression in the aged would be altered to a greater degree or with different temporal characteristics, correlating with the increased reductions in specific force and atrophy observed in aged mice after I/R injury.

EXPERIMENTAL PROCEDURES

Animals: C57Bl/6 mice were used in these experiments. The young mice were 6-7 months old, and the old mice were 24-27 months old. Prior to utilization in experiments, the mice were acclimatized to their new surroundings for one week. Upon completion of the experiments, animals were euthanized using sodium pentabarbitol. For one-dimensional gel electrophoresis and Western blots, 3 animals were used per time

point, with the exception of the young at 1 day, which had 2 animals. Plantaris and flexor hallicus longus muscles were collected for the one dimensional gels.   Time points examined for young and old were 2 hours of ischemia followed by either 1, 3, 5, or 7 days of reperfusion.   For the young mice, an additional time point with 2 hours of ischemia and no reperfusion was also examined. For RNA extraction and PCR analysis, plantaris muscle from 6 young animals and 3 old animals was collected after 2 hours of ischemia followed by 5 days of reperfusion.

Ischemia/Reperfusion Protocol: Tourniquet-induced ischemia/reperfusion was performed in the lab of Dr. Roger Farrar at UT-Austin as previously described [40]. Anesthesia was induced and maintained using 2% isofluorane.   One of the animal's hindlimbs was selected at random.   The tourniquet (Hokanson) was placed on the proximal thigh and inflated to 250 mm Hg by using the Portable Tourniquet System (New Delphi Medical Innovations). A heat lamp was used to maintain the animal's body temperature during the tourniquet procedure. After 2 hours, the tourniquet was removed, and the animal returned to its cage to recover.   After the appropriate length of reperfusion, the muscles were taken, snap frozen in liquid nitrogen, and shipped on dry ice to our laboratory. The samples were stored at -80^oC until analysis.

Protein Extraction: Flexor hallicus longus and plantaris muscles were homogenized together in 2D lysis buffer (8 M urea, 4% CHAPS, 40 mM DTT, protease inhibitors) using the Ettan Sample grinding kit (Amersham BioSciences), according to manufacturer's instructions.   Briefly, the samples were homogenized in the sample grinding tube with abrasive resin by using the provided plastic pestles. The samples were centrifuged at 5 minutes at 10,000g to pellet the resin and debris.   Supernatant was

removed to a fresh tube. Additional 2D lysis buffer was added, and the previous steps repeated to maximize yield. Supernatants were combined.

Protein Assays: Bradford protein assays (BioRad) were used to measure protein concentrations, using bovine serum albumin as a protein standard. The Bradford assays were performed in triplicate after the sample was homogenized, and the average value used. The results of this assay were used to dilute all samples to an equal concentration. The samples were then aliquoted and frozen at -80° C. Prior to gel loading, protein concentrations for each sample were measured once via Bradford assay, and any variations were taken into account before the samples were mixed with loading buffer.

One Dimensional Gel Electrophoresis: Thirty micrograms of sample protein was mixed with 5X Laemli loading buffer (10% SDS, 500 mM DTT, 300 mM Tris, 50% glycerol, 0.05% bromophenol blue, pH 6.8) and brought up to 25 µL with additional 2D lysis buffer. Samples were separated on a 4-20% tris-glycine gradient gel (Bio-Rad) at 135 volts for 2 hours in SDS running buffer (25 mM Tris base, 0.1% SDS (w/v), 192 mM glycine).   Immobilon PVDF membranes (Millipore) were prepared by wetting the membrane for 15 seconds in methanol, equilibrating the membrane in distilled water for 2 minutes, and then equilibrating the membrane in transfer buffer (25 mM Tris base, 10% methanol (v/v), 192 mM glycine) for 5 minutes. Gel transfer was performed in a Hoeffer wire transfer tank at 50 volts for 2 hours at 4^oC.

Western Blotting: Membranes were blocked for one hour with 5% non-fat dried milk (NFDM) in tris-buffered saline/Tween-20 (TBS-T): 49.5 mM tris, 200 mM NaCl, 0.05% Tween-20, pH 7.4. Membranes were then incubated for 1 hour with GAPDH

antibody (clone CA6, Santa Cruz) diluted 1:5000 in 5% non-fat dried milk/ TBS-T, while on an oscillating platform shaker at room temperature. Membranes were washed 3 times for 5 minutes per wash in TBS-T and incubated with anti-mouse secondary antibody (Amersham) for 1 hour at room temperature on an oscillating platform shaker.   The membrane was washed twice for 5 minutes and once for 15 minutes in TBS-T. The blot was then incubated in substrate (Immobilon, Millipore; or Lumiglo, Kirkegaard & Perry Laboratories) on parafilm for 5 minutes. Excess substrate was blotted off the underside of the membrane using chromatography paper (Whatmann). The membranes were placed into a transparent plastic cover.   Film (Biomax MR, Kodak) was exposed to the membranes in a dark room and developed on an SRX-101A developer (Konica Minolta).

Membranes previously used for anti-nitrotyrosine blots were stripped for 30 minutes at room temperature and 30 minutes at 37° C using Restore Western Blot Stripping Buffer (Pierce). Blots were washed twice in TBS-T and blocked for 1 hour in 5% NFDM. Blots were then probed with anti-mouse antibody (Amersham, 1:12,500) for 1 hour to insure complete removal of anti-nitrotyrosine antibody.

Protein Normalization: After one-dimensional gel electrophoresis and transfer to PVDF membranes, the post-transfer gels used for each membrane were stained in Imperial Protein stain (Pierce, USA).   After destaining in water, the gels were photographed using the FluorChem 8900 system (AlphaInnotech). Using the FluorChem 8900 spot densitometry analysis software, a rectangular area of equal size (approximately 25% of the width of a well) was examined for each well. The analysis area extended from approximately 250 kD to <6kD. The stained density of each individual lane of the gel was calculated. Automatic background subtraction was used in the analysis.   Each gel was normalized independently of the others. A ratio of the density of an individual

lane divided by the most dense lane in that gel was calculated. The lane with the highest density was assigned 100% of the appropriate density for the amount of protein loaded. Other lanes were expressed as a percentage of this maximal value. The percent was converted to decimal form, and the reciprocal of the decimal was multiplied by the densities generated by Western blots for GAPDH to normalize for decreased amounts of full-length protein in the I/R samples.

A correction factor was also applied between gels of the same age group for measuring GAPDH pool levels, as the samples for the entire time course were too numerous to allow separation on the same gel. This was done by including 4 samples from the first gel in the second gel (see appendix for images of the Coomassie-stained gels). The last 4 lanes of each gel were loaded with repeated samples, which were not shown in the "Results" section, as they were used for standardization and not analyzed as data. A ratio was taken between the density of the 37 kD GAPDH immunoreactivity in the first and second gels. The average of the ratios was used as a correction factor to adjust the density values of the other samples.

RNA Extraction: Total RNA extraction was accomplished using the RNAqueous-4PCR kit (Applied Biosystems), according to manufacturer's instructions. Plantaris muscle was collected from young (n=6) and old (n=3) mice which had been subjected to 2 hours of ischemia and 5 days of reperfusion. The muscle was snap-frozen in liquid nitrogen after collection and stored at -80° C until use. The plantaris was cut in half on dry ice using a razor blade, and one half of the muscle was transferred to a microfuge tube and homogenized by hand into the lysis/binding solution supplied with the kit using a plastic pestle. An equal volume of 64% ethanol was added to the solution and mixed. This mixture was pipetted into a tube containing a filter cartridge from the

kit. The cartridge and solution were centrifuged at 15,000 g for 1 minute. Wash solution #1 was added to the retentate, and the tube was centrifuged as in the previous step. The previous wash and centrifugation was repeated twice using wash solution #2/3. The filter cartridge was then placed into a new tube, and elution buffer which had been warmed to 70-80° C was added. The cartridge and tube were centrifuged at 15,000 g for 1 minute. Another volume of heated elution buffer was added, and the cartridge was centrifuged again. Finally, the cartridge was removed and the total filtrate was centrifuged again. The supernatant was removed to a fresh tube, leaving any glass fibers from the cartridge in the pellet. Residual amounts of DNA were removed by treating the samples with DNase 1 provided in the RNAqueous kit. The samples were incubated at 37°C for 20 minutes, and DNase inactivation reagent was added. The samples were then gently vortexed and incubated with the inactivation reagent for 2 minutes. The samples were then centrifuged at 10,000g for 1 minute and the supernatant removed to fresh tubes.

To ascertain the quality of the extracted mRNA, the RNA 6000 Nano Assay kit (Agilent Technologies) was used according to manufacturer's instructions, in conjunction with the Agilent 2100 bioanalyzer. This chip-based capillary gel electrophoresis unit utilizes a proprietary dye-based reagent that binds to nucleic acids for detection and quantitation of ribosomal RNA.

cDNA synthesis: Synthesis of cDNA was done using the SuperScript First-Strand Synthesis System for RT-PCR (Invitrogen) according to manufacturer's instructions. For each sample, an equal volume (8 µl) of DNAase-treated total RNA, 1 µl of 10 mM dNTP mix, and 1 µl of 0.5 µg/ µl oligo(dT)$_{12-18}$ was added to one well of a PCR reaction plate. A 2X reaction mixture was prepared which contained the following: 2 µl of 10X reaction buffer, 4 µl of 25 mM MgCl$_2$, 2 µl of 0.1M DTT, and 1 µl

RNaseOUT (provided in the kit). The RNA/primer mix was incubated at 65°C for 5 minutes using an Applied Biosystems GeneAmp 9700. The mixture was then placed on ice for 1 minute. Nine µl of the 2X reaction mixture was added to each reaction and mixed by pipetting. The reaction was incubated at 42°C for 2 minutes in the Applied Biosystems GeneAmp 9700 prior to the addition of 1 µl of SuperScript II reverse transcriptase to each reaction (with the exception that no reverse transcriptase was added to the negative control). The reaction plate was incubated at 42°C for 50 minutes in the GeneAmp 9700; subsequently, the temperature was increased to 70°C for 15 minutes to terminate the reaction. The reaction plate was chilled on ice for 5 minutes. To each well, 1 µl of RNase H was added; the plate was incubated at $37\,^{o}$C for 20 minutes.

PCR: PCR was performed using a Taq polymerase-based fluorogenic assay and primers specific for GAPDH mRNA (Primetime qPCR, Integrated DNA Technologies). Primer sequences used were: 5'-AATCTCCACTTTGCCACTG-3' and 5'-CCTCGTCCCGTAGACAAAA-3'. Reactions were performed using the iCycler (Biorad). Protocol was as follows: One period of 1.5 minutes at $95.0^{o}\,$C, followed by 50 cycles of 0.5 minutes at $95.0^{o}\,$C, 0.5 minutes at $55.0\,^{o}\,$C, and 0.5 minutes at $70.0\,^{o}\,$C.

Statistical Analysis: The developed films from Western blots were photographed using the FluorChem 8900 system (AlphaInnotech). Using the FluorChem 8900 spot densitometry analysis software, a rectangular area was selected which encompassed the region of interest. Selections for each lane were of equal area. The imaging software's automatic background subtraction was used; the density of immunostaining for each band was examined. After normalization, statistical analysis was performed similarly to Hsieh *et al.* [48,50]. Welch's modified version of the paired Student's t-test was used to

compare means between control and ischemic of each time point or between the difference in average response between young and old (within each time point). Welch's modified version of the student t-test does not require that the sample variances be equal. Graphs represent the average of individual values (for example, the average GAPDH immunoreactivity of young controls versus the average of young I/R samples, at one day reperfusion). Error bars represent the standard deviation.

RESULTS

Ischemia leads to the stabilization and subsequent increases in pool level of hypoxia-inducible factor-α (HIF-1α) in most tissues, driving an increase in vascular endothelial growth factor expression and a switch to increased glycolytic metabolism [105,108]. However, whether the stimulation of glycolysis by HIF-1α in skeletal muscle in response to ischemia leads to an increase in GAPDH protein expression during reperfusion is not well-described, as the response of skeletal muscle to ischemia may not be equivalent to the response to hypoxia alone [26]. Further, it has been observed that glycolytic muscle mass is decreased following I/R injury [40], particularly in muscle of the old rats, suggesting decreased protein content. The same study also observed that the maximal force production after I/R injury was decreased, and that the decrease was greater for old muscle. It is possible that the decreased force production is related to decreased expression of contractile proteins or to a decreased expression of glycolytic proteins.

The protein pool levels of GAPDH were assayed by Western blotting for mouse glycolytic skeletal muscle that had been subjected to I/R injury. Prior to any normalization of the Western blot data, the comparison of GAPDH protein levels

26

between young control and ischemic muscle showed no statistically significant difference after 2 hours ischemia with no reperfusion, after 1 day reperfusion, or after 7 days reperfusion. At the 3 and 5 day time points, the GAPDH protein levels were significantly decreased in the I/R tissue, with an average decrease of 89.4% (p=.0004) at 3 days and 71.4% (p=.007) at 5 days.
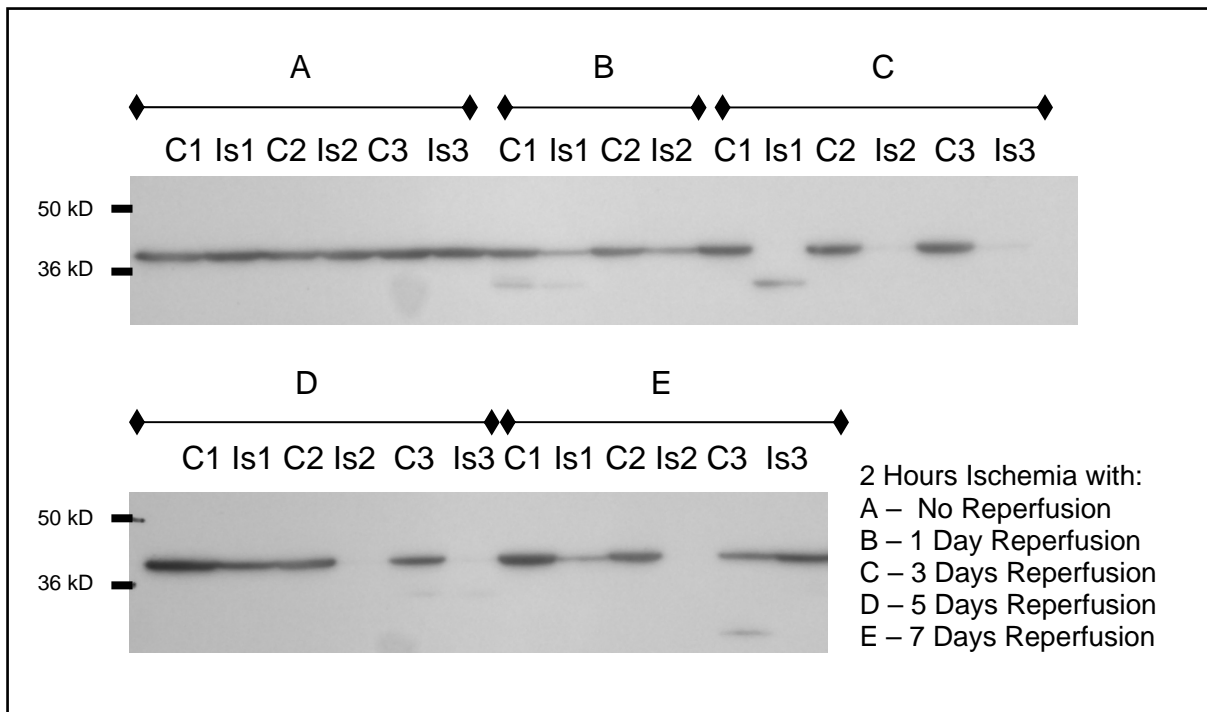
Figure 2.1: GAPDH Pool Levels In Plantaris/FHL Lysate from Young Mice:
Thirty µg of protein from total cell lysate was separated by SDS-PAGE, transferred to PVDF membrane, and blotted with anti-GAPDH antibody. Group A showed no significant difference. Group B was decreased, but not significantly. Group C and Group D showed significant reduction in GAPDH immunoreactivity (p=.0004 and p=.007, respectively). The decrease was not significant for group E.

The no reperfusion time point was not available for the old animals; however, the GAPDH protein levels were significantly decreased at 1 day (61.9%, p= .0005), 3 days

(83.1%, p=.014), 5 days (83.3%, p= .007), and 7 days (73.8%, p= .013) of reperfusion in the muscle samples from the old.
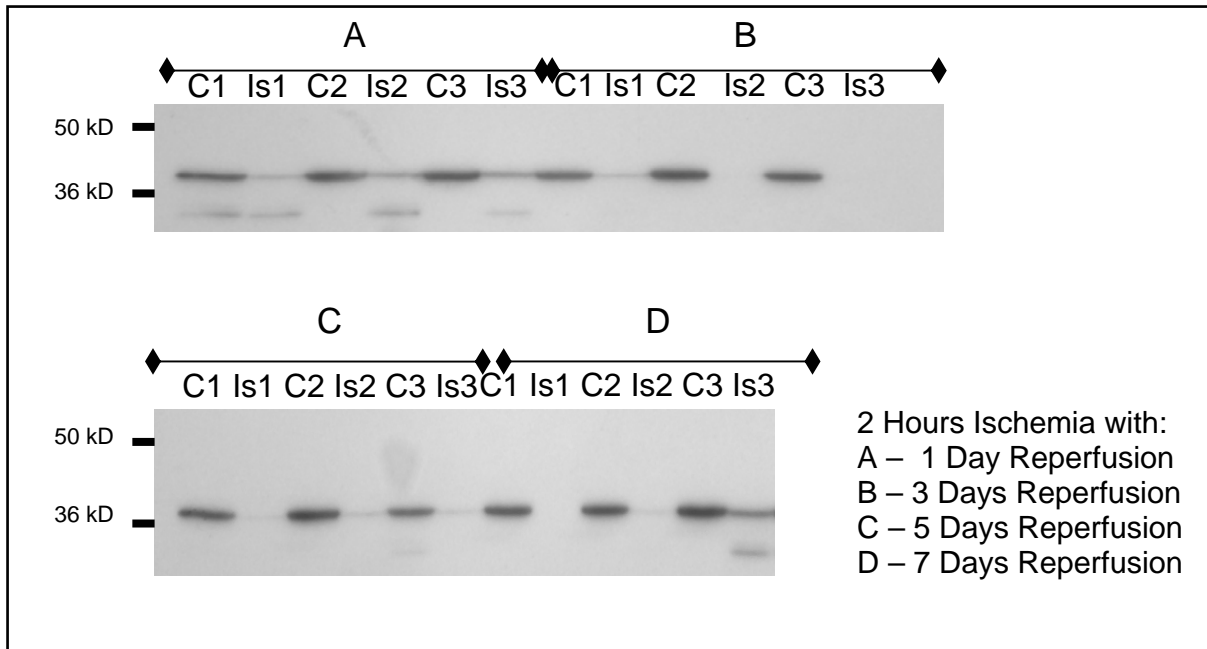
Figure 2.2: GAPDH Pool Levels In Plantaris/FHL Lysate from Old Mice:
Thirty μg of protein from total cell lysate was separated by SDS-PAGE, transferred to PVDF membrane, and blotted with anti-GAPDH. All groups showed statistically significant decreases in GAPDH immunoreactivity.

Although statistically significant differences in GAPDH pool level were seen at several time points in both age groups, one confounding variable in the data was the question of protein degradation in the ischemic muscle, related to the I/R injury. An examination of the post-transfer gels after Coomassie staining revealed an increase in low molecular weight bands (< 16 kD) in the ischemic samples after reperfusion (Figure 2.3). Further, comparison of the total protein staining of the one-dimensional gel

electrophoresis revealed that the average decrease over all days of reperfusion in the young was 16.2% (p= .003 compared to young control).
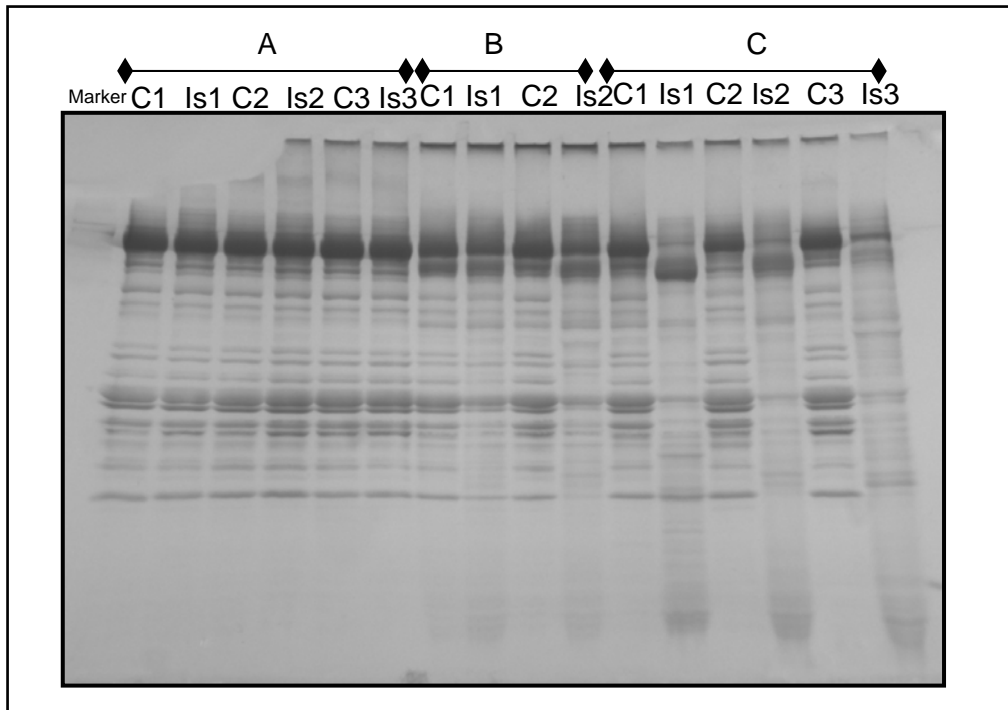
Figure 2.3: Post-transfer Gel Stained with Coomassie for Plantaris/FHL Lysate from Young Mice:
 Total Protein was normalized based upon Bradford assay prior to gel loading. Samples from the group with 2 hours of ischemia but no reperfusion show equal loading. Samples with 2 hours of ischemia and 1 or 3 days reperfusion time show increased low molecular weight staining. (A) No reperfusion; (B) 1 Day Reperfusion; (C) 3 Days Reperfusion; Staining suggests increased protein degradation in the I/R samples compared to contralateral control muscle.

In the old muscle, there was a 16.6% decrease compared to old controls (p< .0001) in staining in the ischemic samples after reperfusion when considered in aggregate, in spite of balancing protein input prior to loading of the gels. Significantly, the samples from the young animals which had been received 2 hours of ischemia but no

reperfusion showed no statistically significant differences in protein loading between control and ischemic muscle. In order to correct for differences in the amount of protein actually present in the gel, a normalization factor based on the Coomassie staining of the post-transfer gels was used.

After normalizing for background levels of protein degradation, the pool level of GAPDH in glycolytic skeletal muscle from young mice was still significantly decreased at 3 and 5 days of reperfusion (p=.001 and .005 respectively), with no significant alterations at 2 hours of ischemia without reperfusion, at 1 day of reperfusion, or at 7 days of reperfusion.
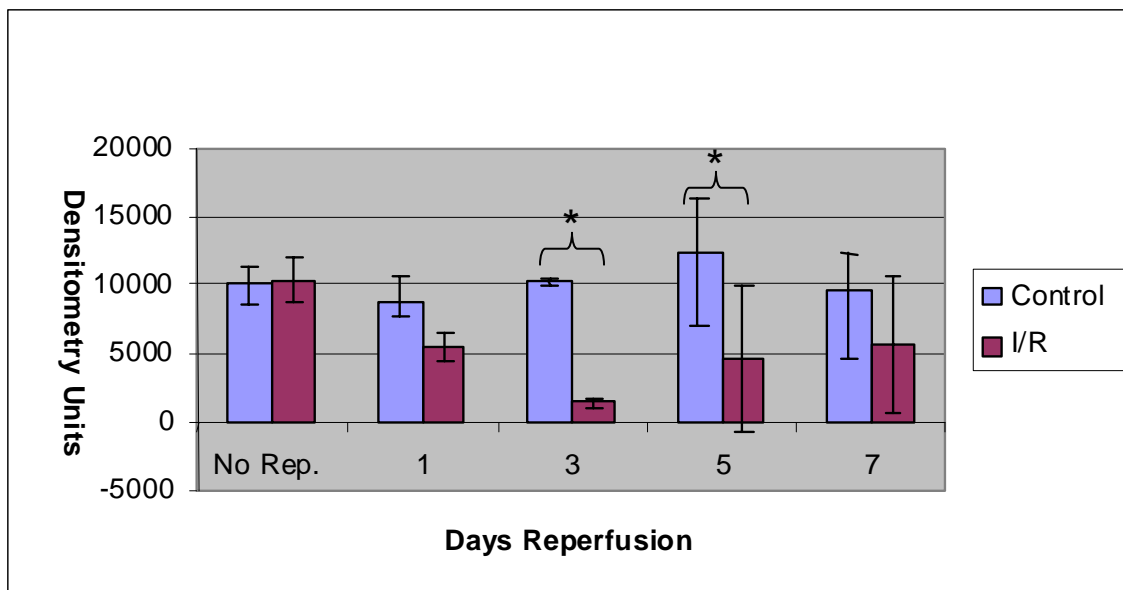
Figure 2.4: Average GAPDH Pool Levels for Plantaris/FHL Lysate from Young Mice, Normalized to Total Protein: * = p < .05 compared to control

After normalization for background protein degradation, the GAPDH protein pool levels in skeletal muscle from the old mice were still significantly decreased at 1, 3, 5, and 7 days reperfusion (p= .001, .015, .011, and .007, respectively).
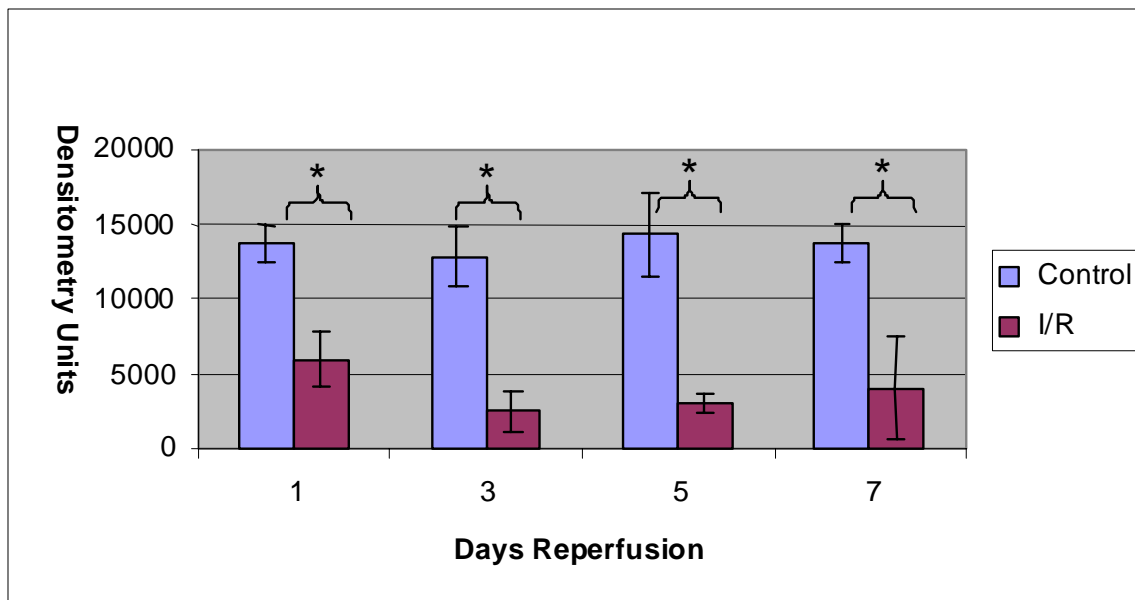
Figure 2.5: Average GAPDH Pool Levels for Plantaris/FHL Lysate from Old Mice, Normalized to Total Protein: * = p < .05 compared to control

We examined the possibility that altered GAPDH transcription may play a role in the decrease in GAPDH pool levels. Total RNA from plantaris muscle was isolated from young and old mice subjected to 2 hours of ischemia and 5 days of reperfusion. An equal percentage of total RNA from each sample was analyzed using a chip-based gel electrophoresis assay to determine the quality of isolated RNA.

Surprisingly, the yield of total RNA from the ischemic samples was substantially increased compared to the contralateral control, regardless of age. While both mRNA

and rRNA appeared to contribute to the increased total RNA, the bulk of the increase was from rRNA.
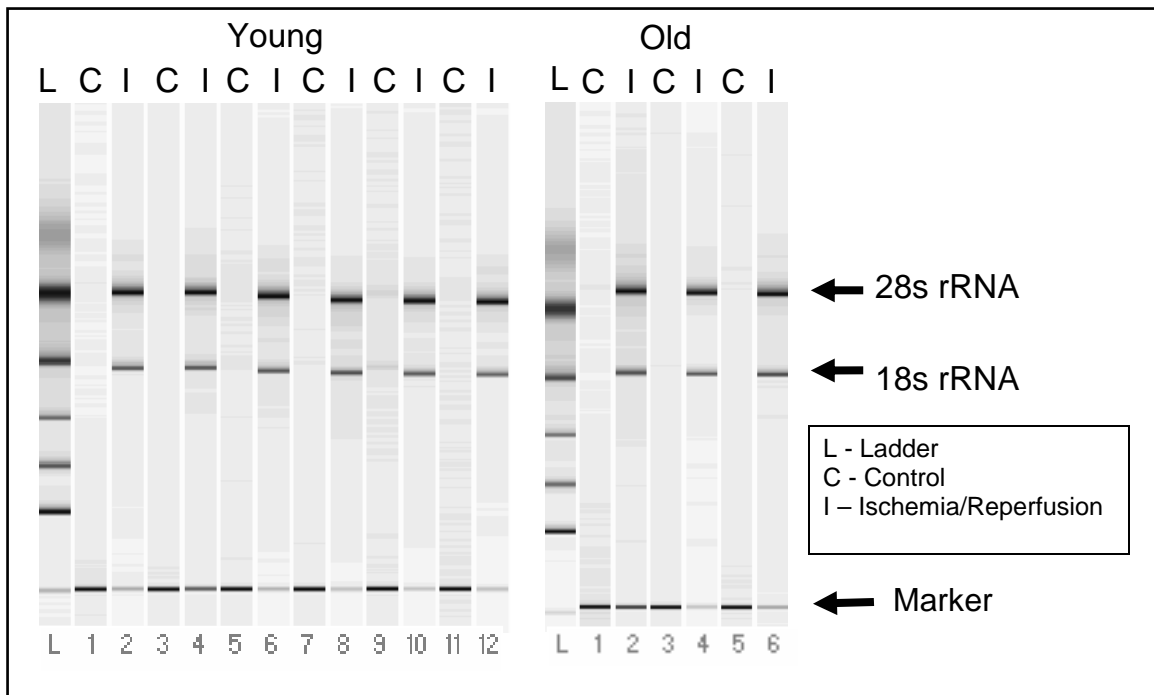
Figure 2.6: Pseudogel of Total RNA from Plantaris:
Equal Amount of Plantaris muscle, isolated in equal volume of regent, shows substantially increased yield of total RNA, especially rRNA, in the I/R samples. I - I/R and C - control (contralateral) limb, pair-wise, beginning with the lane following the ladder (L). Band intensity is autoscaled to the darkest band in each lane.

An equal percentage of total RNA from each sample was reverse transcribed using oligo(d)T to construct an mRNA-cDNA library. One µL of cDNA from each sample was analyzed by capillary gel electrophoresis. The cDNA yield from the ischemic samples was found to be increased compared to the controls in both young and old (Figures 2.7 and 2.8), suggesting that both mRNA and rRNA levels are increased following ischemia and 5 days of reperfusion.
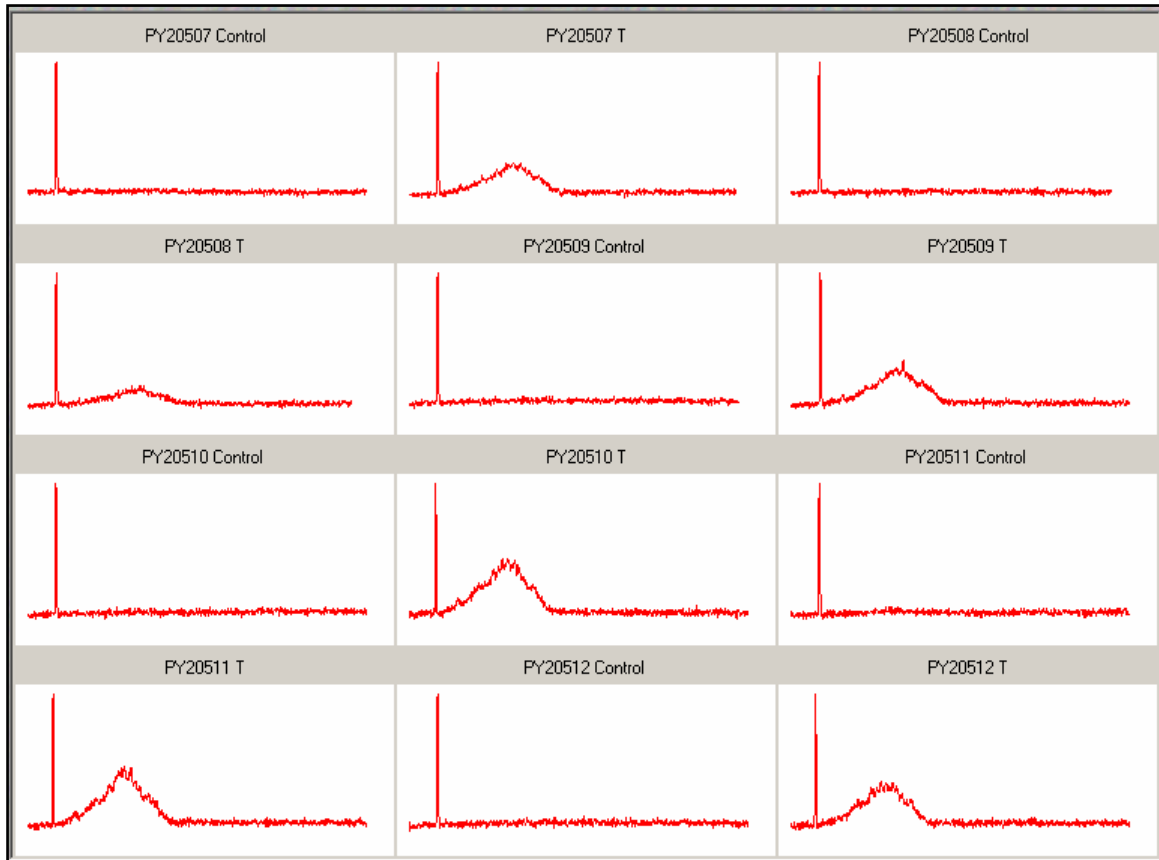
Figure 2.7: Analysis of cDNA from Young Control and I/R Plantaris Muscle Following 5 Days of Reperfusion:

An equal percentage of total cDNA (reverse transcribed from mRNA using oligo(d)T primers) was analyzed by capillary gel electrophoresis. The initial peak in each sample is an exogenous marker. Samples are paired from left to right, beginning with control. T = ischemia/reperfusion

GAPDH specific primers were used to perform PCR on an equal percent of the total cDNA. Significant differences were noticed in the number of cycles to threshold (Ct) between young ischemic and young controls, with an average difference of 6.2 cycles (p=.0009).
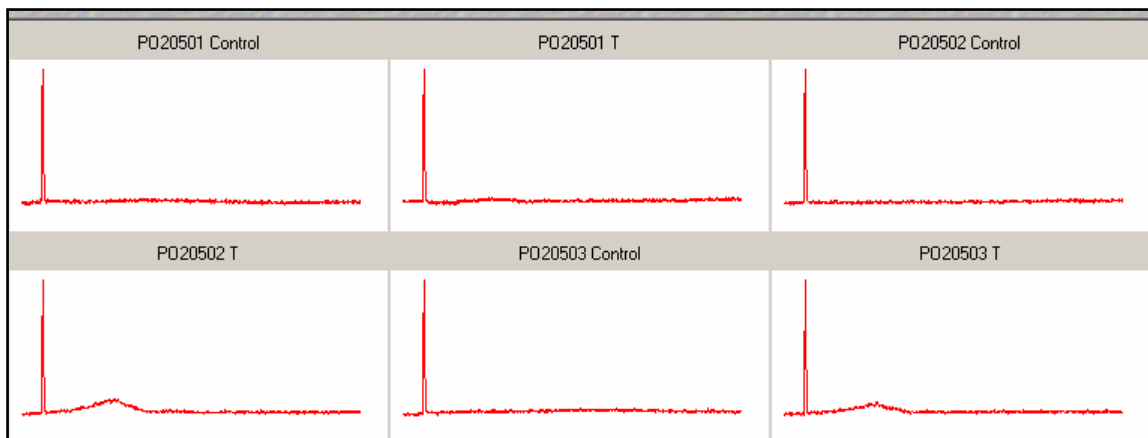
Figure 2.8: Analysis of cDNA from Old Control and I/R Plantaris Muscle Following 5 Days of Reperfusion:

An equal percentage of total cDNA (reverse transcribed from mRNA using oligo(d)T primers) was analyzed by capillary gel electrophoresis. The initial peak in each sample is an exogenous marker. Samples are paired from left to right, beginning with control. T = ischemia/reperfusion

The difference between the old controls and old ischemic was also significant (p=.049), with an average difference of 5.4 cycles. The difference in GAPDH transcript levels in response to I/R between the young and the old was not statistically significant; however, it does suggest that the average increase in GAPDH mRNA level in the young is nearly twice the increase in the old.

Chapter 3: Tyrosine Nitration in Glycolytic Skeletal Muscle Following Ischemia/Reperfusion Injury

SUMMARY

As nitric oxide and reactive oxygen species (ROS) are increased during the period of reperfusion following skeletal muscle ischemia [64], we hypothesized that proteins are subject to tyrosine nitration in the setting of ischemia/reperfusion (I/R) injury. The reaction of nitric oxide with superoxide to form peroxynitrite and the reaction of various heme peroxidases (especially myeloperoxidase from immune cells) with hydrogen peroxide and nitrite are believed to be the reactions leading to tyrosine nitration *in vivo* [90]. Considering either of these mechanisms, it is reasonable to hypothesize that the levels of tyrosine nitration will increase following I/R injury to skeletal muscle. In these studies, whole cell lysate from ischemic and non-ischemic skeletal muscle of young and old mice was separated by one-dimensional gel electrophoresis. Levels of protein-bound nitrotyrosine were compared by Western blot with antibody specific for nitrotyrosine. I/R samples were separated by two-dimensional gel electrophoresis, and proteins were selected for identification by mass spectrometry by comparing the gel to two-dimensional nitrotyrosine western blot. Glyceraldehyde-3-phosphate dehydrogenase, fructose bisphosphate aldolase, triosephosphate isomerase, and phosphoglycerate mutase were identified as nitrated proteins via this methodology from young and aged post-ischemic skeletal muscle from the 5 day reperfusion time point. Nitration of these proteins suggests that the glycolytic pathway is a target for tyrosine nitration in ischemia/reperfusion injury. It is expected that tyrosine nitration of these proteins would alter the degradation rate or function of glycolytic proteins following ischemia and

reperfusion. These experiments suggest that I/R leads to increases in protein tyrosine nitration for specific proteins.

INTRODUCTION

Oxidative protein modification is believed to play a role in age-related muscle loss and in skeletal muscle dysfunction in ischemia/reperfusion (I/R) injury [54,72]. While force production in glycolytic skeletal muscle is decreased after I/R injury in both young and old rats, the decrease in force production was greater in the muscle from old rats compared to the young at 7 and 14 days of recovery [40]. Old rats also show diminished upregulation of local IGF-1 mRNA levels compared to the young. However, it is not clear whether these data represent increased damage to the aged muscle in addition to a failure of muscle repair. As oxidative stress is believed to contribute to skeletal muscle dysfunction in aging and ischemia, we hypothesized that oxidative protein modification would increase in I/R injury and that it would increase to a greater extent in the aged muscle compared to the young, reflecting the role of oxidative protein modification in both conditions.

One form of oxidative protein modification is nitration of tyrosine. While tyrosine nitration has been well-documented as a marker for oxidative stress, it is also recognized that tyrosine nitration of proteins affects both the structure and function of the modified protein. Nitrotyrosine shifts the pK_a of the targeted region of the tyrosine ring structure by approximately 3 pH units [109]. Nitration of tyrosine can also increase the

hydrophobicity of digested peptides [9] and introduce steric and electrostatic alterations in protein structure [101].   Oxidative modification of proteins has also been shown to increase the rate of protein degradation [12,65], raising the question whether oxidative modification could play a role in the lower pool levels of GAPDH that we observed following I/R injury.

EXPERIMENTAL PROCEDURES

Animals: Aliquots of muscle lysate from the young and old animals used in the time course described in chapter 2 were used for these experiments. For one dimensional gels, 3 mice were used at each time point, with the exception that the one day reperfusion time point in the young was represented by 2 mice. For two dimensional gels, a representative sample from the 5 day time point was selected from the young and the old samples.

Protein Extraction and Protein Assays: Protein extraction and protein assays were performed as described in chapter 2.

Two Dimensional Gel Electrophoresis: One hundred eighty micrograms of sample isolated in 2D lysis buffer was mixed with Destreak reagent (GE –BioSciences) plus 0.75% IPG 4-7 pH IPG buffer. Samples were made up to 200 microliters with additional volumes of 2D lysis buffer. The sample was pippetted into an 11 cm Ettan IPGphor strip holder (Amersham Biosciences) and overlaid with an 11 cm Immobiline Drystrip 4-7 pH gel strip (GE Biosciences) with the backing strip of the gel uppermost. Immobiline DryStrip cover fluid (Amersham BioSciences) was pippetted over the strip

and sample to prevent evaporation, the cover placed on the holder, and the assembly rehydrated on an Ettan IPGphor isoelectric focusing system (Amersham Biosciences). Conditions used were as follows: 12 hours in-gel rehydration at 20°C, followed by 3 focusing steps – 500V for 1 hour, 1000V for 1 hour, and 8000V for 2 hours. A constant current of 50 μA/strip was maintained.

Strips were equilibrated for 15 minutes in SDS equilibration buffer (6 M urea, 29.3% glycerol (v/v), 2% SDS (w/v), .002% bromophenol blue (w/v), and 75 mM Tris-HCl pH 8.8). Immediately prior to equilibration, DTT (1% w/v) was added to the SDS equilibration buffer. The gel strip was then placed in the sample lane of a 10-20% Tris-HCl IPG +1 well, 1 mm Criterion gel (BioRad) and sealed with agarose sealing solution (25 mM tris, 192 mM glycine, 0.1% SDS (w/v), 0.5% agarose, 0.002% (w/v) bromophenol blue). After the agarose solidified (approximately 5 minutes at room temperature), the gels were placed in a Criterion running tank (BioRad), the tank filled with running buffer (25 mM Tris base, 0.1% SDS (w/v), and 192 mM glycine), and the sample separated at 135 volts for approximately 2 hours. The gel was transferred using a Criterion blotter system (BioRad) with conditions as described in Chapter 2 for transfer of 1D electrophoresis gels.

Normalization: Western blot data was normalized to account for generalized protein degradation due to the I/R injury. Normalization for total nitration was performed as described for GAPDH pool levels in chapter 2. For nitration of the 37 kD band, a ratio computed from the GADPH western blot was used to normalize for the amount of GAPDH present (rather than total protein).

The data were also normalized between the gels of the same age group by repeating samples in both gels. This normalization is the same as that discussed in more

detail in the methods of Chapter 2, with the exception that the ratio was based on total nitration of the repeated samples rather than GAPDH immunoreactivity (as in Chapter 2).

Western Blotting: Western blotting was done as described previously, with the modifications described hereafter. Membranes were incubated overnight at 4° C in anti-nitrotyrosine antibody (Abcam) diluted 1:2000 in 5% non-fat dried milk/ TBS-T. Membranes were incubated with anti-mouse secondary antibody diluted 1:12500 (Amersham).

Sample Preparation for Mass Spectrometry: Preparation of samples for mass spectrometry and mass spectrometry analysis were performed by the Mass Spectrometry Core at University of Texas Medical Branch Galveston. Gel samples were cut into 1mm size pieces or smaller and placed into separate 0.5mL polypropylene tubes. 100μl of 50mM ammonium bicarbonate buffer was added to each tube and the samples were then incubated at 37°C for 30min. After incubation, the buffer was removed and 100μl of water was added to each tube. The samples were then incubated again at 37°C for 30min. After incubation, the water was removed and 100μl of acetonitrile was added to each tube to dehydrate the gel pieces. The samples were vortexed, and after 5min the acetonitrile was removed. 100μl of acetonitrile was again added to each of the sample tubes, vortexed, and acetonitrile removed after 5 minutes. The samples were then placed in a speedvac for 45 minutes to remove any excess solvent.

A 25mM ammonium bicarbonate solution was prepared at pH 8.0. To a 20μg vial of lyophilized trypsin (Promega Corporation) was added 2mL of 25mM ammonium

bicarbonate. The trypsin solution was then vortexed. Trypsin solution was added to each sample tube in an amount (approximately 10μL) to just cover the dried gel. The samples were then incubated at 37°C for 6hrs.

After digestion, the samples were removed from the oven and 1 μL of sample solution was spotted directly onto a MALDI target plate and allowed to dry. 1 μL of alpha-cyano-4-hydroxycinnamic acid (Aldrich Chemical Co.) matrix solution (50:50 acetonitrile/water at 5 mg/mL) was then applied on the sample spot and allowed to dry. The dried MALDI spot was blown with compressed air (Decon Laboratories, Inc.) before inserting into the mass spectrometer.

Mass Spectrometry

Matrix-Assisted Laser Desorption Ionization Time-of-Flight Mass Spectrometry (MALDI TOF-MS) was used to analyze the samples and determine protein identification. Data were acquired with an Applied Biosystems 4800 MALDI TOF/TOF Proteomics Analyzer. Applied Biosystems software package included 4000 Series Explorer (v. 3.6 RC1) with Oracle Database Schema Version (v. 3.19.0), Data Version (3.80.0) to acquire both MS and MS/MS spectral data. The instrument was operated in positive ion reflectron mode, mass range was 850 – 3000 Da, and the focus mass was set at 1700 Da. For MS data, 1000-2000 laser shots were acquired and averaged from each sample spot. Automatic external calibration was performed using a peptide mixture with reference masses 904.468, 1296.685, 1570.677, and 2465.199.

Following MALDI MS analysis, MALDI MS/MS was performed on several (5-10) abundant ions from each sample spot. A 1kV positive ion MS/MS method was used to acquire data under post-source decay (PSD) conditions. The instrument precursor selection window was +/- 3 Da. For MS/MS data, 2000 laser shots were acquired and averaged from each sample spot. Automatic external calibration was performed using reference fragment masses 175.120, 480.257, 684.347, 1056.475, and 1441.635 (from precursor mass 1570.700).

Applied Biosystems GPS Explorer[TM] (v. 3.6) software was used in conjunction with MASCOT to search the respective protein database using both MS and MS/MS spectral data for protein identification. Protein match probabilities were determined using expectation values and/or MASCOT protein scores. MS peak filtering included the following parameters: mass range 800 Da to 4000 Da, minimum S/N filter = 10, mass exclusion list tolerance = 0.5 Da, and mass exclusion list (for some trypsin and keratin-containing compounds) included masses 842.51, 870.45, 1045.56, 1179.60, 1277.71, 1475.79, and 2211.1. For MS/MS peak filtering, the minimum S/N filter = 10.

For protein identification, the murine taxonomy was searched in either the SwissProtein database. Other parameters included the following: selecting the enzyme as trypsin; maximum missed cleavages = 1; fixed modifications included carbamidomethyl (C) for 2-D gel analyses only; variable modifications included oxidation (M); precursor tolerance was set at 0.2 Da; MS/MS fragment tolerance was set at 0.3 Da; mass = monoisotopic; and peptide charges were only considered as +1. The significance of a protein match, based on both the peptide mass fingerprint (PMF) in the

first MS and the MS/MS data from several precursor ions, is based on expectation values; each protein match is accompanied by an expectation value. The expectation value is the number of matches with equal or better scores that are expected to occur by chance alone. The default significance threshold is p<0.05, so an expectation value of 0.05 is considered to be on this threshold. We used a more stringent threshold of 10^{-3} for protein identification; the lower the expectation value, the more significant the score.

Statistical Analysis: The statistical analysis was performed as described in Chapter 2.

RESULTS

Previous studies have shown functional impairment of glycolytic skeletal muscle following I/R injury [40]. Oxidative modification of proteins critical for muscle function is a possible mechanism explaining the decline in muscle force production. As levels of reactants necessary to form nitrotyrosine are known to increase during the reperfusion stage of I/R injury, we tested the hypothesis that protein-bound tyrosine nitration would increase following reperfusion. Relative levels of protein tyrosine nitration were assayed in skeletal muscle extract from young and old mice following ischemia and reperfusion by one-dimensional gel electrophoresis and Western blotting with antibody specific for nitrotyrosine. The corresponding contralateral muscles were used as a control for the basal level of nitration.
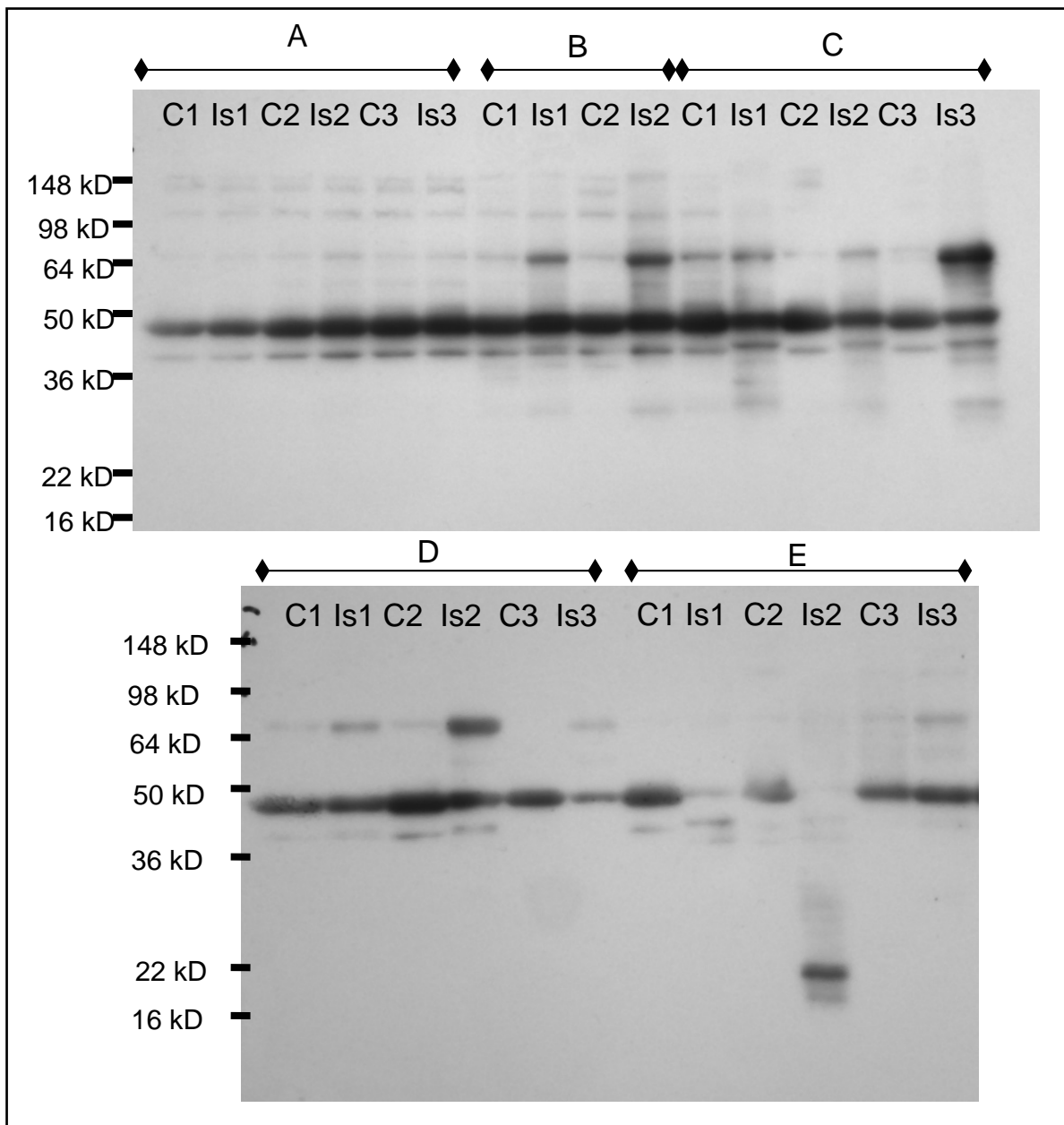
Figure 3.1: Total Tyrosine Nitration of Plantaris/ *FHL* Lysate from Young Mice Following I/R:

Tyrosine nitration of whole cell lysate of glycolytic skeletal muscle from young mice with 2 hours ischemia and variable lengths of reperfusion was examined by Western blot. No statistically significant differences were seen. C = contralateral control Is = I/R; Group A = no reperfusion, B = 1 day reperfusion, Group C = 3 days reperfusion, Group D = 5 days reperfusion, and Group E = 7 days reperfusion

Following normalization for background protein degradation (see previous chapter's methods), there were no statistically significant differences in total nitrotyrosine for the young, although nitration was increased at every time point following reperfusion (range 22% to 67% increase).
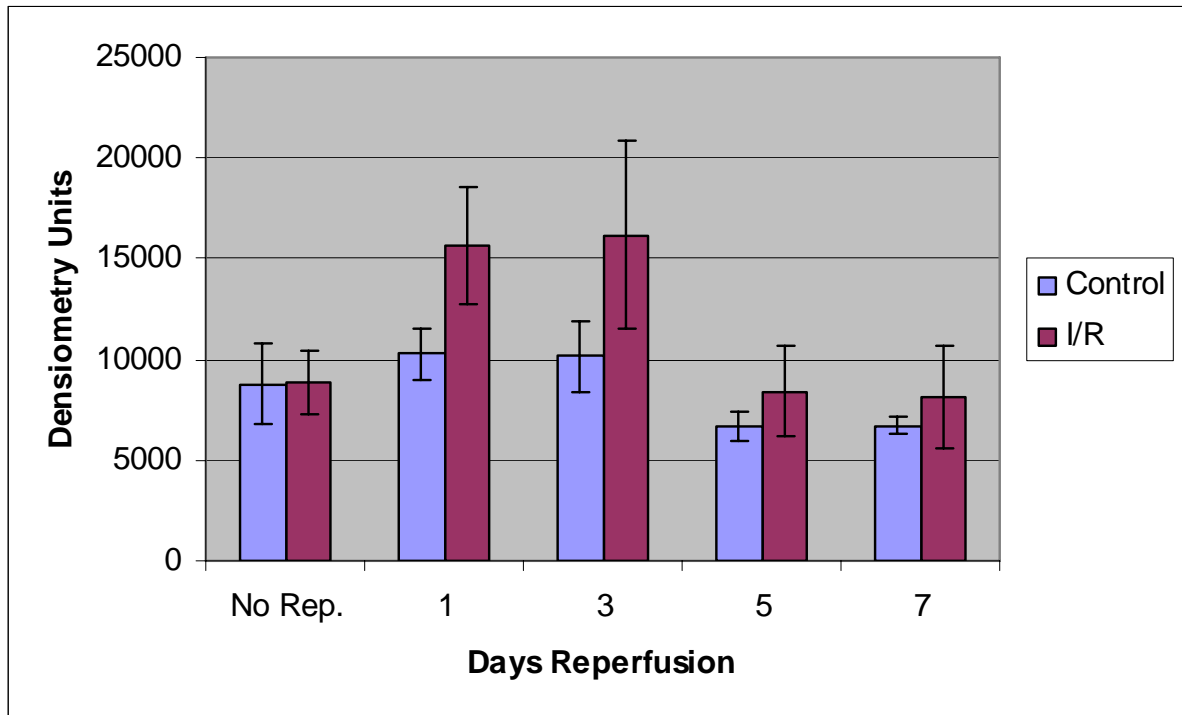
Figure 3.2: Average Total Nitrotyrosine in Plantaris/FHL Lysate from Young Mice Following I/R

In contrast to the young, an analysis of total tyrosine nitration in whole cell lysates of old skeletal muscle following I/R revealed statistically significant increases at the 1, 3, and 5 day time points (p = 0.008, 0.048 and 0.03, respectively). Total nitration was increased at all time points, but the increase was not significant at the 7 day time point.
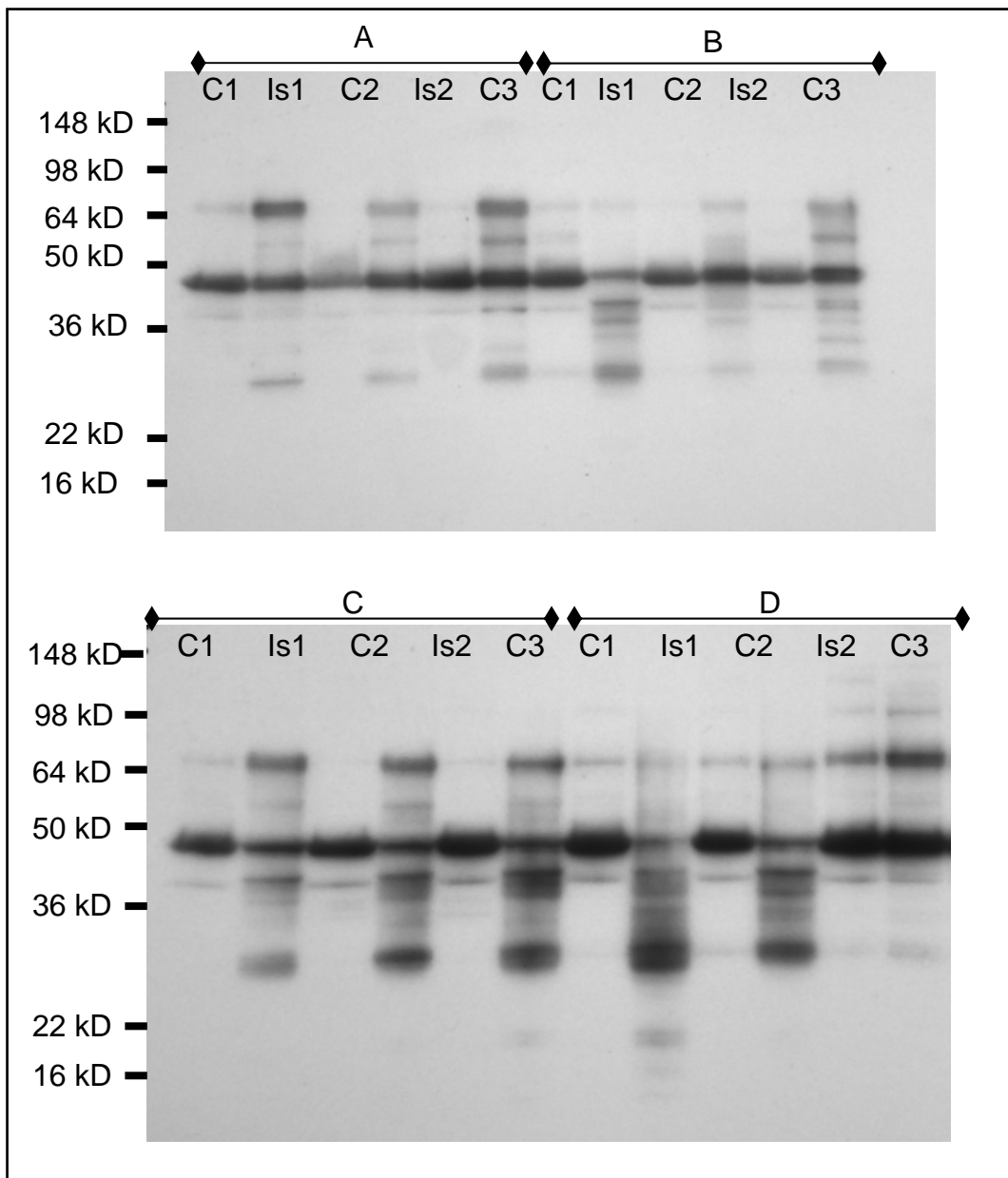
Figure 3.3: Total Tyrosine Nitration of Plantaris/FHL Lysate from Old Mice Following I/R:

Tyrosine nitration of whole cell lysate of glycolytic skeletal muscle from old mice with 2 hours ischemia and variable lengths of reperfusion was examined by Western blot. No statistically significant differences were seen. C = contralateral control Is = I/R; Group A = 1 day reperfusion, Group B = 3 days reperfusion, Group C = 5 days reperfusion, and Group D = 7 days reperfusion
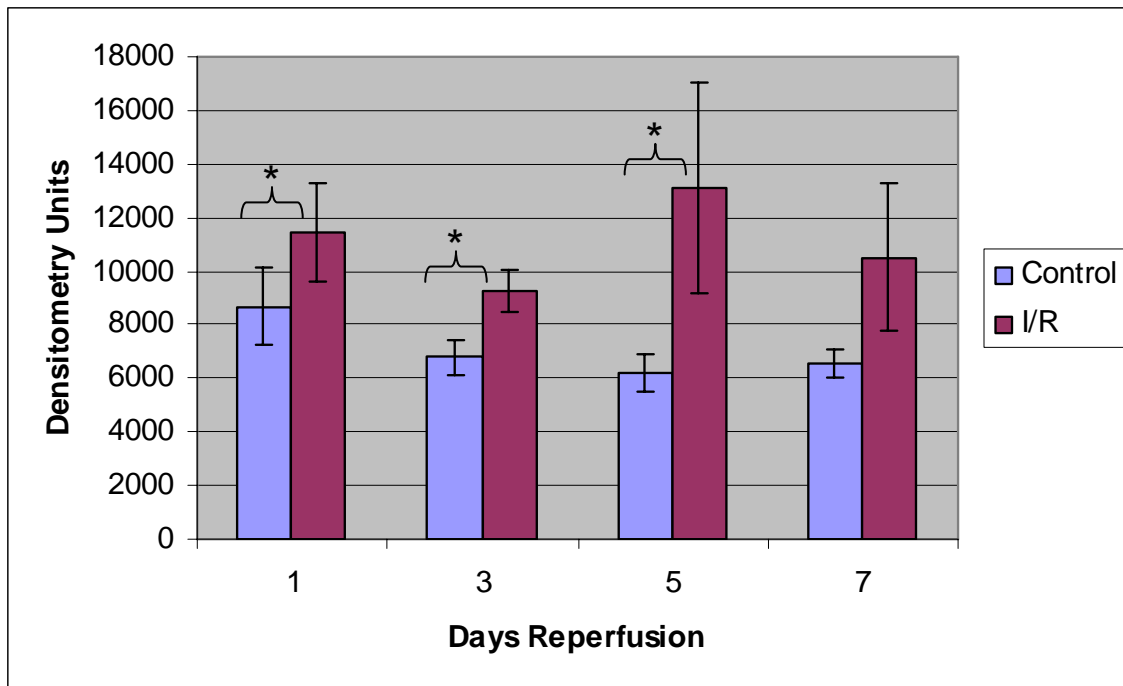
Figure 3.4: Average Total Nitrotyrosine Immunoreactivity in Plantaris/FHL from Old Mice Following I/R, * = p < 0.05

While evaluating overall levels of an oxidative modification is useful as an indication of oxidative stress in a tissue, knowing which proteins are targeted by posttranslational modifications can further an understanding of the consequences of the modifications. Therefore, experiments were undertaken to identify those proteins which were targets of tyrosine nitration in I/R injury. Two-dimensional gel electrophoresis was used to separate lysate from young (6 months) and old (24- 27 months) muscles previously assayed by one dimensional gel electrophoresis and western blot. The five day reperfusion time point was selected for analysis. Anti-nitrotyrosine western blot was used to select spots from a second gel of the same sample (focused concurrently with the gel used for Western blotting) for identification via MALDI-TOF mass spectrometry. A

list of identified proteins is included in Appendix 1. Protein scores greater than 53 are considered significant.

Of the proteins identified by mass spectrometry in the old muscle following I/R, approximately 30% were also identified in the young following I/R. It was noted that several enzymes in the glycolytic pathway were identified as nitrated, based on Western blot selection for MALDI-TOF. Three of these enzymes, glyceraldehyde-3-phosphate dehydrogenase, triosephosphate isomerase, and fructose bis-phosphate aldolase A, were identified from both young and old. During I/R injury, since glycolysis is necessary to maintain adequate ATP levels, any effect on the activities of these enzymes might have a significant effect on ATP levels and consequently on energy availability.

After identifying the nitrated proteins from I/R samples, we re-analyzed the anti-nitrotyrosine Western blots of one-dimensional electrophoresis with respect to a particular nitrated protein. We examined the 37 kD band corresponding to the molecular weight of glyceraldehyde-3-phosphate dehydrogenase (GAPDH). We focused on GAPDH due to its importance in glycolysis, reports of altered GAPDH function with posttranslational modification (i.e., nitrosylation) [41], and a recent report that overexpression of GAPDH can rescue cells in culture from caspase-independent cell death [20]. These reports suggest that GAPDH has multiple functions and may integrate different cellular activities with the metabolic state of the cell [133].

After normalizing the nitration of the 37 kD band to GAPDH protein pool levels as measured by Western blotting, it was found that the nitration of GAPDH in the young was significantly increased at the one and three day time points (p= .001 and .043 respectively). The highest level of nitration in the samples from young mice occurs at the 3 day time point.
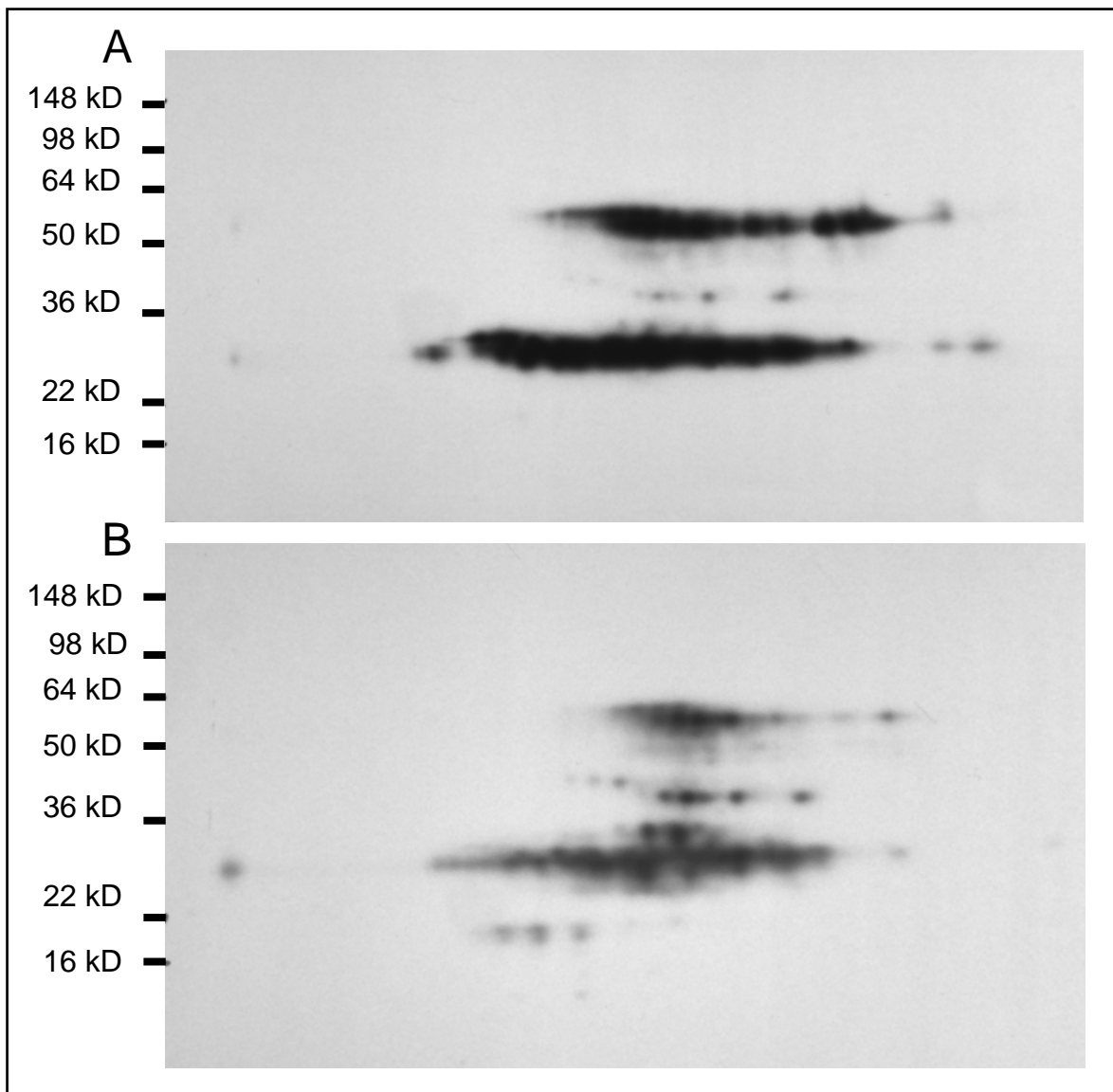
Figure 3.5: 2D Analysis of Nitrated Proteins in Plantaris/FHL from Young and Old Mice Following I/R:

Lysate from the 5 day reperfusion time point of young and old glycolytic skeletal muscle was separated by 2D gel and probed for nitrotyrosine. Spots corresponding to nitrated proteins in the Western blots were selected from duplicate 2D gels and identified by MALDI-TOF (See Appendix 1 for complete list.) A= Young 20 minute exposure; B = Old 30 second exposure

48
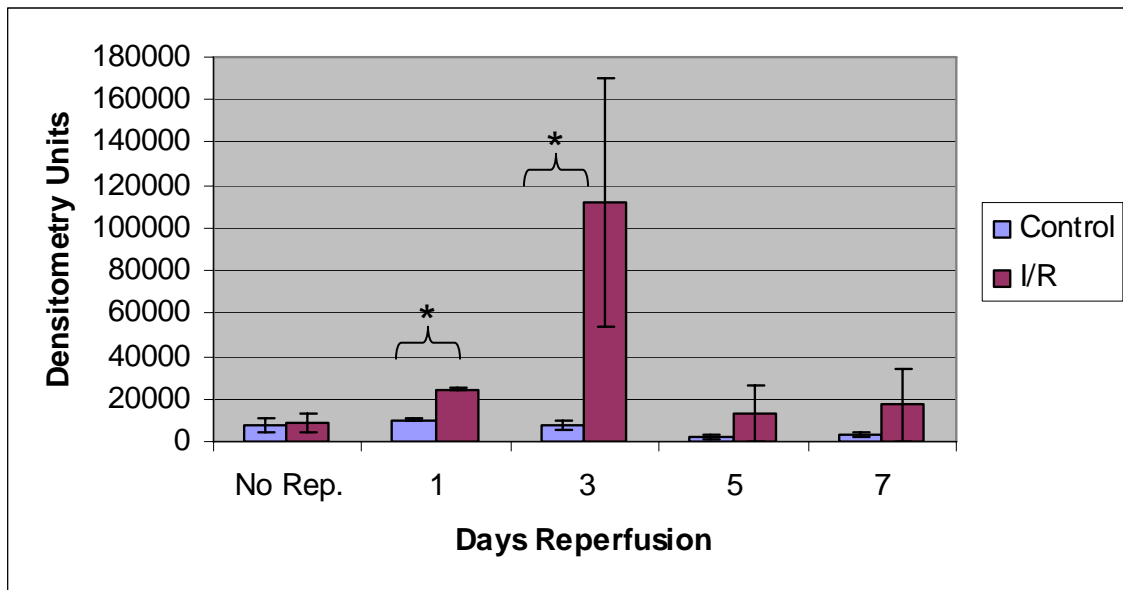
Figure 3.6: Tyrosine Nitration of GAPDH in Plantaris/FHL Lysate from Young Mice:

Tyrosine nitration was assessed by Western blot of one dimensional gel electrophoresis. Nitration was significantly increased for the 37 kD band at 1 and 3 days of reperfusion, with the greatest increase at 3 days reperfusion. $* = p < 0.05$

After normalization to GAPDH pool level, the nitration of the 37 kD band in the samples from old mice was significantly increased at 1, 3, and 5 days reperfusion ($p = .019$, $.048$, and $.011$, respectively). In contrast to the young, the highest levels of nitration measured were at the 5 and 7 day time points; however, the increase in nitration was not statistically significant at 7 days due to the variability within the I/R group.

Comparing the percent increase in nitration (control to I/R) of the 37 kD band, a significant difference ($p= .02$) was noted between the young and old skeletal muscle at the 5 day time point, which was the peak of GAPDH nitration in for the old. The level of nitration in the young had decreased by 5 days, with the peak of the increase in nitration for the young appearing at 3 days reperfusion. In summary, the greatest difference

between control and experimental in the young occurs at 3 days of reperfusion, while the

greatest difference in the old occurs at 5 days of reperfusion.
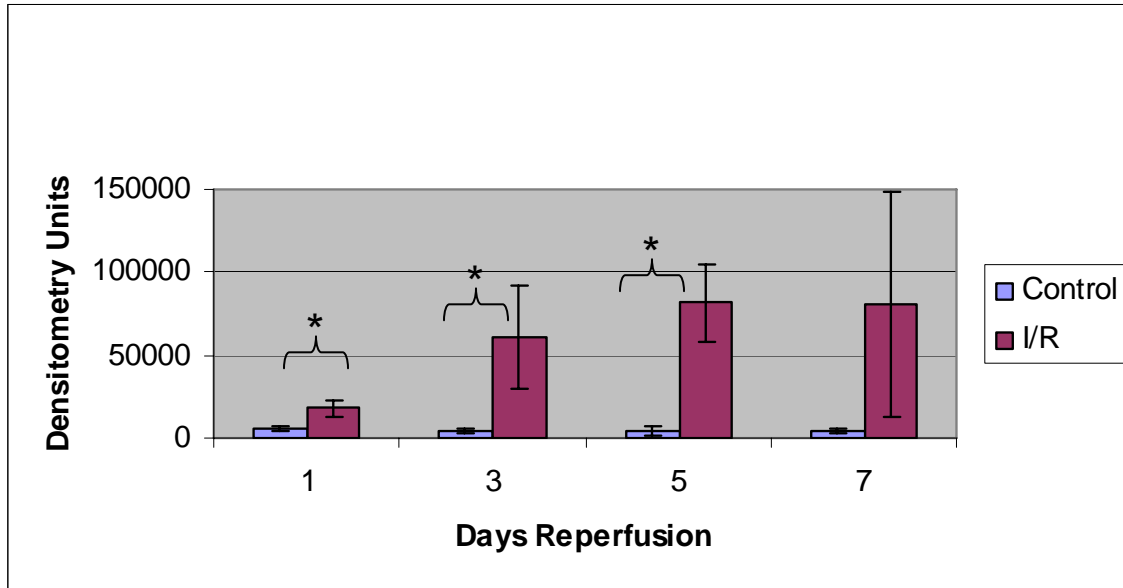
Figure 3.7: Tyrosine Nitration of GAPDH in Plantaris/FHL Lysate from Old Mice:
Tyrosine nitration was assessed by Western blot of one dimensional gel electrophoresis.
Nitration was significantly increased for the 37 kD band at 1, 3, and 5 days of
reperfusion. $* = p < 0.05$
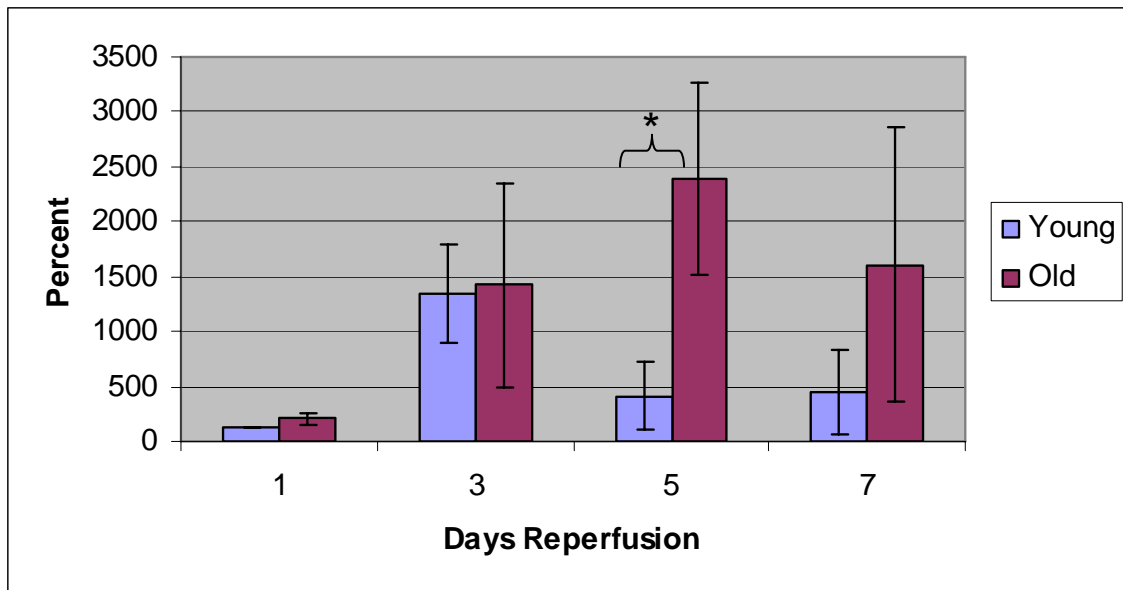
Figure 3.8: Average Percent Increase in Nitration of GAPDH in Plantaris/FHL Lysate from Young and Old Mice Following I/R:

The greatest difference in GAPDH nitration between young control and young I/R occurs at 3 days of reperfusion, while the greatest difference in nitration of GAPDH between the old control and I/R occurs at 5 days of reperfusion. $* = p < 0.05$

Discussion: Chapter 4 - Oxidative Modification, Protein Degradation, and GAPDH

In the present study, we have presented evidence that I/R leads to decreased GAPDH protein levels while increasing levels of nitrated GAPDH. We propose that GAPDH protein levels may be decreased due to increased proteolytic degradation as a result of oxidative protein modification. Oxidative stress and resultant oxidative protein modification have been shown *in vitro* to increase protein degradation by multiple mechanisms [12,65]. Our observations are consistent with these reports. Our results also indicate that GAPDH mRNA levels are increased at 5 days of reperfusion, suggesting that the deficit in GAPDH protein levels is not transcriptionally mediated. However, our results do not rule out a role for dysfunctional/decreased GAPDH translation. This possibility deserves further investigation, considering reports that IGF-1 mRNA is upregulated following I/R (1) and other types of skeletal muscle injury, suggesting that protein translation should be increased.

GAPDH PROTEIN LEVELS

The finding of decreased GAPDH protein in glycolytic skeletal muscle following I/R injury is interesting, as it is known that hypoxia causes a shift towards increased glycolytic metabolism in heart [108] and various cell lines [26,74,104,105]. However, there are conflicting reports concerning the effect of hypoxia on GAPDH transcription, raising the possibility that the response of GAPDH in hypoxia may differ among cell types [35,36,53,75,100], as cell types not only have differing HIF-1α basal expression or inducibility but also may differ in the expression of other HIF family members [35,110].

It is also possible that hypoxia and ischemia have different effects on transcription in skeletal muscle [26]. Furthermore, the relatively brief ischemic time (2 hours) may not lead to a strong induction of GAPDH translation, as one study reported increased GAPDH protein levels in fibroblasts following 18 hours of hypoxia [104]. Finally, the half-life of HIF-1α under normoxic conditions in ferret lung tissue is reported to be less than 1 minute [129]. This suggests that HIF-1α stabilization during ischemia would not mediate increased GAPDH protein levels at the reperfusion time points examined in this study, even if GAPDH protein levels are upregulated by HIF-1α.

PROTEIN DEGRADATION

Another factor that is likely to affect the protein pool level following I/R is protein degradation. We have shown by Western blot that tyrosine nitration increases for GAPDH following I/R injury in both the young and the old muscle. Total tyrosine nitration also increases in the old muscle following I/R. Other investigators have shown that oxidative protein modification leads to protein unfolding [5]. If this unfolding cannot be corrected, the protein is made more susceptible to aggregation or degradation [5,14]. Tyrosine nitration has been used as a marker for oxidative stress, and the increased levels of this modification at time points with lower GAPDH pool levels suggests that oxidative modification may be leading to increased degradation. Supporting this assertion, we see evidence of increased proteolytic products in the I/R samples in both young and aged, in the form of low molecular weight products in the post-transfer gels.

GAPDH has been shown to be degraded by at least two separate proteolytic pathways, i.e., the 20S proteasome [12] and the chaperone-mediated autophagy (CMA)

pathways [65]. Not only is GAPDH degraded by these proteolytic systems, but oxidative modification significantly increased its degradation by both systems *in vitro* [12,62]. For example, *in vitro* tyrosine nitration of GAPDH by peroxynitrite increases the rate of enzyme degradation by the 20S proteasome, compared to the unmodified enzyme [12]. However, degradation rates peak at concentrations of peroxynitrite significantly lower than those required to decrease enzyme activity by half. In addition, the rate of degradation decreased at oxidant concentrations higher than that necessary for maximal stimulation of degradation. Degradation was still higher than control, however, until the peroxynitrite concentration exceeded 2 mM, approximately 20 fold higher than the concentration needed to induce nitration [12]. The decrease in degradation rates appears to involve protein aggregation, oxidative crosslinking, or increasing protein modification [57].

Chaperone-mediated autophagy (CMA) is another mechanism for removing damaged proteins. Kiffin et. al compared the rate of lysosomal import of *in vitro* oxidized GAPDH to the import of untreated GAPDH. They reported that in isolated liver lysosomes from rats starved for 20 hours (a treatment known to increase CMA), oxidized GAPDH was more rapidly imported compared to untreated GAPDH. In addition, liver lysosomes isolated from paraquat-treated rats showed increased uptake of untreated GAPDH, although the rate of proteolytic degradation was slightly lower than for lysosomes from untreated rats [65]. These results suggest that GAPDH which has been nitrated or otherwise oxidatively modified is degraded following I/R injury and offer potential mechanisms for the observed decrease in GAPDH pool levels. In combination with the results in the present study, they also suggest hypotheses for further experiments, which will be discussed later in this chapter. Interestingly, GAPDH pool levels have previously been correlated to oxidative modification in a canine aging model [89]. Dogs

exhibit similar age-related changes in cortical volume and cognitive function as humans. Dogs which were supplemented with a combination of an antioxidant rich diet and behavioral enrichment for a mean of 2.7 years showed decreased carbonylation of GAPDH and increased GAPDH expression in the parietal cortex, compared to age-matched control animals.

From *in vitro* experiments, it appears that high levels of oxidative modification could decrease the proteasomal degradation of oxidatively modified proteins. There is some suggestion of this *in vivo*, as highly oxidized proteins have been detected in the protein aggregates of neurodegenerative diseases such as Alzheimer's and Parkinson's diseases [34] and in lipofuscin in aged tissue [37]. However, the *in vitro* experiments cited represent a "worst case" scenario, where oxidative/nitrosative modifications occur in the absence of antioxidant enzymes, thiol reductants such as glutathione, or chaperones. It is probable that protein degradation *in vivo* would show less inhibition in response to similar levels of protein modification, due to the role of chaperones in preventing protein aggregation.

GAPDH NITRATION

In the young, the levels of GAPDH nitration appear to peak at 3 days reperfusion and decrease by five and seven days. In contrast, GAPDH nitration remains elevated for a longer period of time in the old muscle, with significant increases noted at 5 days of reperfusion. Nitration is still increased (although not significantly) even at 7 days. This is consistent with our hypothesis that (1) oxidative stress and oxidative protein modification in aging and I/R are cumulative, and that (2) I/R injury therefore has a proportionately greater impact upon the old muscle, where antioxidant defenses are

already taxed by chronically elevated ROS. As increased levels of nitration correlate with decreases in GAPDH pool levels for both age groups, it further suggests that oxidative modification may be driving proteolytic degradation of GAPDH following I/R injury.

GAPDH TRANSCRIPTION

One potential cellular response to the decreased GAPDH pool level would be to increase its transcription. Indeed, when we measured GAPDH transcript levels from control and I/R muscle following 5 days of reperfusion, we observed increased GAPDH transcript levels in the I/R samples compared to control. Although it was not statistically significant, it should be noted that our PCR results suggest that GAPDH mRNA in young muscle was upregulated nearly twice as much as in the old (the difference in the average ΔCt between young and old was 0.8). While it is possible that this could play a role in the delayed recovery of GAPDH pool levels in the old, GAPDH is upregulated substantially in both young and old following 5 days of reperfusion when compared to the controls. Therefore, we conclude that it is unlikely that decreased transcriptional response is a sole cause of the persistently decreased GAPDH pool levels in old glycolytic muscle following I/R injury. Analysis of GAPDH mRNA levels at multiple time points would provide more information about the potential of transcriptional differences in the continued decrease in GAPDH pool level in the old glycolytic muscle.

While muscle is a relatively homogenous tissue, the possible contribution of inflammatory cells toward the increased total RNA seen in the I/R samples cannot be discounted without mention. Histological analyses (Farrar *et al*., personal communication) have shown significant levels of immune infiltrate at 5 days in both age

56

groups. While it seems unlikely that RNA isolated from the infiltrating immune cells accounts for the increase in total RNA seen here, we cannot rule out a contribution from these cells with the methods used. Further study using different methods would be required to fully elucidate the contribution made by immune cells in the current results.

TRANSLATION

Another compensatory response to muscle injury and decreased protein pool levels would be to increase translation in conjunction with increased transcription. An important aspect of translation is the ribosomal machinery. During the course of measuring GAPDH mRNA levels, we examined the total RNA by capillary electrophoresis. We found that ribosomal RNA, an integral component of the ribosome, is increased in the muscle following ischemia and 5 days reperfusion. This increase in rRNA may indicate increased ribosomal mass, which would provide increased capacity for protein synthesis.

This is in contrast to what has been reported in rats, where no difference was seen in the level of 18S rRNA in gastrocnemius at 7 days by PCR [40]; however, it should be noted that in addition to the differences in muscle choice, species, and time point, different experimental procedures may explain the discrepancy between these results. In the study by Hammers and Farrar [40], total RNA content was normalized prior to reverse transcription, in accordance with accepted procedure. In our experiments, total RNA quality was assayed prior to balancing. After detecting consistently disparate amounts of total RNA between I/R and control, we felt that the differences were not due to the slight variation in starting muscle weight or to random variation in the isolation procedure. It was decided that balancing the total RNA would eliminate true differences

57

in rRNA abundance and obscure variation in mRNA abundance. As rRNA constitutes the greatest part of total RNA, one could potentially create a paradoxical and artifactual decrease in a specific mRNA if the level of that mRNA was increased to a lesser amount than the rRNA. Therefore we continued to examine equal percentages of the total RNA isolated. In agreement with our findings that the ribosomal RNA is increased, Hammers *et al*. reported increased local insulin-like growth factor-1 (IGF-1) mRNA in rat gastrocnemius following 2 hours of ischemia and 7 days of reperfusion [40]. IGF-1 has been reported to increase the transcriptional activity of RNA polymerase I in HEK293 cells [55] to allow increased capacity for protein synthesis. Increases in local IGF-1 have been reported following muscle injury in several different models, including motor neuron lesion [132], damaging muscle-lengthening contractions [81], cardiotoxin [115], and I/R or hypoxia/reoxygenation [3]. The mechanism for this stimulation of ribosomal transcription was reported to be primarily via activation of the PI3K/Akt/mTOR pathway, although the Ras-MAPK pathway also contributes in HEK293 cells. Amino acid availability appears to play an essential stimulatory role in IGF-1-mediated rRNA transcription as well, as amino acid-starved HEK293 cells in which autophagy (and hence amino acid salvage) had been inhibited did not increase rRNA synthesis in response to IGF-1 [55]. We did not examine IGF-1 mRNA levels in this study, but the data and literature suggest that it would be increased in mouse plantaris following I/R.

With the observed increases in transcription, it would be expected that protein pool levels would rapidly return to normal, given intact translation. In addition to increased protein degradation, another possible explanation for the observed decrease in GAPDH pool level following I/R is a deficient or dysfunctional translation. This seems more likely than alterations in transcription, considering our observation of increased GAPDH mRNA in the I/R samples. Decreased production of anabolic growth factors

with aging [40] and age-related dysfunction in the signaling pathways leading to protein translation [23,68] have been described. Either of these could be potential mechanisms of decreased/dysfunctional translation and the persistence of decreased GAPDH pool levels seen in the aged muscle. However, the decrease in the GAPDH pool levels of the young in the presence of increased transcript (relative to control) is more difficult to rationalize. It is possible that dysfunction of translation may also be involved in the young following I/R, but this remains to be tested directly. The presence of decreased GAPDH protein with increased transcript and increased IGF-1 mRNA argues that an examination of translation would be an important step in understanding the observed phenomena. Of course, it would also be important to examine the changes in GAPDH transcript at earlier time points, particularly in the young. This would show whether the GAPDH transcript is elevated at all time points where the protein level is decreased. If this were the case, it would strongly suggest that translation may also be impaired. There is a precedent for translational arrest following I/R injury from studies examining cerebral I/R injury [25,56] and in kidney [85], although to our knowledge this has not been extended to skeletal muscle. It is noted, however, that the increase in IGF-1 mRNA in this I/R model has only been tested at the 7 day time point. It is possible that IGF-1 levels do not increase until 7 days of reperfusion, causing translation to lag behind transcription until IGF-1 levels rise to stimulate protein synthesis; however, the increase in ribosomal RNA observed at 5 days in plantaris suggests that IGF-1 signaling is already increased by that time point. In summary, we see increases in GAPDH mRNA and rRNA concomitantly with decreases in GAPDH protein levels, suggesting alterations in protein homeostasis during recovery from I/R injury.

SUMMARY

The central observation of this study is that GAPDH protein levels are decreased in both old and young muscle following I/R injury. There are several possible general mechanisms which might explain this finding. Decreased transcription, decreased translation, increased extracellular secretion, or increased degradation could all explain a decrease in protein pool levels from tissue. Our data suggest a model of protein homeostasis following I/R injury in which increased oxidative modification and subsequent degradation of proteins leads to decreases in protein pool levels. Cessation of oxidative stress would allow transcription (and presumably translation) to return protein pools to normal. The observed increase in transcription of GAPDH may be a compensatory response to the decreased protein levels. As we found no evidence in the literature for extracellular secretion of GAPDH in eukaryotes, we did not examine this possibility. The question that remains, however, is "Why are GAPDH protein levels still decreased in the presence of increased transcript level?" As our data does not support the hypothesis that the decrease in GAPDH is transcriptionally mediated, this leaves the possibilities that translation is decreased/dysfunctional or that degradation is increased. Although there is still a statistically significant decrease in GAPDH protein levels in the young following 5 days of reperfusion, the degree of the decrease is more variable than at 3 days, as protein levels had begun to recover in one animal at 5 days. By 7 days reperfusion, the GAPDH pool level is no longer statistically different between the control and I/R limb in the young, suggesting that with declining levels of oxidative modification, the young are able to normalize GAPDH pool levels. For the old animals, however, GAPDH pool levels do not return to normal by the 7 day time point, in spite of evidence for increased GAPDH transcription at 5 days reperfusion. This correlates with significantly increased GAPDH nitration in the old through the 5 day time point (and

higher but not significantly increased levels of nitration at 7 days). This suggests that at time points at which the young have begun to recover the GAPDH pool level, either the prolonged oxidative stress and oxidative modification in the old continues to drive protein degradation or that translation is impaired in the old muscle. Our data support the hypothesis that degradation is responsible for the decreased GAPDH pool levels, although further experiments would be necessary to demonstrate this conclusively. We do not discount a significant role for decreased translation, however; an examination of translation would be a necessary step in further understanding the effects of I/R injury.

FUTURE EXPERIMENTS

The observations and data from the present studies provide information about the aftermath of I/R injury and the contribution of aging to the effects of I/R. However, as is often the case in science, the results of the present study result in a net positive number of questions. Some possible future experiments suggested by this work, related to I/R injury and other pathologic situations, will be discussed below.

One question remaining at the conclusion of the present studies is the effect of tyrosine nitration on GAPDH enzymatic activity in I/R injury. It is unlikely that tyrosine nitration results in the initial loss of GAPDH activity seen in situations of oxidative/nitrative stress, as *in vitro* experiments report loss of glycolytic enzyme activity prior to detection of nitration [12,103]. This is consistent with studies showing that mutation of cysteines in the GAPDH active site abolishes GAPDH glycolytic activity [20]. Other reports have shown that oxidative modification by numerous agents results in loss of activity following modification of these active site cysteines [15,51,83,84],

suggesting that cysteine oxidation following I/R injury in young and aged muscle may be an important physiological factor.

Regardless, this does not mean that tyrosine nitration has no effect on enzyme activity. It is also known that modifications outside of the active site of an enzyme can still cause alterations in enzyme activity. For example, the *in vitro* modification and inactivation of GAPDH by 4-hydroxy-2-nonenal occurred at surface accessible sites rather than the active site [52]. Further, as discussed in the introductory chapter, several forms of cysteine modifications (including nitrosylation) are reversible upon treatment with thiol reductants such as DTT or glutathione. *In vitro* experiments consistently report that following treatment with a reducing agent, a portion of the enzymatic activity of GAPDH is recovered [29,51]. The fraction of the activity that cannot be recovered following reductant treatment may be attributable to higher redox state cysteine modifications which are not reversible by treatment with reducing agents. It is also possible, when peroxynitrite was used as the oxidizing agent, the refractory loss of activity may be the result of nitration. The consequence of this is that while other modifications may initially inactivate GAPDH, nitration of the same molecule may prevent re-activation following the resolution of oxidative stress and return to normal glutathione levels.

Another set of experiments that would expand upon the present results would be an investigation into the activation of the chaperone-mediated autophagy (CMA) pathway following I/R injury in young and aged muscle. As detailed previously, CMA is a mechanism for selectively degrading proteins. GAPDH is a known CMA substrate. As oxidative modification increases uptake of GAPDH by the lysosome and oxidative stress has been shown to activate CMA [65], the decrease in GAPDH pool levels suggests that CMA may act as a mechanism for degrading oxidatively modified GAPDH following I/R

injury. Techniques for isolating lysosomes for the purposes of evaluating CMA have recently been described [63]. Following isolation of lysosomes from post-ischemic muscle, Western blotting for GAPDH would allow a direct means for testing the hypothesis that increased degradation of GAPDH by the CMA pathway following I/R injury contributes to the observed decreases in GAPDH pool level. Further, an increase in oxidative modification (including tyrosine nitration) in the GAPDH recovered from lysosomes would provide direct support for the hypothesis that oxidative modification of GAPDH leads to increased degradation and lower pool levels of the enzyme.

Our studies raise the question as to what extent our findings might be generalized to muscle fibers with a more oxidative phenotype. Metabolic phenotype strongly correlates with sensitivity to oxidative stress [19,33,73,130]. As skeletal muscle with an oxidative phenotype is believed to be more resistant to oxidative stress, a comparison of GAPDH levels within predominately oxidative and predominately glycolytic muscles following I/R would provide a means of testing the hypothesis that oxidative stress and protein modification plays a major role in the observed decrease in GAPDH pool levels. Two possible experimental designs might prove useful in this regard. The first would be to continue the strategy employed in these experiments of selecting muscles with predominately one metabolic fiber type to allow for biochemical experiments. A second strategy would be to select a muscle with a mixture of oxidative and glycolytic fibers such as mouse soleus, which has a nearly even distribution of fiber types [121]. Immunolabeling with fluorescent antibodies might allow colocalization of fiber type markers with GAPDH and nitrotyrosine staining, enabling a comparison of GAPDH or nitrotyrosine levels between fiber types within the same muscle.

A growing body of literature suggests that GAPDH is a multifunctional protein with diverse cellular roles. As part of the glycolytic pathway, GAPDH is directly

responsible for generating reducing equivalents in the form of NADH, as well contributing to ATP generation. While GAPDH is well-known as a glycolytic enzyme, it has also been shown to possess other activities that might be altered due to decreased GAPDH pool levels following I/R injury or to increased oxidative modification in I/R injury or in aging. One intriguing finding is that GAPDH has been shown to physically interact with apurinic/apyrimidinic endonuclease-1 (APE-1) [4]. APE-1 functions both as a DNA endonuclease to remove apurinic/apyrimidinic lesions and as a regulatory molecule which controls the redox state of a number of transcription factors, including NFκB, AP-1, c-Jun, c-Fos, p53, and HIF-1 [31]. The redox state of APE-1 (also known as Ref-1) is believed to be important in the ability of APE-1 to control transcription, and inhibitors of APE-1 redox activity are being investigated as therapeutic options for cancer treatment [32,76] The small cysteine-containing protein thioredoxin has been reported to be responsible for regulating APE-1 activation of the transcription factor AP-1, via a mechanism dependent on the active site cysteines of thioredoxin [47]. This suggests that the regulatory mechanism involves the reduction of APE-1. It has recently been demonstrated that GAPDH also reduces oxidized APE-1. This reduction of APE-1 was shown to be dependent on the active site Cys^{152} and Cys^{156} of GAPDH by independent mutation of each cysteine [4]. In the same study, it was reported that knockdown of GAPDH by siRNA caused increased apurinic lesions in two human colon carcinoma cell lines and correlated with decreased APE-1 activity in cell lysates from these cells. Knockdown of GAPDH by siRNA (80% of control cells) also sensitized cells to bleomycin and methyl methane sulfonate, which both cause DNA lesions in the absence of the repair activity of APE-1. The authors speculate that GAPDH may be able to substitute for thioredoxin in the regulation of c-Jun transcription by APE-1, although this hypothesis was not tested [4]. As mentioned previously, APE-1/Ref-1 is important in the

regulation of many transcription factors, including HIF-1α, the master regulatory transcription factor controlling the cellular response to hypoxia [134]. It has been shown in rat pulmonary artery endothelial cells that the formation of a transcriptional activation complex on the vascular endothelial growth factor hypoxia response element during hypoxia is dependent upon the presence of APE-1 [134]. Earlier work suggest that the recruitment of transcriptional coactivators to the hypoxia response element was potentiated by APE-1/Ref-1 in a redox-dependent manner [16]. More recently, an inhibitor of APE-1 redox function has been developed. Experiments with this compound in endothelial cells and endothelial cell progenitors show that blocking the redox activity of APE-1 decreased the DNA-binding of HIF-1α as well as VEGF secretion [135], further reinforcing the idea that activational capacity of some transcription factors is regulated at least in part by the redox activity of APE-1. If GAPDH has a significant role *in vivo* in maintaining a reduced (and therefore functional) pool of APE-1, it is possible that oxidation or depletion of GAPDH may impair the activity of some transcription factors by diminishing the pool of reduced APE-1/ref-1. Examining the expression of well-characterized targets of transcription factors regulated by APE-1 following I/R could provide information concerning whether loss of GAPDH would affect APE-1 transcriptional regulation. Alternately, expression in cell culture of a GAPDH mutant lacking the putative nuclear import sequence [11] would allow maintenance of glycolytic activity but abolish nuclear localization and activity [20], thus preventing APE-1/GAPDH interaction without disrupting the glycolytic function of GAPDH. Oxidative modification of GAPDH, particularly cysteine oxidation of the active site, could have important consequences in the setting of aging. If GAPDH-mediated reduction of APE-1/ref-1 is an important regulator of transcriptional activity *in vivo*, then increased cysteine oxidation of GAPDH in aging could decrease the repair of apurinic lesions and

predispose to oncogenesis, potentially providing another mechanistic link between increased ROS production with the observed increases in cancer incidence in aging. As oxidative modification of GAPDH has previously been reported in aged muscle [60] and overall cysteine oxidation is increased in mice during aging [91], it is reasonable to hypothesize that (a) cysteine oxidation of GAPDH will be increased during aging, and (b) that decreases in reduced GAPDH would lead to a decreased activity of APE-1 in transcription and repair of apurinic DNA lesions.

Another potential consequence of decreased GAPDH expression is that loss of GAPDH could sensitize the surviving muscle to further insults, such as ROS/RNS from a prolonged inflammatory response, such as that seen in old rats following I/R injury [40]. It has been shown in cell culture that over-expression of GAPDH can prevent caspase-independent cell death in response to treatment with etoposide, staurosporine, or actinomycin D [20]. A recently published study of chronic myelogenous leukemia (CML) demonstrated that the chemotherapeutic agent imatinib mesylate induces both caspase dependent and caspase independent cell death pathways in sensitive clones. However, some CML cells are resistant to therapy with this agent. Cells resistant to imatinib mesylate were reported to have spontaneously upregulated GAPDH expression. Further, it was demonstrated that sensitive cells in culture could be made resistant to imatinib mesylate by overexpression of GAPDH; conversely, resistant clones could be sensitized by siRNA knockdown of GAPDH expression [69].

In the present work, GAPDH protein expression in both young and aged glycolytic skeletal muscle has been shown to be decreased following I/R injury. The decrease in GAPDH expression appears to persist for a longer period of time in the aged muscle, which correlates with a longer period of increased tyrosine nitration. The total RNA and GAPDH mRNA are also increased after 5 days of reperfusion in the I/R muscle

compared to the contralateral control, suggesting a compensatory upregulation responding to the decreased protein pool level of GAPDH. In summary, we have shown significant alterations in GAPDH protein expression following I/R injury in glycolytic skeletal muscle. These alterations may be due to oxidative modification and subsequent protein degradation. This significant decrease in GAPDH could impact subsequent muscle function due to the decrease in glycolysis or other GAPDH functions.

Appendix

POST TRANSFER STAINED GELS:

YOUNG REPERFUSION TIME COURSE
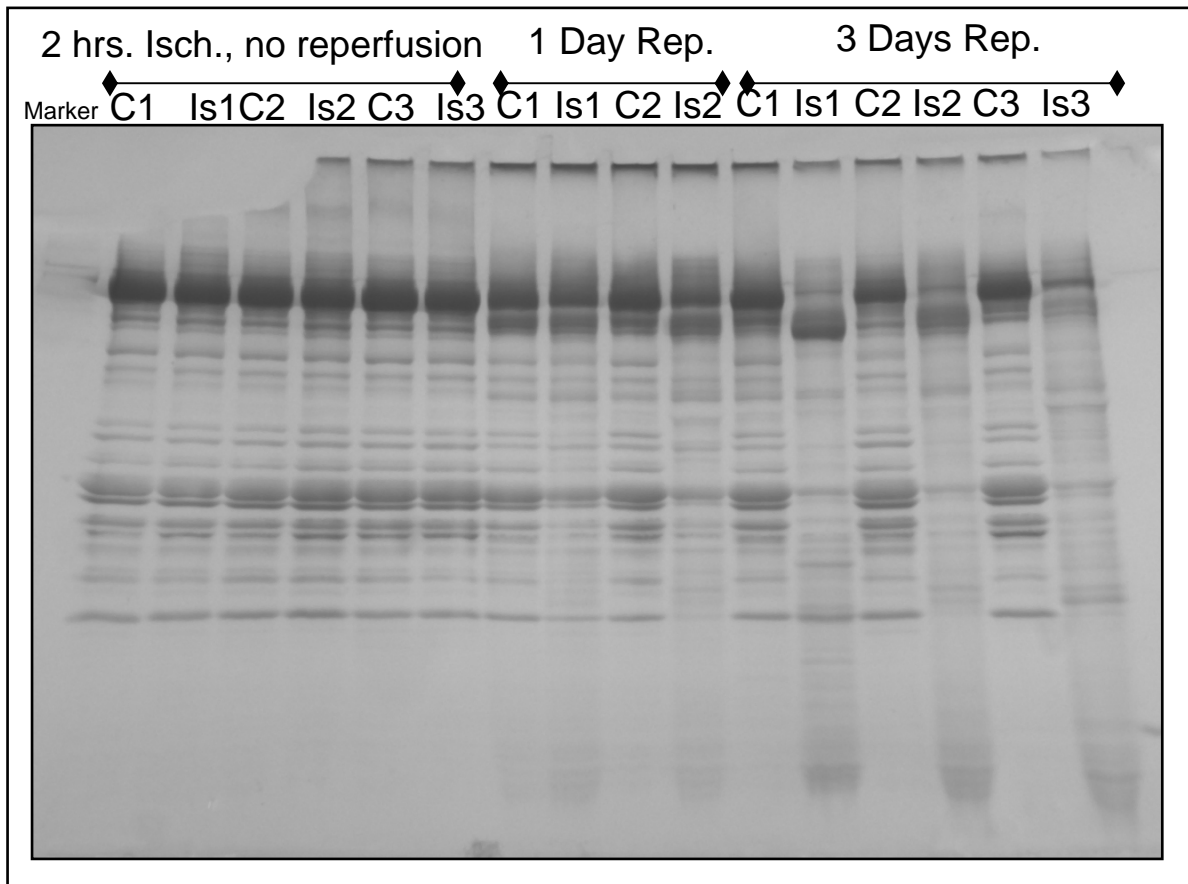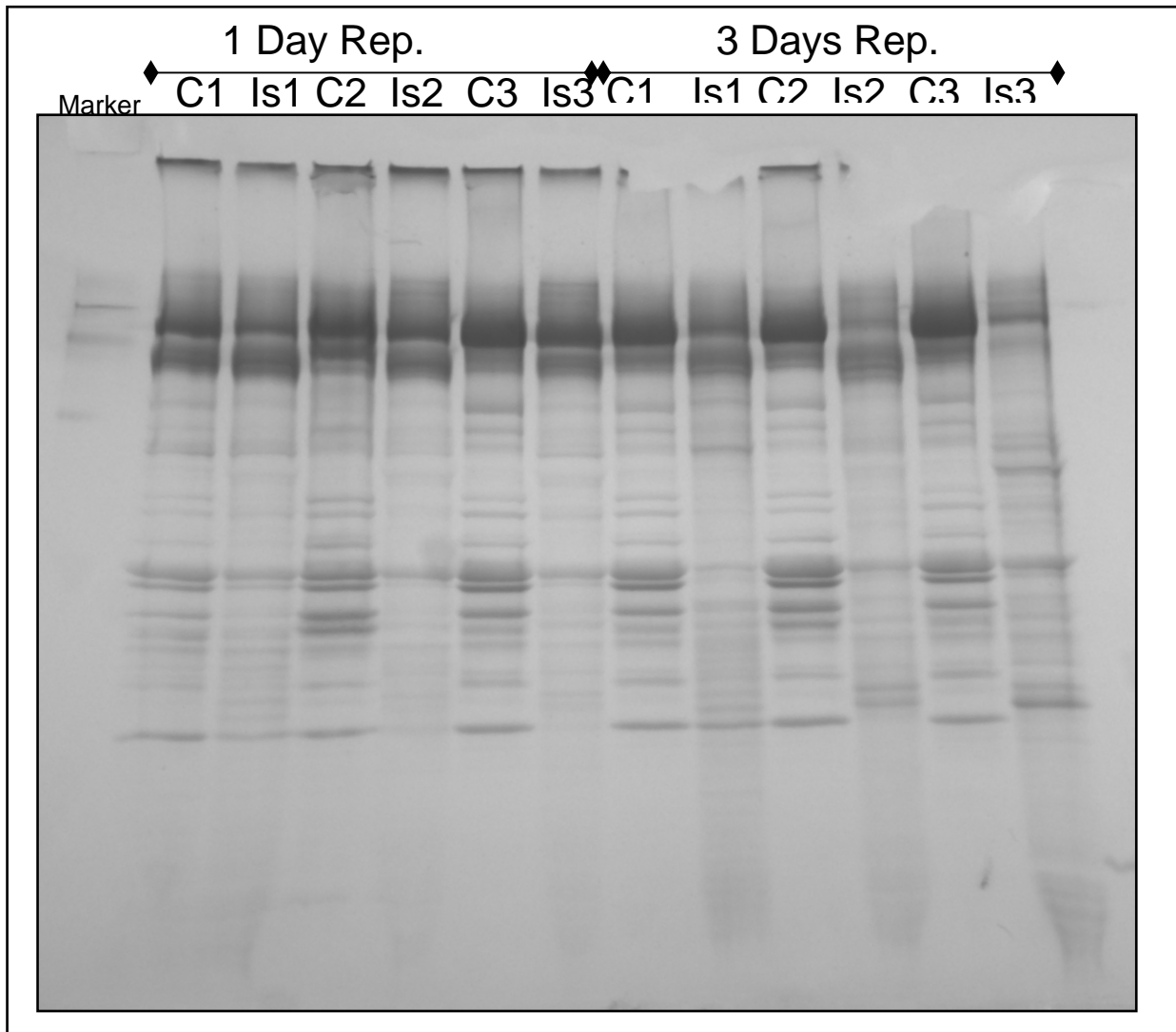
Post-Transfer Gel of Plantaris/FHL Lysate from Young Control and I/R: Coommassie staining of post-transfer gel from the No Reperfusion, 1 Day Reperfusion, and 3 days Reperfusion Time Points

68

Post-Transfer Gel of Young Plantaris/FHL Lysate from Young Control and I/R: Coommassie staining of post-transfer gel from the 5 Days Reperfusion and 7 days Reperfusion Time Points

Post-Transfer Gel of Plantaris/FHL Lysate from Old Control and I/R:
Coommassie staining of post-transfer gel from the 1 Day Reperfusion and 3 days
Reperfusion Time Points
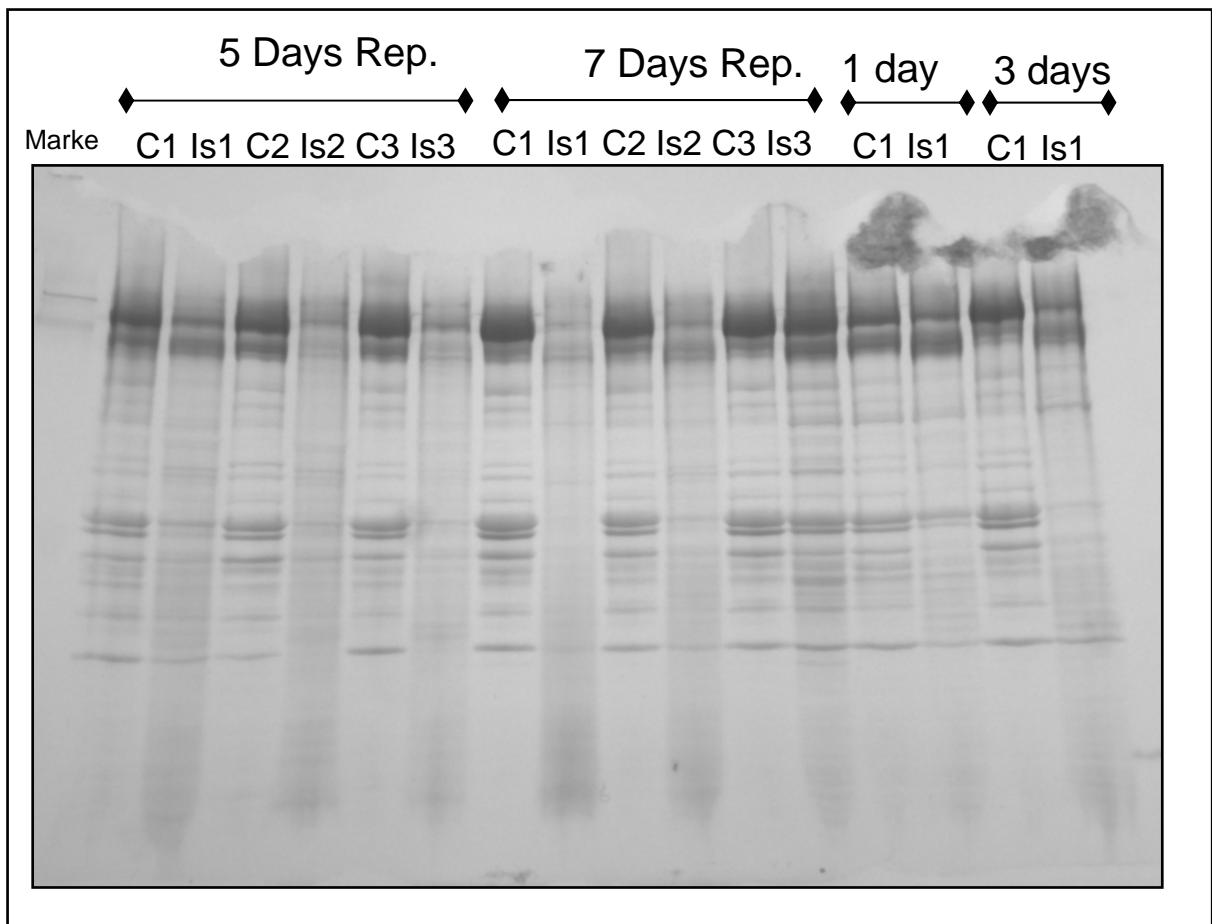
Post-Transfer Gel of Plantaris/FHL Lysate from Old Control and I/R: Coommassie staining of post-transfer gel from the 5 Days Reperfusion and 7 days Reperfusion Time Points

PROTEINS IDENTIFIED BY MASS SPECTROMETRY FOLLOWING 2D ELECTROPHORESIS AND NITRATION WESTERN BLOT

YOUNG – 5 DAYS REPERFUSION

Analysis Information							
	Report Type	Protein-Peptide Summary by Spot		**Analysis Type**	Combined (MS+MS/MS)		
	Sample Set Name	080404c8		**Database**	SwissProt		
	Analysis Name	Mouse SwissProt		**Creation Date**	04/07/2008 09:41:21		
	Reported By	04/07/2008 16:28:37 - admin		**Last Modified**	04/07/2008 10:18:49		
	MS Acq. : Proc. Methods						
	Interpretation Method						

Gel Idx/Pos		49/B22		**Instr./Gel Origin**	AK082/080404c8		
Plate [#] Name		[1] 001300009085		**Instrument Sample Name**			
Rank	**Protein Name**			**Protein MW**	**Pep. Count**	**Protein Score**	**Protein PI**	**Expectation Score**

Rank	**Protein Name**	**Protein MW**	**Pep. Count**	**Protein Score**	**Protein PI**	**Expectation Score**
1	Triosephosphate isomerase - Mus musculus (Mouse)	26695.8	6	199	6.9	1.58114E-16

Gel Idx/Pos	50/B23	**Instr./Gel Origin**	AK082/080404c8			
Plate [#] Name	[1] 001300009085	**Instrument Sample Name**				

Rank	**Protein Name**	**Protein MW**	**Pep. Count**	**Protein Score**	**Protein PI**	**Expectation Score**
1	Triosephosphate isomerase - Mus musculus (Mouse)	26695.8	6	126	6.9	3.15479E-09
2	Fructose-bisphosphate aldolase A - Mus musculus (Mouse)	39331.3	10	108	8.31	1.99054E-07
3	Carbonic anhydrase 3 - Mus musculus (Mouse)	29347.6	5	57	6.89	0.025059362

Gel Idx/Pos	51/B24	**Instr./Gel Origin**	AK082/080404c8			
Plate [#] Name	[1] 001300009085	**Instrument Sample Name**				

Rank	**Protein Name**	**Protein MW**	**Pep. Count**	**Protein Score**	**Protein PI**	**Expectation Score**
1	Triosephosphate isomerase - Mus musculus (Mouse)	26695.8	9	413	6.9	6.29463E-38
2	Carbonic anhydrase 3 - Mus musculus (Mouse)	29347.6	11	289	6.89	1.58114E-25
3	ETS-related transcription factor Elf-3 - Mus musculus (Mouse)	44245.6	10	59	5.75	0.015811388

Gel Idx/Pos	52/C1	**Instr./Gel Origin**	AK082/080404c8			
Plate [#] Name	[1] 001300009085	**Instrument Sample Name**				

Rank	**Protein Name**	**Protein MW**	**Pep. Count**	**Protein Score**	**Protein PI**	**Expectation Score**
1	Triosephosphate isomerase - Mus musculus (Mouse)	26695.8	10	583	6.9	6.29463E-55

Gel Idx/Pos	53/C2	**Instr./Gel Origin**	AK082/080404c8			
Plate [#] Name	[1] 001300009085	**Instrument Sample Name**				

Rank	**Protein Name**	**Protein MW**	**Pep. Count**	**Protein Score**	**Protein PI**	**Expectation Score**
1	Creatine kinase M-type - Mus musculus (Mouse)	43017.8	16	562	6.58	7.92447E-53
2	Triosephosphate isomerase - Mus musculus (Mouse)	26695.8	8	240	6.9	1.25594E-20

Gel Idx/Pos	54/C3	Instr./Gel Origin		AK082/080404c8			
Plate [#] Name	[1] 001300009085	Instrument Sample Name					
Rank	Protein Name		Protein MW	Pep. Count	Protein Score	Protein PI	Expectation Score
1	Peroxiredoxin-6 - Mus musculus (Mouse)		24855	5	149	5.71	1.58114E-11
2	Triosephosphate isomerase - Mus musculus (Mouse)		26695.8	4	78	6.9	0.000199054
3	Creatine kinase M-type - Mus musculus (Mouse)		43017.8	7	76	6.58	0.000315479

Gel Idx/Pos	55/C4	Instr./Gel Origin		AK082/080404c8			
Plate [#] Name	[1] 001300009085	Instrument Sample Name					
Rank	Protein Name		Protein MW	Pep. Count	Protein Score	Protein PI	Expectation Score
1	Heat shock protein beta-1 - Mus musculus (Mouse)		22999.7	8	254	6.12	5E-22
2	Creatine kinase M-type - Mus musculus (Mouse)		43017.8	9	151	6.58	9.97631E-12
3	Triosephosphate isomerase - Mus musculus (Mouse)		26695.8	6	148	6.9	1.99054E-11

Gel Idx/Pos	56/C5	Instr./Gel Origin		AK082/080404c8			
Plate [#] Name	[1] 001300009085	Instrument Sample Name					
Rank	Protein Name		Protein MW	Pep. Count	Protein Score	Protein PI	Expectation Score
1	Triosephosphate isomerase - Mus musculus (Mouse)		26695.8	11	593	6.9	6.29463E-56

Gel Idx/Pos	57/C6	Instr./Gel Origin		AK082/080404c8			
Plate [#] Name	[1] 001300009085	Instrument Sample Name					
Rank	Protein Name		Protein MW	Pep. Count	Protein Score	Protein PI	Expectation Score
1	Serum albumin precursor - Mus musculus (Mouse)		68647.7	5	207	5.75	2.50594E-17

Gel Idx/Pos	58/C7	Instr./Gel Origin		AK082/080404c8			
Plate [#] Name	[1] 001300009085	Instrument Sample Name					
Rank	Protein Name		Protein MW	Pep. Count	Protein Score	Protein PI	Expectation Score
1	Heat shock protein beta-1 - Mus musculus (Mouse)		22999.7	10	432	6.12	7.92447E-40

Gel Idx/Pos	59/C8	Instr./Gel Origin		AK082/080404c8			
Plate [#] Name	[1] 001300009085	Instrument Sample Name					
Rank	Protein Name		Protein MW	Pep. Count	Protein Score	Protein PI	Expectation Score
1	Actin, alpha skeletal muscle - Mus musculus (Mouse)		42023.9	12	482	5.23	7.92447E-45
2	Actin, alpha cardiac muscle 1 - Mus musculus (Mouse)		41991.9	10	450	5.23	1.25594E-41
3	Actin, gamma-enteric smooth muscle - Mus musculus (Mouse)		41849.8	8	304	5.31	5E-27
4	Actin, cytoplasmic 2 - Mus musculus (Mouse)		41765.8	7	220	5.31	1.25594E-18

Gel Idx/Pos		60/C9	Instr./Gel Origin		AK082/080404c8				
Plate [#] Name		[1] 001300009085	Instrument Sample Name						
Rank	Protein Name			Protein MW	Pep.	Protein	Protein	Expectation	
					Count	Score	PI	Score	
1	Serum albumin precursor - Mus musculus (Mouse)			68647.7	5	160	5.75	1.25594E-12	
2	Triosephosphate isomerase - Mus musculus (Mouse)			26695.8	4	130	6.9	1.25594E-09	
3	NADH dehydrogenase [ubiquinone] flavoprotein 2,			27267.9	4	54	7	0.05	
	mitochondrial precursor - Mus musculus (Mouse)								

Gel Idx/Pos		61/C10	Instr./Gel Origin		AK082/080404c8				
Plate [#] Name		[1] 001300009085	Instrument Sample Name						
Rank	Protein Name			Protein MW	Pep.	Protein	Protein	Expectation	
					Count	Score	PI	Score	
1	Actin, alpha cardiac muscle 1 - Mus musculus (Mouse)			41991.9	10	368	5.23	1.99054E-33	
2	Actin, gamma-enteric smooth muscle - Mus musculus			41849.8	9	356	5.31	3.15479E-32	
	(Mouse)								
3	Actin, cytoplasmic 2 - Mus musculus (Mouse)			41765.8	7	261	5.31	9.97631E-23	

Gel Idx/Pos		62/C11	Instr./Gel Origin		AK082/080404c8				
Plate [#] Name		[1] 001300009085	Instrument Sample Name						
Rank	Protein Name			Protein MW	Pep.	Protein	Protein	Expectation	
					Count	Score	PI	Score	
1	Rho GDP-dissociation inhibitor 1 - Mus musculus			23392.8	11	270	5.12	1.25594E-23	
	(Mouse)								

Gel Idx/Pos		63/C12	Instr./Gel Origin		AK082/080404c8				
Plate [#] Name		[1] 001300009085	Instrument Sample Name						
Rank	Protein Name			Protein MW	Pep.	Protein	Protein	Expectation	
					Count	Score	PI	Score	
1	ATP synthase subunit alpha, mitochondrial precursor -			59715.6	18	332	9.22	7.92447E-30	
	Mus musculus (Mouse)								

Gel Idx/Pos		64/C13	Instr./Gel Origin		AK082/080404c8				
Plate [#] Name		[1] 001300009085	Instrument Sample Name						
Rank	Protein Name			Protein MW	Pep.	Protein	Protein	Expectation	
					Count	Score	PI	Score	
1	ATP synthase subunit alpha, mitochondrial precursor -			59715.6	17	290	9.22	1.25594E-25	
	Mus musculus (Mouse)								
2	UTP--glucose-1-phosphate uridylyltransferase - Mus			56943.7	6	58	7.18	0.019905359	
	musculus (Mouse)								

Gel Idx/Pos		65/C14		Instr./Gel Origin		AK082/080404c8			
Plate [#] Name		[1] 001300009085		Instrument Sample Name					
Rank	Protein Name				Protein MW	Pep. Count	Protein Score	Protein PI	Expectation Score
1	ATP synthase subunit alpha, mitochondrial precursor - Mus musculus (Mouse)				59715.6	21	349	9.22	1.58114E-31
2	Annexin A11 - Mus musculus (Mouse)				54076.8	11	146	7.53	3.15479E-11
3	Desmin - Mus musculus (Mouse)				53465	12	67	5.21	0.002505936
4	UTP--glucose-1-phosphate uridylyltransferase - Mus musculus (Mouse)				56943.7	11	67	7.18	0.002505936
5	Nebulin-related-anchoring protein - Mus musculus (Mouse)				195651.6	23	59	9.35	0.015811388

Gel Idx/Pos		66/C15		Instr./Gel Origin		AK082/080404c8			
Plate [#] Name		[1] 001300009085		Instrument Sample Name					
Rank	Protein Name				Protein MW	Pep. Count	Protein Score	Protein PI	Expectation Score
1	Glutamate dehydrogenase 1, mitochondrial precursor - Mus musculus (Mouse)				61298.2	8	75	8.05	0.000397164

Gel Idx/Pos		68/C17		Instr./Gel Origin		AK082/080404c8			
Plate [#] Name		[1] 001300009085		Instrument Sample Name					
Rank	Protein Name				Protein MW	Pep. Count	Protein Score	Protein PI	Expectation Score
1	Dihydrolipoyl dehydrogenase, mitochondrial precursor - Mus musculus (Mouse)				54238.2	10	269	7.99	1.58114E-23
2	Pyruvate kinase isozymes M1/M2 - Mus musculus (Mouse)				57808	13	128	7.18	1.99054E-09
3	Desmin - Mus musculus (Mouse)				53465	10	71	5.21	0.000997631
4	Aconitate hydratase, mitochondrial precursor - Mus musculus (Mouse)				85410	13	70	8.08	0.001255943

Gel Idx/Pos		69/C18		Instr./Gel Origin		AK082/080404c8			
Plate [#] Name		[1] 001300009085		Instrument Sample Name					
Rank	Protein Name				Protein MW	Pep. Count	Protein Score	Protein PI	Expectation Score
1	Pyruvate kinase isozymes M1/M2 - Mus musculus (Mouse)				57808	8	94	7.18	0.000005

Gel Idx/Pos		70/C19		Instr./Gel Origin		AK082/080404c8			
Plate [#] Name		[1] 001300009085		Instrument Sample Name					
Rank	Protein Name				Protein MW	Pep. Count	Protein Score	Protein PI	Expectation Score
1	Creatine kinase M-type - Mus musculus (Mouse)				43017.8	18	361	6.58	9.97631E-33
2	Fructose-bisphosphate aldolase A - Mus musculus (Mouse)				39331.3	15	167	8.31	2.50594E-13
3	NADH dehydrogenase [ubiquinone] flavoprotein 1, mitochondrial precursor - Mus musculus (Mouse)				50801.7	11	62	8.51	0.007924466

Gel Idx/Pos		71/C20		Instr./Gel Origin			AK082/080404c8		
Plate [#] Name		[1] 001300009085		Instrument Sample Name					
Rank		**Protein Name**				**Protein MW**	**Pep.**	**Protein Protein**	**Expectation**
							Count	**Score** **PI**	**Score**
1		Carbonic anhydrase 3 - Mus musculus (Mouse)				29347.6	8	183 6.89	6.29463E-15
2		Glyceraldehyde-3-phosphate dehydrogenase - Mus				35787.2	9	180 8.44	1.25594E-14
		musculus (Mouse)							
3		Fructose-bisphosphate aldolase A - Mus musculus				39331.3	12	144 8.31	5E-11
		(Mouse)							
4		Actin, alpha skeletal muscle - Mus musculus (Mouse)				42023.9	9	80 5.23	0.000125594
5		Actin, alpha cardiac muscle 1 - Mus musculus (Mouse)				41991.9	8	71 5.23	0.000997631
Gel Idx/Pos		72/C21		Instr./Gel Origin			AK082/080404c8		
Plate [#] Name		[1] 001300009085		Instrument Sample Name					
Rank		**Protein Name**				**Protein MW**	**Pep.**	**Protein Protein**	**Expectation**
							Count	**Score** **PI**	**Score**
1		Glycerol-3-phosphate dehydrogenase [NAD+],				37548.4	13	311 6.75	9.97631E-28
		cytoplasmic - Mus musculus (Mouse)							
2		Fructose-bisphosphate aldolase A - Mus musculus				39331.3	11	107 8.31	2.50594E-07
		(Mouse)							
3		Actin, alpha skeletal muscle - Mus musculus (Mouse)				42023.9	8	65 5.23	0.003971641
4		Creatine kinase M-type - Mus musculus (Mouse)				43017.8	10	57 6.58	0.025059362
5		Actin, alpha cardiac muscle 1 - Mus musculus (Mouse)				41991.9	7	56 5.23	0.031547867
Gel Idx/Pos		73/C22		Instr./Gel Origin			AK082/080404c8		
Plate [#] Name		[1] 001300009085		Instrument Sample Name					
Rank		**Protein Name**				**Protein MW**	**Pep.**	**Protein Protein**	**Expectation**
							Count	**Score** **PI**	**Score**
1		Malate dehydrogenase, cytoplasmic - Mus musculus				36488.1	7	188 6.16	1.99054E-15
		(Mouse)							
2		Actin, alpha skeletal muscle - Mus musculus (Mouse)				42023.9	10	92 5.23	7.92447E-06
3		Actin, alpha cardiac muscle 1 - Mus musculus (Mouse)				41991.9	9	81 5.23	9.97631E-05

OLD– 5 DAYS REPERFUSION

Analysis Information							
	Report Type	Protein-Peptide Summary by Spot	**Analysis Type**	Combined (MS+MS/MS)	**P-Value**		0.05
	Sample Set Name	080404c8	**Database**	SwissProt	**Protein**		
	Analysis Name	Mouse SwissProt	**Creation Date**	04/07/2008 09:41:21	**Sig Score**		54
	Reported By	04/07/2008 16:28:28 - admin	**Last Modified**	04/07/2008 10:18:49			

Gel Idx/Pos	2/A2			AK082/080404c8			
Plate [#] Name	[1] 001300009085						
Rank		**Protein Name**		**Protein MW**	**Pep. Count**	**Protein Score**	**Protein PI**	**Expectation Score**

Rank		Protein Name		Protein MW	Pep. Count	Protein Score	Protein PI	Expectation Score
1		ATP synthase subunit alpha, mitochondrial precursor Mus musculus (Mouse)		59715.6	16	383	9.22	6.29463E-35
2		Fibrinogen beta chain precursor [Contains: Fibrinopeptide B] - Mus musculus (Mouse)		54717.7	8	90	6.68	1.25594E-05
3		Strumpellin - Mus musculus (Mouse)		134024.8	12	57	6.72	0.025059362

Gel Idx/Pos	4/A4	AK082/080404c8
Plate [#] Name	[1] 001300009085	

Rank		Protein Name		Protein MW	Pep. Count	Protein Score	Protein PI	Expectation Score
1		Annexin A11 - Mus musculus (Mouse)		54076.8	10	299	7.53	1.58114E-26

Gel Idx/Pos	5/A5	AK082/080404c8
Plate [#] Name	[1] 001300009085	

Rank		Protein Name		Protein MW	Pep. Count	Protein Score	Protein PI	Expectation Score
1		Lamin-A/C - Mus musculus (Mouse)		74192.7	7	72	6.54	0.000792447
2		Serum albumin precursor - Mus musculus (Mouse)		68647.7	8	57	5.75	0.025059362
3		Fibrinogen beta chain precursor [Contains: Fibrinopeptide B] - Mus musculus (Mouse)		54717.7	5	56	6.68	0.031547867

Gel Idx/Pos	9/A9	AK082/080404c8
Plate [#] Name	[1] 001300009085	

Rank		Protein Name		Protein MW	Pep. Count	Protein Score	Protein PI	Expectation Score
1		Serotransferrin precursor - Mus musculus (Mouse)		76673.7	13	294	6.94	5E-26
2		Serum albumin precursor - Mus musculus (Mouse)		68647.7	6	54	5.75	0.05

Gel Idx/Pos	11/A11	AK082/080404c8
Plate [#] Name	[1] 001300009085	

Rank		Protein Name		Protein MW	Pep. Count	Protein Score	Protein PI	Expectation Score
1		Fructose-bisphosphate aldolase A - Mus musculus (Mouse)		39331.3	11	350	8.31	1.25594E-31
2		L-lactate dehydrogenase A chain - Mus musculus (Mouse)		36475.2	7	117	7.62	2.50594E-08

Gel Idx/Pos	13/A13				AK082/080404c8			
Plate [#] Name	[1] 001300009085							
Rank		Protein Name		Protein MW	Pep.		Protein	Protein	Expectation
					Count		Score	PI	Score
1		Glyceraldehyde-3-phosphate dehydrogenase - Mus musculus (Mouse)		35787.2	5		150	8.44	1.25594E-11

Gel Idx/Pos	14/A14				AK082/080404c8			
Plate [#] Name	[1] 001300009085							
Rank		Protein Name		Protein MW	Pep.		Protein	Protein	Expectation
					Count		Score	PI	Score
1		Actin, alpha cardiac muscle 1 - Mus musculus (Mous		41991.9	4		98	5.23	1.99054E-06
2		Actin, alpha skeletal muscle - Mus musculus (Mouse)		42023.9	4		97	5.23	2.50594E-06
3		Actin, gamma-enteric smooth muscle - Mus musculus (Mouse)		41849.8	3		63	5.31	0.006294627
4		Serum albumin precursor - Mus musculus (Mouse)		68647.7	5		59	5.75	0.015811388
5		Actin, cytoplasmic 2 - Mus musculus (Mouse)		41765.8	2		57	5.31	0.025059362

Gel Idx/Pos	15/A15				AK082/080404c8			
Plate [#] Name	[1] 001300009085							
Rank		Protein Name		Protein MW	Pep.		Protein	Protein	Expectation
					Count		Score	PI	Score
1		Ig gamma-2B chain C region secreted form - Mus musculus (Mouse)		36635.3	3		175	7.19	3.97164E-14
2		Ig gamma-2B chain C region, membrane-bound form - Mus musculus (Mouse)		44231.2	3		174	6.1	5E-14
3		Serum albumin precursor - Mus musculus (Mouse)		68647.7	5		124	5.75	0.000000005
4		Actin, alpha cardiac muscle 1 - Mus musculus (Mous		41991.9	4		55	5.23	0.039716412
5		Actin, alpha skeletal muscle - Mus musculus (Mouse)		42023.9	4		54	5.23	0.05

Gel Idx/Pos	16/A16				AK082/080404c8			
Plate [#] Name	[1] 001300009085							
Rank		Protein Name		Protein MW	Pep.		Protein	Protein	Expectation
					Count		Score	PI	Score
1		Actin, alpha cardiac muscle 1 - Mus musculus (Mous		41991.9	4		57	5.23	0.025059362
2		Actin, alpha skeletal muscle - Mus musculus (Mouse)		42023.9	4		57	5.23	0.025059362

Gel Idx/Pos	17/A17				AK082/080404c8			
Plate [#] Name	[1] 001300009085							
Rank		Protein Name		Protein MW	Pep.		Protein	Protein	Expectation
					Count		Score	PI	Score
1		Phosphoglycerate mutase 1 - Mus musculus (Mouse)		28813.9	8		175	6.67	3.97164E-14
2		Phosphoglycerate mutase 2 - Mus musculus (Mouse)		28808.8	4		103	8.65	6.29463E-07
3		Serum albumin precursor - Mus musculus (Mouse)		68647.7	4		65	5.75	0.003971641

Gel Idx/Pos	18/A18					AK082/080404c8		
Plate [#] Name	[1] 001300009085							
Rank		Protein Name		Protein MW	Pep.		Protein	Protein	Expectation
					Count		Score	PI	Score
1		Creatine kinase M-type - Mus musculus (Mouse)		43017.8	6		104	6.58	0.0000005
2		Serum albumin precursor - Mus musculus (Mouse)		68647.7	4		81	5.75	9.97631E-05
3		Fructose-bisphosphate aldolase A - Mus musculus (Mouse)		39331.3	5		68	8.31	0.001990536

Gel Idx/Pos	19/A19					AK082/080404c8		
Plate [#] Name	[1] 001300009085							
Rank		Protein Name		Protein MW	Pep.		Protein	Protein	Expectation
					Count		Score	PI	Score
1		Myosin-4 - Mus musculus (Mouse)		222719.9	9		264	5.58	5E-23
2		Myosin-8 - Mus musculus (Mouse)		222569.5	10		231	5.65	9.97631E-20
3		Myosin-1 - Mus musculus (Mouse)		223203.4	8		161	5.6	9.97631E-13
4		Myosin-3 - Mus musculus (Mouse)		223652.4	8		121	5.62	9.97631E-09

Gel Idx/Pos	21/A21					AK082/080404c8		
Plate [#] Name	[1] 001300009085							
Rank		Protein Name		Protein MW	Pep.		Protein	Protein	Expectation
					Count		Score	PI	Score
1		Creatine kinase M-type - Mus musculus (Mouse)		43017.8	13		456	6.58	3.15479E-42
2		Triosephosphate isomerase - Mus musculus (Mouse)		26695.8	6		246	6.9	3.15479E-21

Gel Idx/Pos	22/A22					AK082/080404c8		
Plate [#] Name	[1] 001300009085							
Rank		Protein Name		Protein MW	Pep.		Protein	Protein	Expectation
					Count		Score	PI	Score
1		Serum albumin precursor - Mus musculus (Mouse)		68647.7	11		527	5.75	2.50594E-49
2		Fructose-bisphosphate aldolase A - Mus musculus (Mouse)		39331.3	7		99	8.31	1.58114E-06

Gel Idx/Pos	23/A23					AK082/080404c8		
Plate [#] Name	[1] 001300009085							
Rank		Protein Name		Protein MW	Pep.		Protein	Protein	Expectation
					Count		Score	PI	Score
1		Serum albumin precursor - Mus musculus (Mouse)		68647.7	13		616	5.75	3.15479E-58

Gel Idx/Pos	24/A24					AK082/080404c8		
Plate [#] Name	[1] 001300009085							
Rank		Protein Name		Protein MW	Pep.		Protein	Protein	Expectation
					Count		Score	PI	Score
1		Serum albumin precursor - Mus musculus (Mouse)		68647.7	12		491	5.75	9.97631E-46

Gel Idx/Pos		28/B1					AK082/080404c8			
Plate [#] Name		[1] 001300009085								
Rank		Protein Name			Protein MW	Pep.		Protein	Protein	Expectation
						Count		Score	PI	Score
1		Serum albumin precursor - Mus musculus (Mouse)			68647.7	8		238	5.75	1.99054E-20
2		Myosin-4 - Mus musculus (Mouse)			222719.9	13		183	5.58	6.29463E-15
3		Myosin-1 - Mus musculus (Mouse)			223203.4	13		178	5.6	1.99054E-14
4		Myosin-8 - Mus musculus (Mouse)			222569.5	11		123	5.65	6.29463E-09
5		Myosin-3 - Mus musculus (Mouse)			223652.4	8		113	5.62	6.29463E-08
Gel Idx/Pos		29/B2					AK082/080404c8			
Plate [#] Name		[1] 001300009085								
Rank		Protein Name			Protein MW	Pep.		Protein	Protein	Expectation
						Count		Score	PI	Score
1		Serum albumin precursor - Mus musculus (Mouse)			68647.7	10		377	5.75	2.50594E-34
Gel Idx/Pos		30/B3					AK082/080404c8			
Plate [#] Name		[1] 001300009085								
Rank		Protein Name			Protein MW	Pep.		Protein	Protein	Expectation
						Count		Score	PI	Score
1		Serum albumin precursor - Mus musculus (Mouse)			68647.7	10		331	5.75	9.97631E-30
Gel Idx/Pos		31/B4					AK082/080404c8			
Plate [#] Name		[1] 001300009085								
Rank		Protein Name			Protein MW	Pep.		Protein	Protein	Expectation
						Count		Score	PI	Score
1		Serum albumin precursor - Mus musculus (Mouse)			68647.7	8		442	5.75	7.92447E-41
2		Actin, cytoplasmic 2 - Mus musculus (Mouse)			41765.8	9		143	5.31	6.29463E-11
3		Actin, cytoplasmic 1 - Mus musculus (Mouse)			41709.7	8		134	5.29	5E-10
4		Actin, alpha skeletal muscle - Mus musculus (Mouse)			42023.9	7		125	5.23	3.97164E-09
5		Actin, alpha cardiac muscle 1 - Mus musculus (Mous			41991.9	6		115	5.23	3.97164E-08
Gel Idx/Pos		32/B5					AK082/080404c8			
Plate [#] Name		[1] 001300009085								
Rank		Protein Name			Protein MW	Pep.		Protein	Protein	Expectation
						Count		Score	PI	Score
1		Apolipoprotein A-I precursor - Mus musculus (Mouse			30568.7	17		622	5.64	7.92447E-59
2		Serum albumin precursor - Mus musculus (Mouse)			68647.7	10		181	5.75	9.97631E-15
3		Actin, alpha skeletal muscle - Mus musculus (Mouse)			42023.9	6		67	5.23	0.002505936
4		Actin, alpha cardiac muscle 1 - Mus musculus (Mous			41991.9	5		60	5.23	0.012559432
5		Actin, gamma-enteric smooth muscle - Mus musculus (Mouse)			41849.8	4		53	5.31	0.062946271

Gel Idx/Pos	33/B6				AK082/080404c8			
Plate [#] Name	[1] 001300009085							
Rank		Protein Name		Protein MW	Pep.	Protein	Protein	Expectation
					Count	Score	PI	Score
1		Serum albumin precursor - Mus musculus (Mouse)		68647.7	5	161	5.75	9.97631E-13
2		Actin, gamma-enteric smooth muscle - Mus musculus		41849.8	4	87	5.31	2.50594E-05
		(Mouse)						
3		Actin, alpha cardiac muscle 1 - Mus musculus (Mous		41991.9	4	87	5.23	2.50594E-05
4		Actin, alpha skeletal muscle - Mus musculus (Mouse)		42023.9	4	86	5.23	3.15479E-05
5		Actin, cytoplasmic 2 - Mus musculus (Mouse)		41765.8	4	62	5.31	0.007924466
Gel Idx/Pos	34/B7				AK082/080404c8			
Plate [#] Name	[1] 001300009085							
Rank		Protein Name		Protein MW	Pep.	Protein	Protein	Expectation
					Count	Score	PI	Score
1		Serum albumin precursor - Mus musculus (Mouse)		68647.7	11	376	5.75	3.15479E-34
2		Actin, alpha skeletal muscle - Mus musculus (Mouse)		42023.9	10	341	5.23	9.97631E-31
3		Actin, cytoplasmic 2 - Mus musculus (Mouse)		41765.8	9	333	5.31	6.29463E-30
4		Actin, alpha cardiac muscle 1 - Mus musculus (Mous		41991.9	8	321	5.23	9.97631E-29
5		Actin, gamma-enteric smooth muscle - Mus musculus		41849.8	6	203	5.31	6.29463E-17
		(Mouse)						
Gel Idx/Pos	35/B8				AK082/080404c8			
Plate [#] Name	[1] 001300009085							
Rank		Protein Name		Protein MW	Pep.	Protein	Protein	Expectation
					Count	Score	PI	Score
1		Serum albumin precursor - Mus musculus (Mouse)		68647.7	11	316	5.75	3.15479E-28
2		Actin, alpha skeletal muscle - Mus musculus (Mouse)		42023.9	6	158	5.23	1.99054E-12
3		Actin, alpha cardiac muscle 1 - Mus musculus (Mous		41991.9	5	148	5.23	1.99054E-11
4		Actin, cytoplasmic 2 - Mus musculus (Mouse)		41765.8	5	93	5.31	6.29463E-06
5		Actin, gamma-enteric smooth muscle - Mus musculus		41849.8	4	85	5.31	3.97164E-05
		(Mouse)						
Gel Idx/Pos	36/B9				AK082/080404c8			
Plate [#] Name	[1] 001300009085							
Rank		Protein Name		Protein MW	Pep.	Protein	Protein	Expectation
					Count	Score	PI	Score
1		Serum albumin precursor - Mus musculus (Mouse)		68647.7	4	135	5.75	3.97164E-10
2		Ig kappa chain C region - Mus musculus (Mouse)		11770.5	2	68	5.23	0.001990536
Gel Idx/Pos	37/B10				AK082/080404c8			
Plate [#] Name	[1] 001300009085							
Rank		Protein Name		Protein MW	Pep.	Protein	Protein	Expectation
					Count	Score	PI	Score
1		Serum albumin precursor - Mus musculus (Mouse)		68647.7	6	168	5.75	1.99054E-13
2		Myosin-1 - Mus musculus (Mouse)		223203.4	4	57	5.6	0.025059362

Gel Idx/Pos	38/B11						AK082/080404c8		
Plate [#] Name	[1] 001300009085								
Rank		Protein Name		Protein MW	Pep.		Protein	Protein	Expectation
					Count		Score	PI	Score
1		Serum albumin precursor - Mus musculus (Mouse)		68647.7	18		943	5.75	6.29463E-91

Gel Idx/Pos	39/B12						AK082/080404c8		
Plate [#] Name	[1] 001300009085								
Rank		Protein Name		Protein MW	Pep.		Protein	Protein	Expectation
					Count		Score	PI	Score
1		Serum albumin precursor - Mus musculus (Mouse)		68647.7	15		614	5.75	5E-58
2		Actin, alpha skeletal muscle - Mus musculus (Mouse)		42023.9	11		162	5.23	7.92447E-13
3		Actin, cytoplasmic 2 - Mus musculus (Mouse)		41765.8	11		162	5.31	7.92447E-13
4		Actin, alpha cardiac muscle 1 - Mus musculus (Mous		41991.9	10		153	5.23	6.29463E-12
5		Actin, gamma-enteric smooth muscle - Mus musculus (Mouse)		41849.8	9		144	5.31	5E-11

Gel Idx/Pos	40/B13						AK082/080404c8		
Plate [#] Name	[1] 001300009085								
Rank		Protein Name		Protein MW	Pep.		Protein	Protein	Expectation
					Count		Score	PI	Score
1		Tropomyosin alpha-1 chain - Mus musculus (Mouse)		32660.7	26		687	4.69	2.50594E-65
2		Tropomyosin beta chain - Mus musculus (Mouse)		32816.6	18		275	4.66	3.97164E-24
3		Tropomyosin alpha-3 chain - Mus musculus (Mouse)		32842.8	13		206	4.68	3.15479E-17
4		Tropomyosin alpha-4 chain - Mus musculus (Mouse)		28450.4	6		68	4.65	0.001990536
5		Ankyrin repeat domain-containing protein 49 - Mus musculus (Mouse)		27094.5	7		54	5.04	0.05

Gel Idx/Pos	41/B14						AK082/080404c8		
Plate [#] Name	[1] 001300009085								
Rank		Protein Name		Protein MW	Pep.		Protein	Protein	Expectation
					Count		Score	PI	Score
1		Myosin-4 - Mus musculus (Mouse)		222719.9	47		795	5.58	3.97164E-76
2		Myosin-7 - Mus musculus (Mouse)		222740.5	28		537	5.59	2.50594E-50
3		Myosin-8 - Mus musculus (Mouse)		222569.5	26		480	5.65	1.25594E-44
4		Myosin-1 - Mus musculus (Mouse)		223203.4	34		453	5.6	6.29463E-42
5		Myosin-6 - Mus musculus (Mouse)		223426.5	24		441	5.57	9.97631E-41

Gel Idx/Pos	42/B15						AK082/080404c8		
Plate [#] Name	[1] 001300009085								
Rank		Protein Name		Protein MW	Pep.		Protein	Protein	Expectation
					Count		Score	PI	Score
1		Superoxide dismutase [Cu-Zn] - Mus musculus (Mous		15932.8	9		406	6.02	3.15479E-37
2		Serum albumin precursor - Mus musculus (Mouse)		68647.7	3		86	5.75	3.15479E-05

Gel Idx/Pos	44/B17				AK082/080404c8			
Plate [#] Name	[1] 001300009085							
Rank		Protein Name		Protein MW	Pep.		Protein	Protein	Expectation
					Count		Score	PI	Score
1		Transthyretin precursor - Mus musculus (Mouse)		15766	9		446	5.77	3.15479E-41

Gel Idx/Pos	45/B18				AK082/080404c8			
Plate [#] Name	[1] 001300009085							
Rank		Protein Name		Protein MW	Pep.		Protein	Protein	Expectation
					Count		Score	PI	Score
1		Peptidyl-prolyl cis-trans isomerase A - Mus musculus (Mouse)		17959.8	2		50	7.74	0.125594322

Gel Idx/Pos	46/B19				AK082/080404c8			
Plate [#] Name	[1] 001300009085							
Rank		Protein Name		Protein MW	Pep.		Protein	Protein	Expectation
					Count		Score	PI	Score
1		Putative RNA-binding protein 3 - Mus musculus (Mouse)		16594.7	8		258	6.84	1.99054E-22
2		Nucleoside diphosphate kinase B - Mus musculus (Mouse)		17351.9	4		60	6.97	0.012559432
3		Peptidyl-prolyl cis-trans isomerase A - Mus musculus (Mouse)		17959.8	6		55	7.74	0.039716412

Bibliography

[1] Anderson, P. L.; Gelijns, A.; Moskowitz, A.; Arons, R.; Gupta, L.; Weinberg, A.; Faries, P. L.; Nowygrod, R.; Kent, K. C. Understanding trends in inpatient surgical volume: vascular interventions, 1980-2000. *J. Vasc. Surg.* **39**:1200-1208; 2004.

[2] Aniento, F.; Roche, E.; Cuervo, A. M.; Knecht, E. Uptake and degradation of glyceraldehyde-3-phosphate dehydrogenase by rat liver lysosomes. *J. Biol. Chem.* **268**:10463-10470; 1993.

[3] Aravindan, N.; Williams, M. T.; Riedel, B. J.; Shaw, A. D. Transcriptional responses of rat skeletal muscle following hypoxia-reoxygenation and near ischaemia-reperfusion. *Acta Physiol Scand.* **183**:367-377; 2005.

[4] Azam, S.; Jouvet, N.; Jilani, A.; Vongsamphanh, R.; Yang, X.; Yang, S.; Ramotar, D. Human glyceraldehyde-3-phosphate dehydrogenase plays a direct role in reactivating oxidized forms of the DNA repair enzyme APE1. *J. Biol. Chem.* **283**:30632-30641; 2008.

[5] Bader, N.; Grune, T. Protein oxidation and proteolysis. *Biol. Chem.* **387**:1351-1355; 2006.

[6] Baker, J. E.; Su, J.; Fu, X.; Hsu, A.; Gross, G. J.; Tweddell, J. S.; Hogg, N. Nitrite confers protection against myocardial infarction: role of xanthine oxidoreductase, NADPH oxidase and K(ATP) channels. *J. Mol. Cell Cardiol.* **43**:437-444; 2007.

[7] Beckman, J. S.; Koppenol, W. H. Nitric oxide, superoxide, and peroxynitrite: the good, the bad, and ugly. *Am. J. Physiol* **271**:C1424-C1437; 1996.

[8] Blaisdell, F. W. The pathophysiology of skeletal muscle ischemia and the reperfusion syndrome: a review. *Cardiovasc. Surg.* **10**:620-630; 2002.

[9] Blanchard-Fillion, B.; Souza, J. M.; Friel, T.; Jiang, G. C.; Vrana, K.; Sharov, V.; Barron, L.; Schoneich, C.; Quijano, C.; Alvarez, B.; Radi, R.; Przedborski, S.; Fernando, G. S.; Horwitz, J.; Ischiropoulos, H. Nitration and inactivation of tyrosine hydroxylase by peroxynitrite. *J. Biol. Chem.* **276**:46017-46023; 2001.

[10] Brovkovych, V.; Stolarczyk, E.; Oman, J.; Tomboulian, P.; Malinski, T. Direct electrochemical measurement of nitric oxide in vascular endothelium. *J. Pharm. Biomed. Anal.* **19**:135-143; 1999.

[11] Brown, V. M.; Krynetski, E. Y.; Krynetskaia, N. F.; Grieger, D.; Mukatira, S. T.; Murti, K. G.; Slaughter, C. A.; Park, H. W.; Evans, W. E. A novel CRM1-mediated nuclear export signal governs nuclear accumulation of glyceraldehyde-3-phosphate dehydrogenase following genotoxic stress. *J. Biol. Chem.* **279**:5984-5992; 2004.

[12] Buchczyk, D. P.; Grune, T.; Sies, H.; Klotz, L. O. Modifications of glyceraldehyde-3-phosphate dehydrogenase induced by increasing concentrations of peroxynitrite: early recognition by 20S proteasome. *Biol. Chem.* **384**:237-241; 2003.

[13] Buchner, D. M.; Larson, E. B.; Wagner, E. H.; Koepsell, T. D.; de Lateur, B. J. Evidence for a non-linear relationship between leg strength and gait speed. *Age Ageing* **25**:386-391; 1996.

[14] Calloni, G.; Zoffoli, S.; Stefani, M.; Dobson, C. M.; Chiti, F. Investigating the effects of mutations on protein aggregation in the cell. *J. Biol. Chem.* **280**:10607-10613; 2005.

[15] Campian, E. C.; Cai, J.; Benz, F. W. Acrylonitrile irreversibly inactivates glyceraldehyde-3-phosphate dehydrogenase by alkylating the catalytically active cysteine 149. *Chem. Biol. Interact.* **140**:279-291; 2002.

[16] Carrero, P.; Okamoto, K.; Coumailleau, P.; O'Brien, S.; Tanaka, H.; Poellinger, L. Redox-regulated recruitment of the transcriptional coactivators CREB-binding protein and SRC-1 to hypoxia-inducible factor 1alpha. *Mol. Cell Biol.* **20**:402-415; 2000.

[17] Cheng, Y. J.; Chien, C. T.; Chen, C. F. Oxidative stress in bilateral total knee replacement, under ischaemic tourniquet. *J. Bone Joint Surg. Br.* **85**:679-682; 2003.

[18] Chirico, W. J.; Waters, M. G.; Blobel, G. 70K heat shock related proteins stimulate protein translocation into microsomes. *Nature* **332**:805-810; 1988.

[19] Choksi, K. B.; Nuss, J. E.; Deford, J. H.; Papaconstantinou, J. Age-related alterations in oxidatively damaged proteins of mouse skeletal muscle mitochondrial electron transport chain complexes. *Free Radic. Biol. Med.* **45**:826-838; 2008.

[20] Colell, A.; Ricci, J. E.; Tait, S.; Milasta, S.; Maurer, U.; Bouchier-Hayes, L.; Fitzgerald, P.; Guio-Carrion, A.; Waterhouse, N. J.; Li, C. W.; Mari, B.; Barbry, P.; Newmeyer, D. D.; Beere, H. M.; Green, D. R. GAPDH and autophagy

preserve survival after apoptotic cytochrome c release in the absence of caspase activation. *Cell* **129**:983-997; 2007.

[21] Crane, B. R. The enzymology of nitric oxide in bacterial pathogenesis and resistance. *Biochem. Soc. Trans.* **36**:1149-1154; 2008.

[22] Cuervo, A. M.; Terlecky, S. R.; Dice, J. F.; Knecht, E. Selective binding and uptake of ribonuclease A and glyceraldehyde-3-phosphate dehydrogenase by isolated rat liver lysosomes. *J. Biol. Chem.* **269**:26374-26380; 1994.

[23] Cuthbertson, D.; Smith, K.; Babraj, J.; Leese, G.; Waddell, T.; Atherton, P.; Wackerhage, H.; Taylor, P. M.; Rennie, M. J. Anabolic signaling deficits underlie amino acid resistance of wasting, aging muscle. *FASEB J.* **19**:422-424; 2005.

[24] Dairou, J.; Pluvinage, B.; Noiran, J.; Petit, E.; Vinh, J.; Haddad, I.; Mary, J.; Dupret, J. M.; Rodrigues-Lima, F. Nitration of a critical tyrosine residue in the allosteric inhibitor site of muscle glycogen phosphorylase impairs its catalytic activity. *J. Mol. Biol.* **372**:1009-1021; 2007.

[25] DeGracia, D. J.; Jamison, J. T.; Szymanski, J. J.; Lewis, M. K. Translation arrest and ribonomics in post-ischemic brain: layers and layers of players. *J. Neurochem.* **106**:2288-2301; 2008.

[26] Dehne, N.; Kerkweg, U.; Otto, T.; Fandrey, J. The HIF-1 response to simulated ischemia in mouse skeletal muscle cells neither enhances glycolysis nor prevents myotube cell death. *Am. J. Physiol Regul. Integr. Comp Physiol* **293**:R1693-R1701; 2007.

[27] Deshaies, R. J.; Koch, B. D.; Werner-Washburne, M.; Craig, E. A.; Schekman, R. A subfamily of stress proteins facilitates translocation of secretory and mitochondrial precursor polypeptides. *Nature* **332**:800-805; 1988.

[28] Draetta, G.; Piwnica-Worms, H.; Morrison, D.; Druker, B.; Roberts, T.; Beach, D. Human cdc2 protein kinase is a major cell-cycle regulated tyrosine kinase substrate. *Nature* **336**:738-744; 1988.

[29] Eaton, P.; Wright, N.; Hearse, D. J.; Shattock, M. J. Glyceraldehyde phosphate dehydrogenase oxidation during cardiac ischemia and reperfusion. *J. Mol. Cell Cardiol.* **34**:1549-1560; 2002.

[30] El Haber, N.; Erbas, B.; Hill, K. D.; Wark, J. D. Relationship between age and measures of balance, strength and gait: linear and non-linear analyses *Clin. Sci. (Lond)* **114**:719-727; 2008.

[31] Evans, A. R.; Limp-Foster, M.; Kelley, M. R. Going APE over ref-1. *Mutat. Res.* **461**:83-108; 2000.

[32] Fishel, M. L.; Kelley, M. R. The DNA base excision repair protein Ape1/Ref-1 as a therapeutic and chemopreventive target. *Mol. Aspects Med.* **28**:375-395; 2007.

[33] Fugere, N. A.; Ferrington, D. A.; Thompson, L. V. Protein nitration with aging in the rat semimembranosus and soleus muscles. *J. Gerontol. A Biol. Sci. Med. Sci.* **61**:806-812; 2006.

[34] Giasson, B. I.; Duda, J. E.; Murray, I. V.; Chen, Q.; Souza, J. M.; Hurtig, H. I.; Ischiropoulos, H.; Trojanowski, J. Q.; Lee, V. M. Oxidative damage linked to neurodegeneration by selective alpha-synuclein nitration in synucleinopathy lesions. *Science* **290**:985-989; 2000.

[35] Graven, K. K.; Bellur, D.; Klahn, B. D.; Lowrey, S. L.; Amberger, E. HIF-2alpha regulates glyceraldehyde-3-phosphate dehydrogenase expression in endothelial cells. *Biochim. Biophys. Acta* **1626**:10-18; 2003.

[36] Graven, K. K.; Yu, Q.; Pan, D.; Roncarati, J. S.; Farber, H. W. Identification of an oxygen responsive enhancer element in the glyceraldehyde-3-phosphate dehydrogenase gene. *Biochim. Biophys. Acta* **1447**:208-218; 1999.

[37] Grune, T.; Jung, T.; Merker, K.; Davies, K. J. Decreased proteolysis caused by protein aggregates, inclusion bodies, plaques, lipofuscin, ceroid, and 'aggresomes' during oxidative stress, aging, and disease. *Int. J. Biochem. Cell Biol.* **36**:2519-2530; 2004.

[38] Guzy, R. D.; Hoyos, B.; Robin, E.; Chen, H.; Liu, L.; Mansfield, K. D.; Simon, M. C.; Hammerling, U.; Schumacker, P. T. Mitochondrial complex III is required for hypoxia-induced ROS production and cellular oxygen sensing. *Cell Metab* **1**:401-408; 2005.

[39] Hallstrom, S.; Gasser, H.; Neumayer, C.; Fugl, A.; Nanobashvili, J.; Jakubowski, A.; Huk, I.; Schlag, G.; Malinski, T. S-nitroso human serum albumin treatment reduces ischemia/reperfusion injury in skeletal muscle via nitric oxide release. *Circulation* **105**:3032-3038; 2002.

[40] Hammers, D. W.; Merritt, E. K.; Matheny, W.; Adamo, M. L.; Walters, T. J.; Estep, J. S.; Farrar, R. P. Functional deficits and insulin-like growth factor-I gene expression following tourniquet-induced injury of skeletal muscle in young and old rats *J. Appl. Physiol* **105**:1274-1281; 2008.

[41] Hara, M. R.; Agrawal, N.; Kim, S. F.; Cascio, M. B.; Fujimuro, M.; Ozeki, Y.; Takahashi, M.; Cheah, J. H.; Tankou, S. K.; Hester, L. D.; Ferris, C. D.; Hayward, S. D.; Snyder, S. H.; Sawa, A. S-nitrosylated GAPDH initiates apoptotic cell death by nuclear translocation following Siah1 binding *Nat. Cell Biol.* **7**:665-674; 2005.

[42] Hasegawa, R.; Islam, M. M.; Lee, S. C.; Koizumi, D.; Rogers, M. E.; Takeshima, N. Threshold of lower body muscular strength necessary to perform ADL independently in community-dwelling older adults *Clin. Rehabil.* **22**:902-910; 2008.

[43] Haynes, V.; Elfering, S.; Traaseth, N.; Giulivi, C. Mitochondrial nitric-oxide synthase: enzyme expression, characterization, and regulation. *J. Bioenerg. Biomembr.* **36**:341-346; 2004.

[44] Hess, D. T.; Matsumoto, A.; Kim, S. O.; Marshall, H. E.; Stamler, J. S. Protein S-nitrosylation: purview and parameters. *Nat. Rev. Mol. Cell Biol.* **6**:150-166; 2005.

[45] Hill, B. G.; Bhatnagar, A. Role of glutathiolation in preservation, restoration and regulation of protein function. *IUBMB. Life* **59**:21-26; 2007.

[46] Hirayama, A.; Nagase, S.; Ueda, A.; Oteki, T.; Takada, K.; Obara, M.; Inoue, M.; Yoh, K.; Hirayama, K.; Koyama, A. In vivo imaging of oxidative stress in ischemia-reperfusion renal injury using electron paramagnetic resonance. *Am. J. Physiol Renal Physiol* **288**:F597-F603; 2005.

[47] Hirota, K.; Matsui, M.; Iwata, S.; Nishiyama, A.; Mori, K.; Yodoi, J. AP-1 transcriptional activity is regulated by a direct association between thioredoxin and Ref-1. *Proc. Natl. Acad. Sci. U. S. A* **94**:3633-3638; 1997.

[48] Hsieh, C. C.; Papaconstantinou, J. The effect of aging on p38 signaling pathway activity in the mouse liver and in response to ROS generated by 3-nitropropionic acid. *Mech. Ageing Dev.* **123**:1423-1435; 2002.

[49] Hsieh, C. C.; Papaconstantinou, J. Thioredoxin-ASK1 complex levels regulate ROS-mediated p38 MAPK pathway activity in livers of aged and long-lived Snell dwarf mice. *FASEB J.* **20**:259-268; 2006.

[50] Hsieh, C. C.; Rosenblatt, J. I.; Papaconstantinou, J. Age-associated changes in SAPK/JNK and p38 MAPK signaling in response to the generation of ROS by 3-nitropropionic acid. *Mech. Ageing Dev.* **124**:733-746; 2003.

[51] Ishii, T.; Sunami, O.; Nakajima, H.; Nishio, H.; Takeuchi, T.; Hata, F. Critical role of sulfenic acid formation of thiols in the inactivation of glyceraldehyde-3-

phosphate dehydrogenase by nitric oxide. *Biochem. Pharmacol.* **58**:133-143; 1999.

[52] Ishii, T.; Tatsuda, E.; Kumazawa, S.; Nakayama, T.; Uchida, K. Molecular basis of enzyme inactivation by an endogenous electrophile 4-hydroxy-2-nonenal: identification of modification sites in glyceraldehyde-3-phosphate dehydrogenase. *Biochemistry* **42**:3474-3480; 2003.

[53] Iyer, N. V.; Kotch, L. E.; Agani, F.; Leung, S. W.; Laughner, E.; Wenger, R. H.; Gassmann, M.; Gearhart, J. D.; Lawler, A. M.; Yu, A. Y.; Semenza, G. L. Cellular and developmental control of O2 homeostasis by hypoxia-inducible factor 1 alpha. *Genes Dev.* **12**:149-162; 1998.

[54] Jackson, M. J. Redox regulation of skeletal muscle *IUBMB. Life* **60**:497-501; 2008.

[55] James, M. J.; Zomerdijk, J. C. Phosphatidylinositol 3-kinase and mTOR signaling pathways regulate RNA polymerase I transcription in response to IGF-1 and nutrients. *J. Biol. Chem.* **279**:8911-8918; 2004.

[56] Jamison, J. T.; Kayali, F.; Rudolph, J.; Marshall, M.; Kimball, S. R.; DeGracia, D. J. Persistent redistribution of poly-adenylated mRNAs correlates with translation arrest and cell death following global brain ischemia and reperfusion. *Neuroscience* **154**:504-520; 2008.

[57] Jung, T.; Grune, T. The proteasome and its role in the degradation of oxidized proteins. *IUBMB. Life* **60**:743-752; 2008.

[58] Kamel, H. K. Sarcopenia and aging. *Nutr. Rev.* **61**:157-167; 2003.

[59] Kanski, J.; Behring, A.; Pelling, J.; Schoneich, C. Proteomic identification of 3-nitrotyrosine-containing rat cardiac proteins: effects of biological aging. *Am. J. Physiol Heart Circ. Physiol* **288**:H371-H381; 2005.

[60] Kanski, J.; Hong, S. J.; Schoneich, C. Proteomic analysis of protein nitration in aging skeletal muscle and identification of nitrotyrosine-containing sequences in vivo by nanoelectrospray ionization tandem mass spectrometry. *J. Biol. Chem.* **280**:24261-24266; 2005.

[61] Katula, J. A.; Rejeski, W. J.; Marsh, A. P. Enhancing quality of life in older adults: a comparison of muscular strength and power training *Health Qual. Life Outcomes.* **6**:45; 2008.

[62] Kaushik, S.; Cuervo, A. M. Autophagy as a cell-repair mechanism: activation of chaperone-mediated autophagy during oxidative stress. *Mol. Aspects Med.* **27**:444-454; 2006.

[63] Kaushik, S.; Cuervo, A. M. Methods to monitor chaperone-mediated autophagy. *Methods Enzymol.* **452**:297-324; 2009.

[64] Khanna, A.; Cowled, P. A.; Fitridge, R. A. Nitric oxide and skeletal muscle reperfusion injury: current controversies (research review) *J. Surg. Res.* **128**:98-107; 2005.

[65] Kiffin, R.; Christian, C.; Knecht, E.; Cuervo, A. M. Activation of chaperone-mediated autophagy during oxidative stress. *Mol. Biol. Cell* **15**:4829-4840; 2004.

[66] Kinjo, N.; Kawanaka, H.; Akahoshi, T.; Yamaguchi, S.; Yoshida, D.; Anegawa, G.; Konishi, K.; Tomikawa, M.; Tanoue, K.; Tarnawski, A.; Hashizume, M.; Maehara, Y. Significance of ERK nitration in portal hypertensive gastropathy and its therapeutic implications. *Am. J. Physiol Gastrointest. Liver Physiol* **295**:G1016-G1024; 2008.

[67] Kong, S. K.; Yim, M. B.; Stadtman, E. R.; Chock, P. B. Peroxynitrite disables the tyrosine phosphorylation regulatory mechanism: Lymphocyte-specific tyrosine kinase fails to phosphorylate nitrated cdc2(6-20)NH2 peptide. *Proc. Natl. Acad. Sci. U. S. A* **93**:3377-3382; 1996.

[68] Kumar, V.; Selby, A.; Rankin, D.; Patel, R.; Atherton, P.; Hildebrandt, W.; Williams, J.; Smith, K.; Seynnes, O.; Hiscock, N.; Rennie, M. J. Age-related differences in the dose-response relationship of muscle protein synthesis to resistance exercise in young and old men. *J. Physiol* **587**:211-217; 2009.

[69] Lavallard, V. J.; Pradelli, L. A.; Paul, A.; Beneteau, M.; Jacquel, A.; Auberger, P.; Ricci, J. E. Modulation of Caspase-Independent Cell Death Leads to Resensitization of Imatinib Mesylate-Resistant Cells. *Cancer Res.* **69**:3013-3020; 2009.

[70] Lepore, D. A.; Kozlov, A. V.; Stewart, A. G.; Hurley, J. V.; Morrison, W. A.; Tomasi, A. Nitric oxide synthase-independent generation of nitric oxide in rat skeletal muscle ischemia-reperfusion injury. *Nitric. Oxide.* **3**:75-84; 1999.

[71] Levine, R. L.; Stadtman, E. R. Oxidative modification of proteins during aging. *Exp. Gerontol.* **36**:1495-1502; 2001.

[72] Li, C.; Jackson, R. M. Reactive species mechanisms of cellular hypoxia-reoxygenation injury. *Am. J. Physiol Cell Physiol* **282**:C227-C241; 2002.

[73] Li, P.; Waters, R. E.; Redfern, S. I.; Zhang, M.; Mao, L.; Annex, B. H.; Yan, Z. Oxidative phenotype protects myofibers from pathological insults induced by chronic heart failure in mice. *Am. J. Pathol.* **170**:599-608; 2007.

[74] Lu, C. W.; Lin, S. C.; Chen, K. F.; Lai, Y. Y.; Tsai, S. J. Induction of pyruvate dehydrogenase kinase-3 by hypoxia-inducible factor-1 promotes metabolic switch and drug resistance. *J. Biol. Chem.* **283**:28106-28114; 2008.

[75] Lu, S.; Gu, X.; Hoestje, S.; Epner, D. E. Identification of an additional hypoxia responsive element in the glyceraldehyde-3-phosphate dehydrogenase gene promoter. *Biochim. Biophys. Acta* **1574**:152-156; 2002.

[76] Luo, M.; Delaplane, S.; Jiang, A.; Reed, A.; He, Y.; Fishel, M.; Nyland, R. L.; Borch, R. F.; Qiao, X.; Georgiadis, M. M.; Kelley, M. R. Role of the multifunctional DNA repair and redox signaling protein Ape1/Ref-1 in cancer and endothelial cells: small-molecule inhibition of the redox function of Ape1. *Antioxid. Redox. Signal.* **10**:1853-1867; 2008.

[77] Majeski, A. E.; Dice, J. F. Mechanisms of chaperone-mediated autophagy. *Int. J. Biochem. Cell Biol.* **36**:2435-2444; 2004.

[78] Makhina, T.; Loers, G.; Schulze, C.; Ueberle, B.; Schachner, M.; Kleene, R. Extracellular GAPDH binds to L1 and enhances neurite outgrowth. *Mol. Cell Neurosci.* **41**:206-218; 2009.

[79] Mallozzi, C.; Di Stasi, A. M.; Minetti, M. Nitrotyrosine mimics phosphotyrosine binding to the SH2 domain of the src family tyrosine kinase lyn. *FEBS Lett.* **503**:189-195; 2001.

[80] Martinez, M. C.; Andriantsitohaina, R. Reactive Nitrogen Species: Molecular Mechanisms and Potential Significance in Health and Disease. *Antioxid. Redox. Signal.* **11**: 669-702; 2009.

[81] McKay, B. R.; O'Reilly, C. E.; Phillips, S. M.; Tarnopolsky, M. A.; Parise, G. Co-expression of IGF-1 family members with myogenic regulatory factors following acute damaging muscle-lengthening contractions in humans. *J. Physiol* **586**:5549-5560; 2008.

[82] Michell, B. J.; Harris, M. B.; Chen, Z. P.; Ju, H.; Venema, V. J.; Blackstone, M. A.; Huang, W.; Venema, R. C.; Kemp, B. E. Identification of regulatory sites of phosphorylation of the bovine endothelial nitric-oxide synthase at serine 617 and serine 635. *J. Biol. Chem.* **277**:42344-42351; 2002.

[83] Mohr, S.; Stamler, J. S.; Brune, B. Mechanism of covalent modification of glyceraldehyde-3-phosphate dehydrogenase at its active site thiol by nitric oxide, peroxynitrite and related nitrosating agents. *FEBS Lett.* **348**:223-227; 1994.

[84] Mohr, S.; Stamler, J. S.; Brune, B. Posttranslational modification of glyceraldehyde-3-phosphate dehydrogenase by S-nitrosylation and subsequent NADH attachment. *J. Biol. Chem.* **271**:4209-4214; 1996.

[85] Montie, H. L.; Kayali, F.; Haezebrouck, A. J.; Rossi, N. F.; DeGracia, D. J. Renal ischemia and reperfusion activates the eIF 2 alpha kinase PERK. *Biochim. Biophys. Acta* **1741**:314-324; 2005.

[86] Newman, A. B.; Kupelian, V.; Visser, M.; Simonsick, E. M.; Goodpaster, B. H.; Kritchevsky, S. B.; Tylavsky, F. A.; Rubin, S. M.; Harris, T. B. Strength, but not muscle mass, is associated with mortality in the health, aging and body composition study cohort *J. Gerontol. A Biol. Sci. Med. Sci.* **61**:72-77; 2006.

[87] Oess, S.; Icking, A.; Fulton, D.; Govers, R.; Muller-Esterl, W. Subcellular targeting and trafficking of nitric oxide synthases *Biochem. J.* **396**:401-409; 2006.

[88] Omodeo-Sale, F.; Cortelezzi, L.; Riva, E.; Vanzulli, E.; Taramelli, D. Modulation of glyceraldehyde 3 phosphate dehydrogenase activity and tyr-phosphorylation of Band 3 in human erythrocytes treated with ferriprotoporphyrin IX. *Biochem. Pharmacol.* **74**:1383-1389; 2007.

[89] Opii, W. O.; Joshi, G.; Head, E.; Milgram, N. W.; Muggenburg, B. A.; Klein, J. B.; Pierce, W. M.; Cotman, C. W.; Butterfield, D. A. Proteomic identification of brain proteins in the canine model of human aging following a long-term treatment with antioxidants and a program of behavioral enrichment: relevance to Alzheimer's disease. *Neurobiol. Aging* **29**:51-70; 2008.

[90] Peluffo, G.; Radi, R. Biochemistry of protein tyrosine nitration in cardiovascular pathology. *Cardiovasc. Res.* **75**:291-302; 2007.

[91] Perez, V. I.; Buffenstein, R.; Masamsetti, V.; Leonard, S.; Salmon, A. B.; Mele, J.; Andziak, B.; Yang, T.; Edrey, Y.; Friguet, B.; Ward, W.; Richardson, A.; Chaudhuri, A. Protein stability and resistance to oxidative stress are determinants of longevity in the longest-living rodent, the naked mole-rat. *Proc. Natl. Acad. Sci. U. S. A* **106**:3059-3064; 2009.

[92] Pierce, A.; Mirzaei, H.; Muller, F.; De Waal, E.; Taylor, A. B.; Leonard, S.; Van Remmen, H.; Regnier, F.; Richardson, A.; Chaudhuri, A. GAPDH is conformationally and functionally altered in association with oxidative stress in

mouse models of amyotrophic lateral sclerosis. *J. Mol. Biol.* **382**:1195-1210; 2008.

[93]   Pierce, A. P.; De Waal, E.; McManus, L. M.; Shireman, P. K.; Chaudhuri, A. R. Oxidation and structural perturbation of redox-sensitive enzymes in injured skeletal muscle. *Free Radic. Biol. Med.* **43**:1584-1593; 2007.

[94]   Quint, P.; Reutzel, R.; Mikulski, R.; McKenna, R.; Silverman, D. N. Crystal structure of nitrated human manganese superoxide dismutase: mechanism of inactivation. *Free Radic. Biol. Med.* **40**:453-458; 2006.

[95]   Rantanen, T. Muscle strength, disability and mortality *Scand. J. Med. Sci. Sports* **13**:3-8; 2003.

[96]   Reid, K. F.; Naumova, E. N.; Carabello, R. J.; Phillips, E. M.; Fielding, R. A. Lower extremity muscle mass predicts functional performance in mobility-limited elders *J. Nutr. Health Aging* **12**:493-498; 2008.

[97]   Reinheckel, T.; Sitte, N.; Ullrich, O.; Kuckelkorn, U.; Davies, K. J.; Grune, T. Comparative resistance of the 20S and 26S proteasome to oxidative stress. *Biochem. J.* **335 (Pt 3)**:637-642; 1998.

[98]   Reinheckel, T.; Ullrich, O.; Sitte, N.; Grune, T. Differential impairment of 20S and 26S proteasome activities in human hematopoietic K562 cells during oxidative stress. *Arch. Biochem. Biophys.* **377**:65-68; 2000.

[99]   Rommel, C.; Bodine, S. C.; Clarke, B. A.; Rossman, R.; Nunez, L.; Stitt, T. N.; Yancopoulos, G. D.; Glass, D. J. Mediation of IGF-1-induced skeletal myotube hypertrophy by PI(3)K/Akt/mTOR and PI(3)K/Akt/GSK3 pathways. *Nat. Cell Biol.* **3**:1009-1013; 2001.

[100] Said, H. M.; Hagemann, C.; Stojic, J.; Schoemig, B.; Vince, G. H.; Flentje, M.; Roosen, K.; Vordermark, D. GAPDH is not regulated in human glioblastoma under hypoxic conditions. *BMC. Mol. Biol.* **8**:55; 2007.

[101] Savvides, S. N.; Scheiwein, M.; Bohme, C. C.; Arteel, G. E.; Karplus, P. A.; Becker, K.; Schirmer, R. H. Crystal structure of the antioxidant enzyme glutathione reductase inactivated by peroxynitrite. *J. Biol. Chem.* **277**:2779-2784; 2002.

[102] Schliess, F.; Gorg, B.; Fischer, R.; Desjardins, P.; Bidmon, H. J.; Herrmann, A.; Butterworth, R. F.; Zilles, K.; Haussinger, D. Ammonia induces MK-801-sensitive nitration and phosphorylation of protein tyrosine residues in rat astrocytes. *FASEB J.* **16**:739-741; 2002.

[103] Schroeder, P.; Klotz, L. O.; Buchczyk, D. P.; Sadik, C. D.; Schewe, T.; Sies, H. Epicatechin selectively prevents nitration but not oxidation reactions of peroxynitrite. *Biochem. Biophys. Res. Commun.* **285**:782-787; 2001.

[104] Seagroves, T. N.; Ryan, H. E.; Lu, H.; Wouters, B. G.; Knapp, M.; Thibault, P.; Laderoute, K.; Johnson, R. S. Transcription factor HIF-1 is a necessary mediator of the pasteur effect in mammalian cells. *Mol. Cell Biol.* **21**:3436-3444; 2001.

[105] Semenza, G. L.; Roth, P. H.; Fang, H. M.; Wang, G. L. Transcriptional regulation of genes encoding glycolytic enzymes by hypoxia-inducible factor 1. *J. Biol. Chem.* **269**:23757-23763; 1994.

[106] Sharov, V. S.; Galeva, N. A.; Dremina, E. S.; Williams, T. D.; Schoneich, C. Inactivation of rabbit muscle glycogen phosphorylase b by peroxynitrite revisited: does the nitration of Tyr613 in the allosteric inhibition site control enzymatic function? *Arch. Biochem. Biophys.* **484**:155-166; 2009.

[107] Sharov, V. S.; Galeva, N. A.; Kanski, J.; Williams, T. D.; Schoneich, C. Age-associated tyrosine nitration of rat skeletal muscle glycogen phosphorylase b: characterization by HPLC-nanoelectrospray-tandem mass spectrometry. *Exp. Gerontol.* **41**:407-416; 2006.

[108] Shohet, R. V.; Garcia, J. A. Keeping the engine primed: HIF factors as key regulators of cardiac metabolism and angiogenesis during ischemia *J. Mol. Med.* **85**:1309-1315; 2007.

[109] Souza, J. M.; Peluffo, G.; Radi, R. Protein tyrosine nitration--functional alteration or just a biomarker? *Free Radic. Biol. Med.* **45**:357-366; 2008.

[110] Sowter, H. M.; Raval, R. R.; Moore, J. W.; Ratcliffe, P. J.; Harris, A. L. Predominant role of hypoxia-inducible transcription factor (Hif)-1alpha versus Hif-2alpha in regulation of the transcriptional response to hypoxia. *Cancer Res.* **63**:6130-6134; 2003.

[111] Spickett, C. M.; Pitt, A. R.; Morrice, N.; Kolch, W. Proteomic analysis of phosphorylation, oxidation and nitrosylation in signal transduction. *Biochim. Biophys. Acta* **1764**:1823-1841; 2006.

[112] Stadler, K.; Bonini, M. G.; Dallas, S.; Jiang, J.; Radi, R.; Mason, R. P.; Kadiiska, M. B. Involvement of inducible nitric oxide synthase in hydroxyl radical-mediated lipid peroxidation in streptozotocin-induced diabetes. *Free Radic. Biol. Med.* **45**:866-874; 2008.

[113] Stadtman, E. R.; Levine, R. L. Free radical-mediated oxidation of free amino acids and amino acid residues in proteins. *Amino. Acids* **25**:207-218; 2003.

[114] Stamler, J. S.; Meissner, G. Physiology of nitric oxide in skeletal muscle. *Physiol Rev.* **81**:209-237; 2001.

[115] Straface, G.; Aprahamian, T.; Flex, A.; Gaetani, E.; Biscetti, F.; Smith, R. C.; Pecorini, G.; Pola, E.; Angelini, F.; Stigliano, E.; Castellot, J. J., Jr.; Losordo, D. W.; Pola, R. Sonic Hedgehog Regulates Angiogenesis and Myogenesis During Post-Natal Skeletal Muscle Regeneration. *J. Cell Mol. Med.* 2008. http://www.ncbi.nlm.nih.gov/pubmed/18662193

[116] Sultana, R.; Poon, H. F.; Cai, J.; Pierce, W. M.; Merchant, M.; Klein, J. B.; Markesbery, W. R.; Butterfield, D. A. Identification of nitrated proteins in Alzheimer's disease brain using a redox proteomics approach. *Neurobiol. Dis.* **22**:76-87; 2006.

[117] Tanaka, K. The proteasome: overview of structure and functions. *Proc. Jpn. Acad. Ser. B Phys. Biol. Sci.* **85**:12-36; 2009.

[118] Thomas, D. D.; Ridnour, L. A.; Isenberg, J. S.; Flores-Santana, W.; Switzer, C. H.; Donzelli, S.; Hussain, P.; Vecoli, C.; Paolocci, N.; Ambs, S.; Colton, C. A.; Harris, C. C.; Roberts, D. D.; Wink, D. A. The chemical biology of nitric oxide: implications in cellular signaling. *Free Radic. Biol. Med.* **45**:18-31; 2008.

[119] Thompson, D. D. Aging and sarcopenia *J. Musculoskelet. Neuronal. Interact.* **7**:344-345; 2007.

[120] Thompson, L. V. Age-related muscle dysfunction. *Exp. Gerontol.* **44**:106-111; 2009.

[121] Vaughan, H. S.; Aziz, U.; Goldspink, G.; Nowell, N. W. Sex and stock differences in the histochemical myofibrillar adenosine triphosphatase reaction in the soleus muscle of the mouse. *J. Histochem. Cytochem.* **22**:155-159; 1974.

[122] Visser, M.; Goodpaster, B. H.; Kritchevsky, S. B.; Newman, A. B.; Nevitt, M.; Rubin, S. M.; Simonsick, E. M.; Harris, T. B. Muscle mass, muscle strength, and muscle fat infiltration as predictors of incident mobility limitations in well-functioning older persons. *J. Gerontol. A Biol. Sci. Med. Sci.* **60**:324-333; 2005.

[123] Walsh, S. R.; Tang, T. Y.; Sadat, U.; Gaunt, M. E. Remote ischemic preconditioning in major vascular surgery. *J. Vasc. Surg.* **49**:240-243; 2009.

[124] Wang, W.; Fang, H.; Groom, L.; Cheng, A.; Zhang, W.; Liu, J.; Wang, X.; Li, K.; Han, P.; Zheng, M.; Yin, J.; Wang, W.; Mattson, M. P.; Kao, J. P.; Lakatta, E. G.; Sheu, S. S.; Ouyang, K.; Chen, J.; Dirksen, R. T.; Cheng, H. Superoxide flashes in single mitochondria. *Cell* **134**:279-290; 2008.

[125] Whetzel, T. P.; Stevenson, T. R.; Sharman, R. B.; Carlsen, R. C. The effect of ischemic preconditioning on the recovery of skeletal muscle following tourniquet ischemia *Plast. Reconstr. Surg.* **100**:1767-1775; 1997.

[126] Xu, Z.; Lam, L. S.; Lam, L. H.; Chau, S. F.; Ng, T. B.; Au, S. W. Molecular basis of the redox regulation of SUMO proteases: a protective mechanism of intermolecular disulfide linkage against irreversible sulfhydryl oxidation. *FASEB J.* **22**:127-137; 2008.

[127] Yang, B.; Rizzo, V. TNF-alpha potentiates protein-tyrosine nitration through activation of NADPH oxidase and eNOS localized in membrane rafts and caveolae of bovine aortic endothelial cells. *Am. J. Physiol Heart Circ. Physiol* **292**:H954-H962; 2007.

[128] Ye, Y.; Quijano, C.; Robinson, K. M.; Ricart, K. C.; Strayer, A. L.; Sahawneh, M. A.; Shacka, J. J.; Kirk, M.; Barnes, S.; Accavitti-Loper, M. A.; Radi, R.; Beckman, J. S.; Estevez, A. G. Prevention of peroxynitrite-induced apoptosis of motor neurons and PC12 cells by tyrosine-containing peptides. *J. Biol. Chem.* **282**:6324-6337; 2007.

[129] Yu, A. Y.; Frid, M. G.; Shimoda, L. A.; Wiener, C. M.; Stenmark, K.; Semenza, G. L. Temporal, spatial, and oxygen-regulated expression of hypoxia-inducible factor-1 in the lung. *Am. J. Physiol* **275**:L818-L826; 1998.

[130] Yu, Z.; Li, P.; Zhang, M.; Hannink, M.; Stamler, J. S.; Yan, Z. Fiber type-specific nitric oxide protects oxidative myofibers against cachectic stimuli *PLoS. ONE.* **3**:e2086; 2008. http://www.plosone.org/article/info%3Adoi%2F10.1371%2Fjournal.pone.0002086

[131] Zaid, H.; Talior-Volodarsky, I.; Antonescu, C.; Liu, Z.; Klip, A. GAPDH binds GLUT4 reciprocally to Hexokinase-II and regulates glucose transport activity. *Biochem. J.* **419**:475-484; 2009.

[132] Zeman, R. J.; Zhao, J.; Zhang, Y.; Zhao, W.; Wen, X.; Wu, Y.; Pan, J.; Bauman, W. A.; Cardozo, C. Differential skeletal muscle gene expression after upper or lower motor neuron transection. *Pflugers Arch.* **458**:525-535; 2009.

[133] Zheng, L.; Roeder, R. G.; Luo, Y. S phase activation of the histone H2B promoter by OCA-S, a coactivator complex that contains GAPDH as a key component. *Cell* **114**:255-266; 2003.

[134] Ziel, K. A.; Campbell, C. C.; Wilson, G. L.; Gillespie, M. N. Ref-1/Ape is critical for formation of the hypoxia-inducible transcriptional complex on the hypoxic response element of the rat pulmonary artery endothelial cell VEGF gene. *FASEB J.* **18**:986-988; 2004.

[135] Zou, G. M.; Karikari, C.; Kabe, Y.; Handa, H.; Anders, R. A.; Maitra, A. The Ape-1/Ref-1 redox antagonist E3330 inhibits the growth of tumor endothelium and endothelial progenitor cells: therapeutic implications in tumor angiogenesis. *J. Cell Physiol* **219**:209-218; 2009.

Vita

Christopher Eric Bailey was born in Orange, Texas in 1978, to William and Melissa Bailey. He graduated as the valedictorian of Community Christian High School in 1996 and was subsequently named a National Merit Scholar. He then attended East Texas Baptist University, graduating with a B.A. in psychology. He attended Lamar University- Beaumont, where he completed his premedical requirements. Subsequently, he was accepted into medical school at the University of Texas Medical Branch-Galveston. After the first year of medical school, he applied and was accepted into the MD/PhD program. He joined the Papaconstantinou lab in 2004 to examine the contribution of oxidative stress and posttranslational protein modification to aging and pathology. He is married to Kimberly Shilling Bailey, M.D. He will be continuing his medical education at the James H. Quillen College of Medicine at East Tennessee State University.

Education

B.A., May 2000, East Texas Baptist University

Publications

Jonathan E. Nuss, James K. Amaning, **C. Eric Bailey**, James H. DeFord, Vincent L. Dimayuga, Jeffrey P. Rabek, and John Papaconstantinou   (2009) *Aging* 1 (6)

Permanent address: 378 Oak Grove Road, Gray, TN 37615

This dissertation was typed by Christopher Eric Bailey.